Electronic Supplementary Material (ESI) for ChemComm.
This journal is © The Royal Society of Chemistry 2020

Electronic supplementary Information (ESI)

Synthesis and reactivity of phosphine borohydride compounds

Ramaraj Ayyappan,[a] Yannick Coppel,[a] Laure Vendier,[a] Sundargopal Ghosh,[b] Sylviane Sabo-Etienne,[a] Sébastien Bontemps,[a]*

[a] LCC-CNRS, Université de Toulouse, CNRS, 205 route de Narbonne, 31077 Toulouse Cedex 04, France.

[b] Department of Chemistry, Indian Institute of Technology Madras, Chennai 600036, India.

E-mail: sebastien.bontemps@lcc-toulouse.fr.

Table of content

1. General considerations

All manipulations were carried out under an argon atmosphere using either Schlenk techniques or inside argon filled glove box.[i] Dry and degassed solvents were collected from MBraun solvent purification system (SPS). Deuterated solvents THF-d_8, C_6D_6 and toluene-d_8 were dried over 4 Å molecular sieves, degassed and stored under argon atmosphere. Quick pressure NMR valves and Fischer-Porter assembly was used to carry out reactions with CO_2. 9-BBN (9-borabicyclo[3.3.1]nonane), and CH_3I were purchased from Sigma Aldrich and used as received. Mes_2B-H (Mes = 2,4,6-$Me_3(C_6H_2)$)[ii], $(Ipc)_2B$-H (Ipc = diisopinocampheyl)[iii], *o*-${}^iPr_2P(C_6H_4)Br$[iv] and 1-iodo-8-(diisopropylphosphino)naphthalene[v] were synthesized according to the literature reports. NMR spectra were recorded using Bruker Avance 400 and Avance NEO 600 NMR spectrometers. The ^1H and ^{13}C NMR chemical shifts were referenced to the residual proton and carbon signal of the deuterated solvents respectively. The ^{31}P, ^{11}B and ^7Li NMR spectra were referenced relative to 85% H_3PO_4 aqueous solution, $F_3B.Et_2O$ and 1M LiCl (external reference) respectively. Chemical shifts are reported in ppm (δ) and coupling constants in Hertz (Hz). The following abbreviations were used, s – singlet, d – doublet, t – triplet, quart – quartet, sept – septet, br-broad and m – multiplet. ESI-MS mass spectra were measured on a TSQ 7000 Thermo Electron mass instrument at ICT "Institut de Chimie de Toulouse" (website: ict.ups-tlse.fr). Elemental analyses were performed in the facility available in Laboratoire de Chimie de Coordination du CNRS using PerkinElmer 2400 Series Analyzer, Toulouse. Single crystals were diffracted in Bruker Kappa APEX II diffractometer at 100 – 115 K using Mo Kα radiation (λ = 0.71073 Å) filtered through graphite monochromator.

2. $[Li(OEt_2)]^+[o\text{-}{}^iPr_2P\text{-}C_6H_4\text{-}B(C_8H_{14})\text{-}H]^-$ (1a)

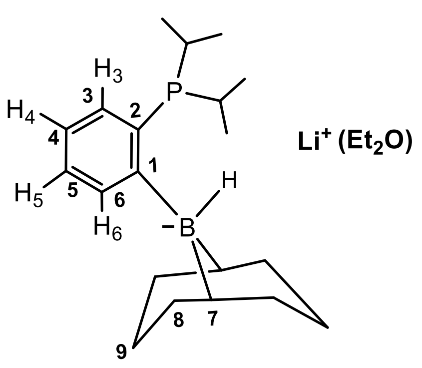

(1a)

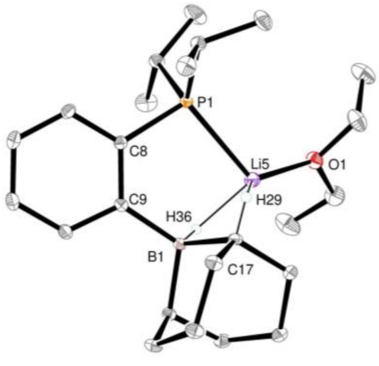

9-BBN dimer (0.400 g, 1.50 mmol) and *o*-Li(0.9 Et_2O)-C_6H_4-P^iPr_2 (0.800 g, 3.00 mmol) were stirred together at rt for 10 h in toluene (10 mL) under an argon atmosphere. Then, the solvent was removed under vacuum and after addition of n-pentane (35 mL) a colourless solid precipitated at –35 °C. (0.800 g, 2.02 mmol, 68 %). Monocrystals suitable for X-ray diffraction were obtained by cooling a saturated n-pentane solution at –35 °C. Compound **1a** features one molecule of Et_2O coordinated to Li^+ as shown in the crystal structure as well as by ^1H NMR spectroscopy.

^1H NMR (600.47 MHz, 298 K, C_6D_6): δ 8.24 (dd, $^3J_{H\text{-}H}$ = 8.0 Hz, $^3J_{H\text{-}P}$ = 3.4 Hz, 1H, H3), 7.41 (tt, $^3J_{H\text{-}H}$ = 7.5 Hz, $^4J_{H\text{-}P}$ = 1.5 Hz, 1H, H4), 7.30 (ddd, $^3J_{H\text{-}H}$ = 6.2 Hz, $^4J_{H\text{-}H}$ = 1.5 Hz, 1H, H6), 7.17 (td, $^3J_{H\text{-}H}$ = 7.3 Hz, $^4J_{H\text{-}H}$ = 1.5 Hz, 1H, H5), 2.47 (m, 3H, CH and CH_2 (9-BBN)), 2.36 (br s, CH_2 (9-BBN), 2H), 2.23 (m, $^3J_{H\text{-}H}$ = 6.4 Hz, 1H, CH (9-BBN)), 2.07 (br s, 2H, CH_2 (9-BBN), 1.94 (m, 6H, $^3J_{H\text{-}H}$ = 7.1 Hz, CH_2 (9-BBN) and CH(^{i}Pr)), 1.61 (brs, 2H, CH_2(9-BBN)), 1.51 (quart, $^1J_{B\text{-}H}$ = 60 Hz, 1H, B-H), 1.02 (dd, $^3J_{H\text{-}P}$ = 14.7 Hz, $^3J_{H\text{-}H}$ = 6.9 Hz, 6H, CH_3(^{i}Pr)), 0.90 (dd, $^3J_{H\text{-}P}$ = 13.2 Hz, $^3J_{H\text{-}H}$ = 7.1 Hz, 6H, CH_3(^{i}Pr)).

$^{31}P\{^1H\}$ NMR (243.07 MHz, 298 K, C_6D_6): δ 0.2 (br s)

$^{31}P\{^1H\}$ NMR (243.07 MHz, 233 K, tol-*d*$_8$): δ –1.6 (quart, $^1J_{P\text{-}Li}$ = 69.4 Hz)

$^{31}P\{^1H\}$ NMR (243.07 MHz, 298 K, THF-*d*$_8$): δ –0.4 (quart, $J_{B\text{-}P}$ = 10.7 Hz)

^{11}B NMR (192.65 MHz, 298 K, C_6D_6): δ –13.3 (d, $^1J_{B\text{-}H}$ = 65.7 Hz)

$^{11}B\{^1H\}$ NMR (192.65 MHz, 298 K, THF-*d*$_8$): δ –13.7 (d, $J_{B\text{-}P}$ = 10.6 Hz)

$^{13}C\{^1H\}$ NMR (151.00 MHz, 298 K, C_6D_6): δ 169.0 (br s, C1), 136.1 (d, $^1J_{C\text{-}P}$ = 15.6 Hz, C2), 131.0 (s, C5), 128.8 (s, C6), 128.3 (s, C4), 123.6 (d, $^2J_{C\text{-}P}$ = 3.2 Hz, C3), 36.8 (s, CH_2(9-BBN), C8), 31.0 (s, CH_2(9-BBN), C8), 25.9 (br, CH(^{i}Pr)), 25.9 (s, CH_2(9-BBN), C9), 25.6 (s, CH_2(9-BBN), C9), 25.5 (br, CH(9-BBN), C7), 21.0 (d, $^2J_{C\text{-}P}$ = 14.0 Hz, CH_3(^{i}Pr)), 20.6 (d, $^2J_{C\text{-}P}$ = 8.1 Hz, CH_3(^{i}Pr)).

Comments: The CH(iPr), CH_2(9-BBN) {C9} and CH(9-BBN) (C7) signals are overlapping. Assignments were based on $^{13}C\{^1H\}\{^{31}P\}$, DEPT-135 and ^1H-^{13}C HSQC experiments.

^7Li NMR (233.37 MHz, 298 K, C_6D_6): δ 0.4 (br s)

^7Li NMR (233.37 MHz, 233 K, tol-*d*$_8$): δ 0.5 (dd, $^1J_{P\text{-}Li}$ = 70.0 Hz, $^1J_{Li\text{-}H}$ = 7.0 Hz)

$^{31}P\{^1H\}$ MAS NMR (168.8 MHz, 298 K): δ 5.4 (quart, $^1J_{P\text{-}Li}$ = 72.9 Hz)

^7Li MAS NMR (155.30 MHz, 298 K): δ –1.0 (d, $^1J_{P\text{-}Li}$ = 72.9 Hz)

Anal. cald. for $C_{24}H_{43}BLiOP$: C, 72.73; H, 10.94. Found: C, 72.13; H, 11.20

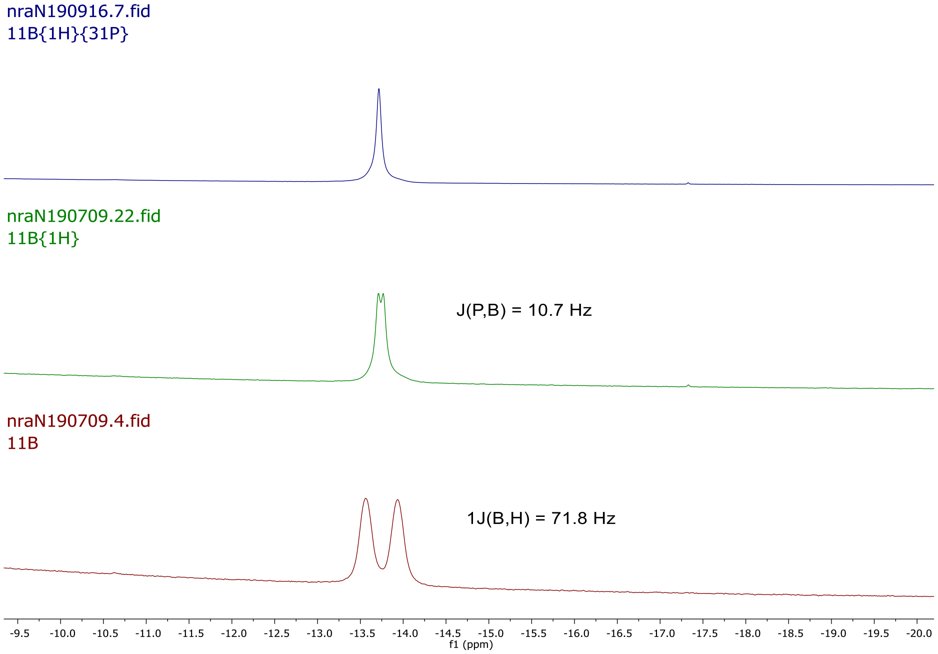

Figure S1. ^{11}B NMR spectral stack plot of **1a** upon decoupling ^{1}H and ^{31}P in THF-d_8 at 298 K.

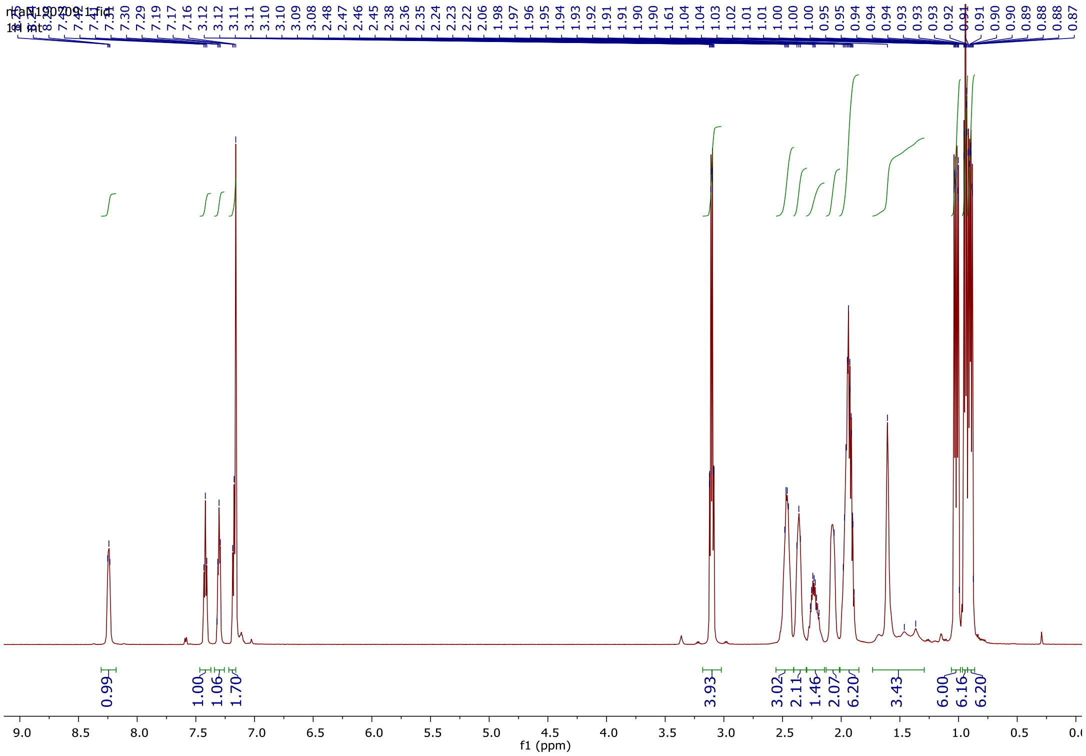

Figure S2. ^{1}H NMR spectrum of **1a** in C_6D_6 at 298 K

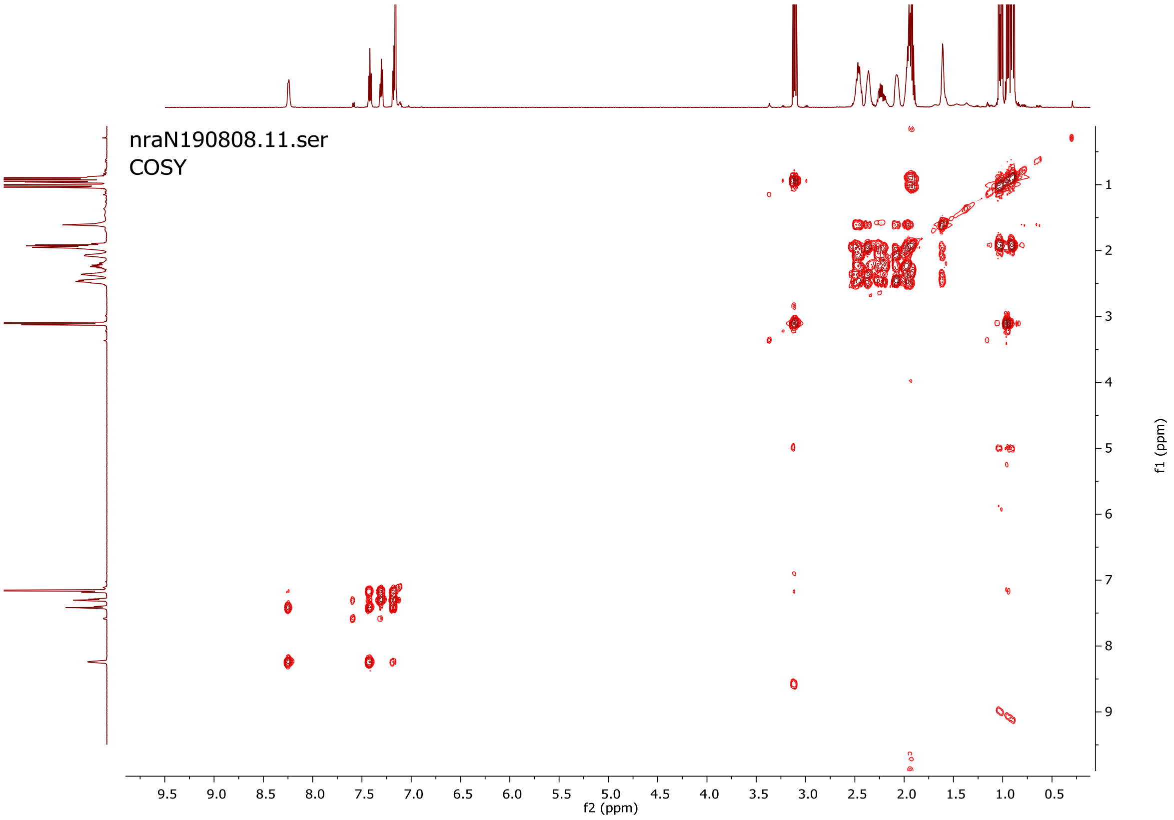

Figure S3. COSY: ^1H / ^1H NMR spectrum of **1a** at 298 K in C_6D_6.

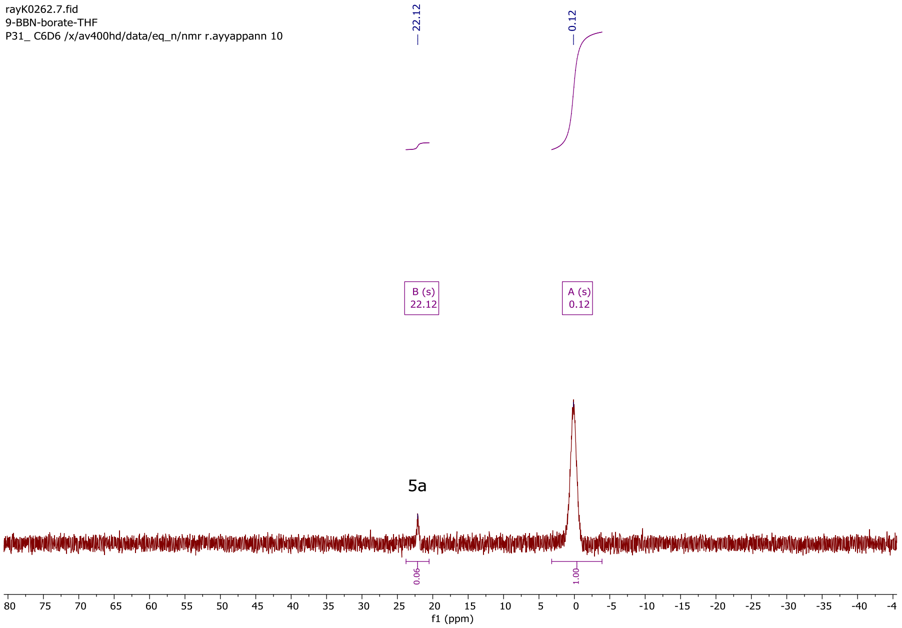

Figure S4. ^{31}P NMR spectrum of **1a** in C_6D_6 at 298 K. with the detection of [*o*-$^iPr_2P-C_6H_4-B(C_8H_{14})$] (P-BBN, **5a**) as a result of partial evolution.

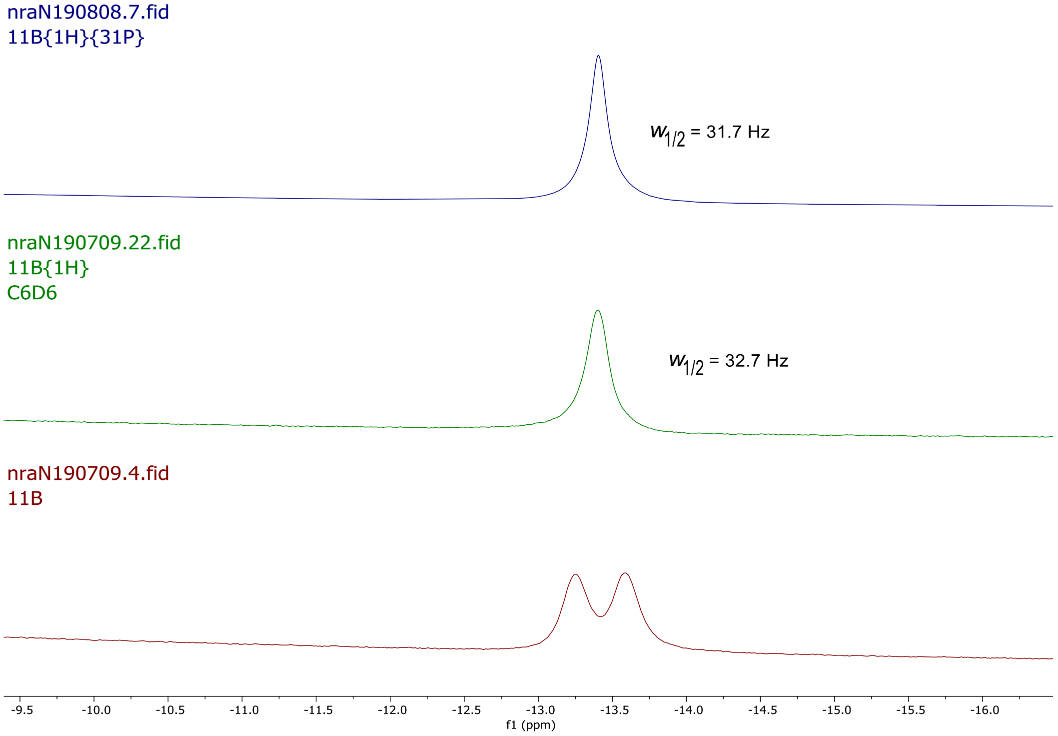

Figure S5. ^{11}B NMR spectral stack plot of **1a** upon decoupling ^{1}H and ^{31}P at 298 K in C_6D_6.

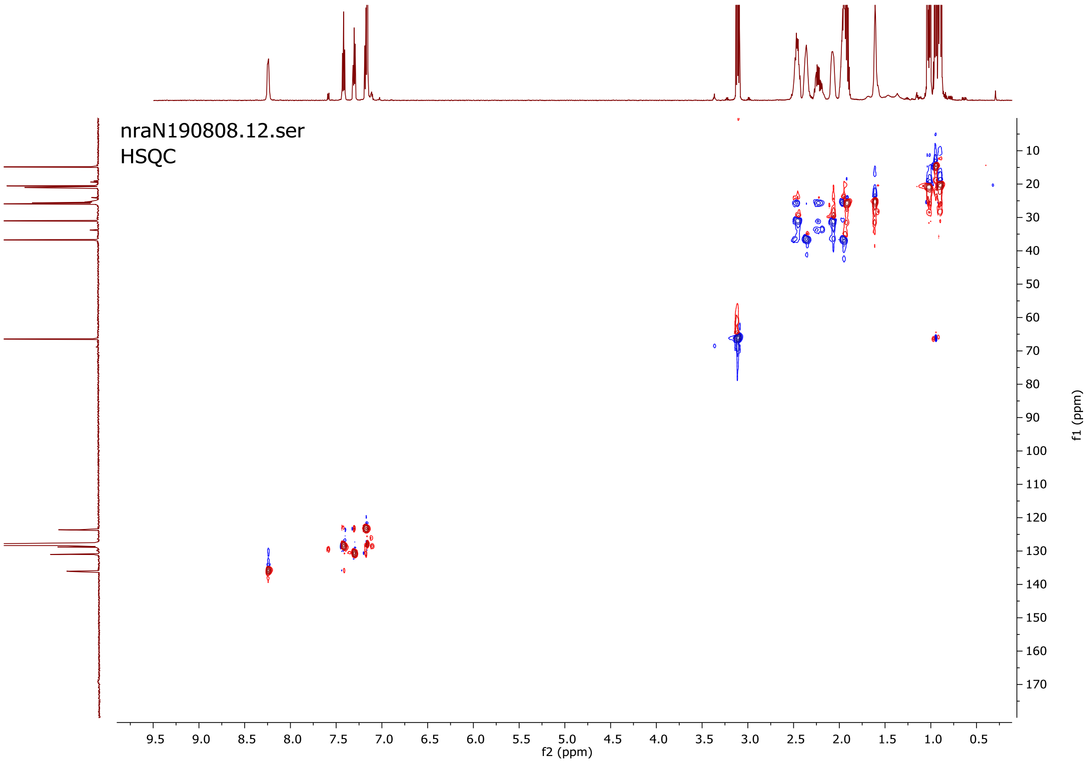

Figure S6. ^{1}H-^{13}C{^{1}H} HSQC spectrum of **1a** at 298 K in C_6D_6.

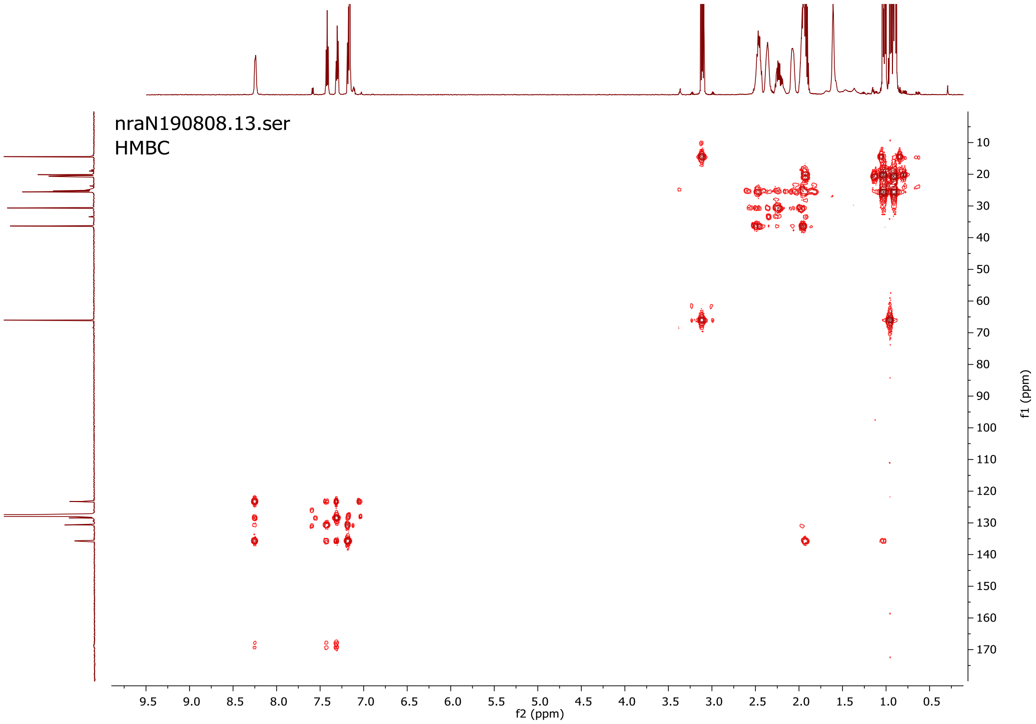

Figure S7. ^{1}H-$^{13}C\{^{1}H\}$ HMBC spectrum of **1a** at 298 K in C_6D_6.

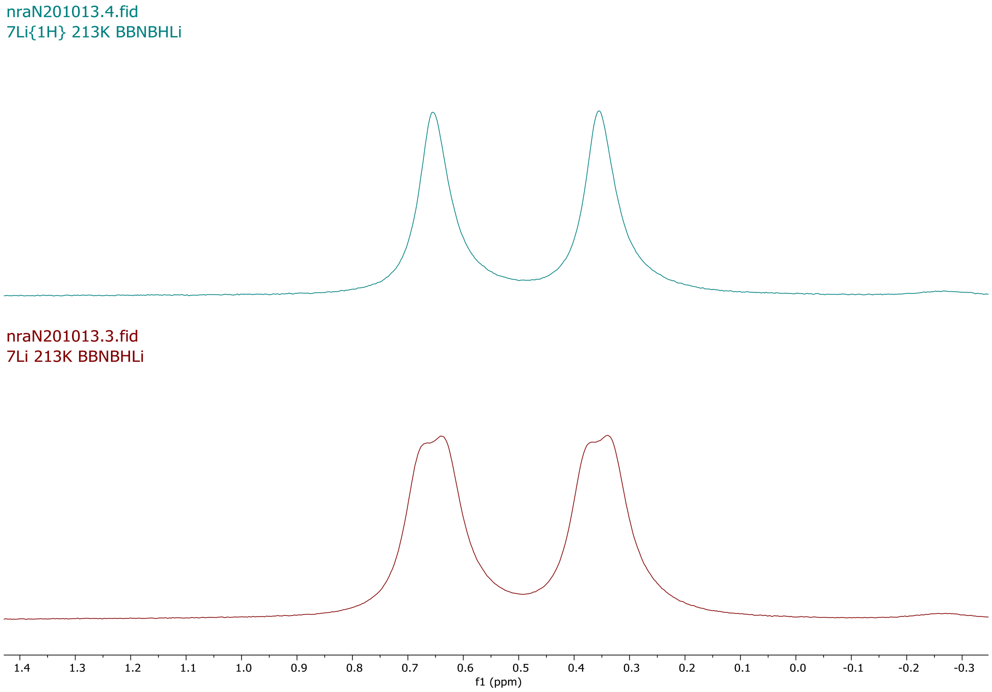

Fig S8. ^{7}Li and $^{7}Li\{^{1}H\}$ NMR spectral stack plot of **1a** in tol-d_8 at 233 K.

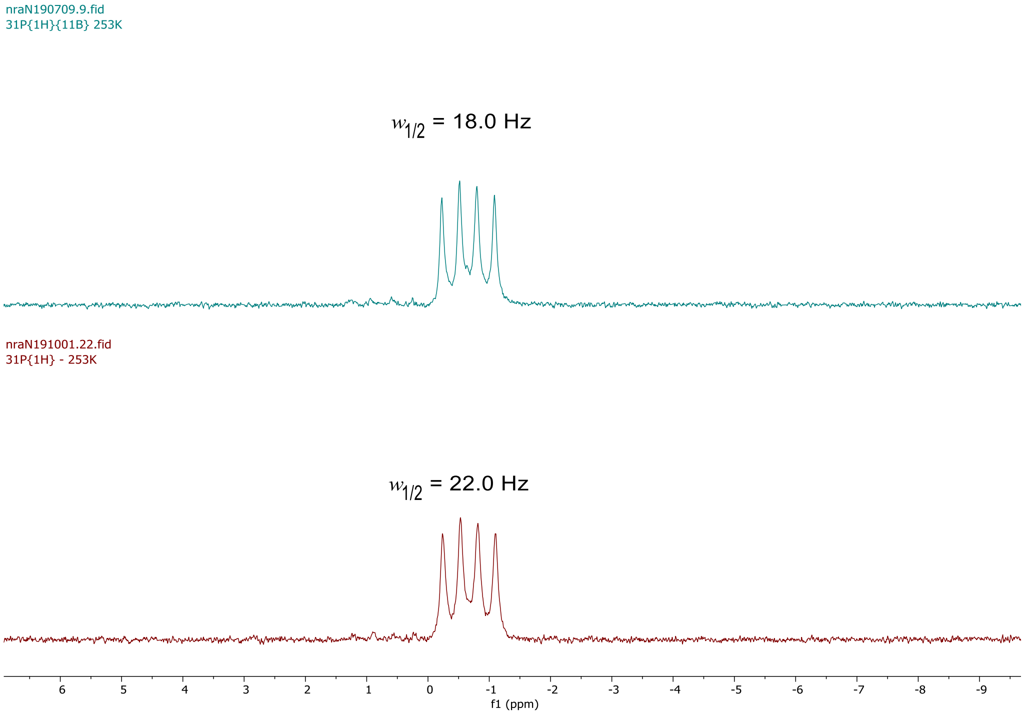

Figure S9. ^{31}P{^{1}H} and ^{31}P{^{11}B}{^{1}H} NMR spectral stack plot of **1a** in tol-d_8 at 253 K. The change in $w_{1/2}$ is 4.0 Hz.

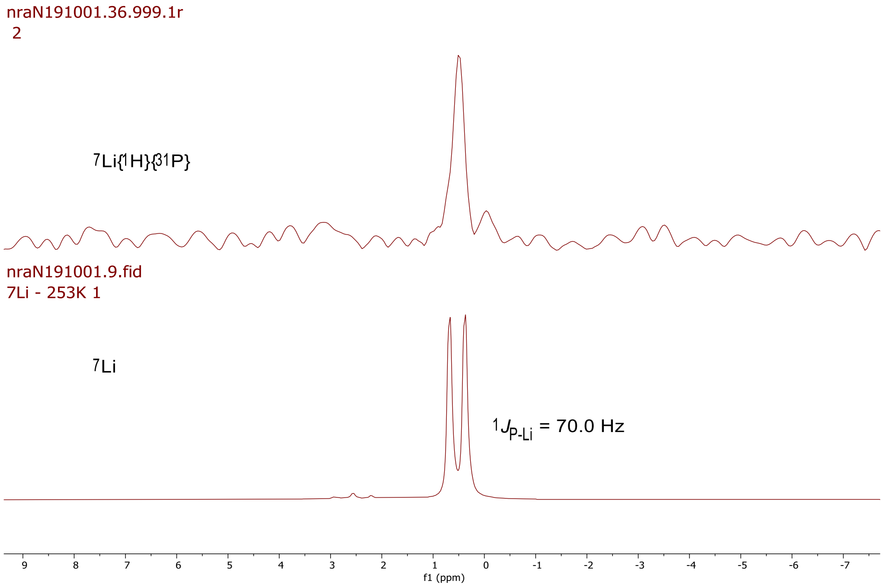

Figure S10. ^{7}Li and ^{7}Li{^{1}H}{^{31}P} stack plot of spectra of **1a** in tol-d_8 at 253 K.

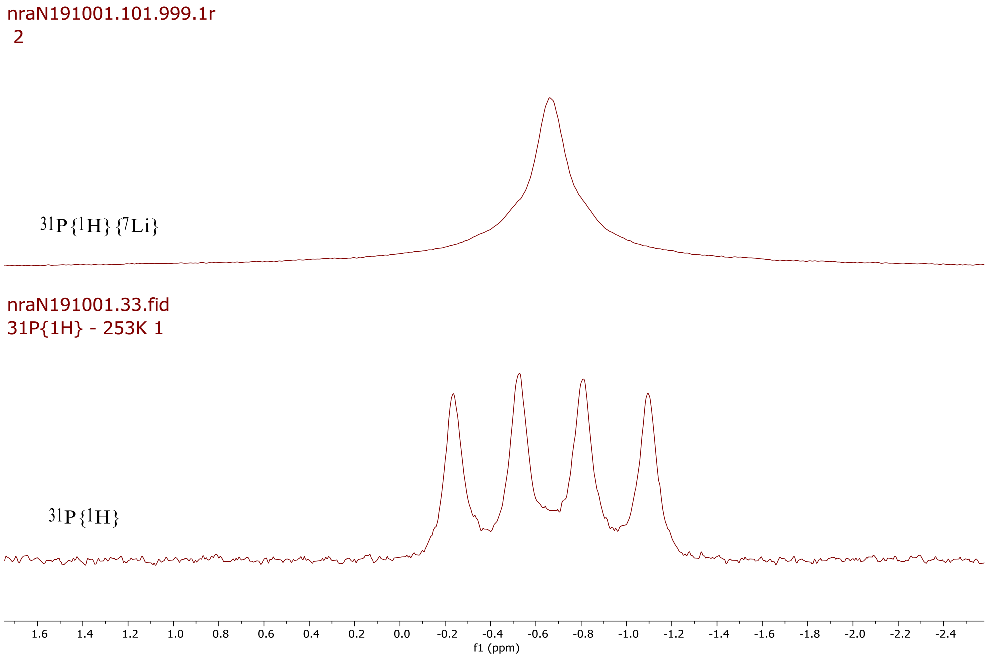

Figure S11. $^{31}P\{^1H\}$ and $^{31}P\{^1H\}\{^7Li\}$ overlapped spectra of **1a** in tol-d_8 at 253 K.

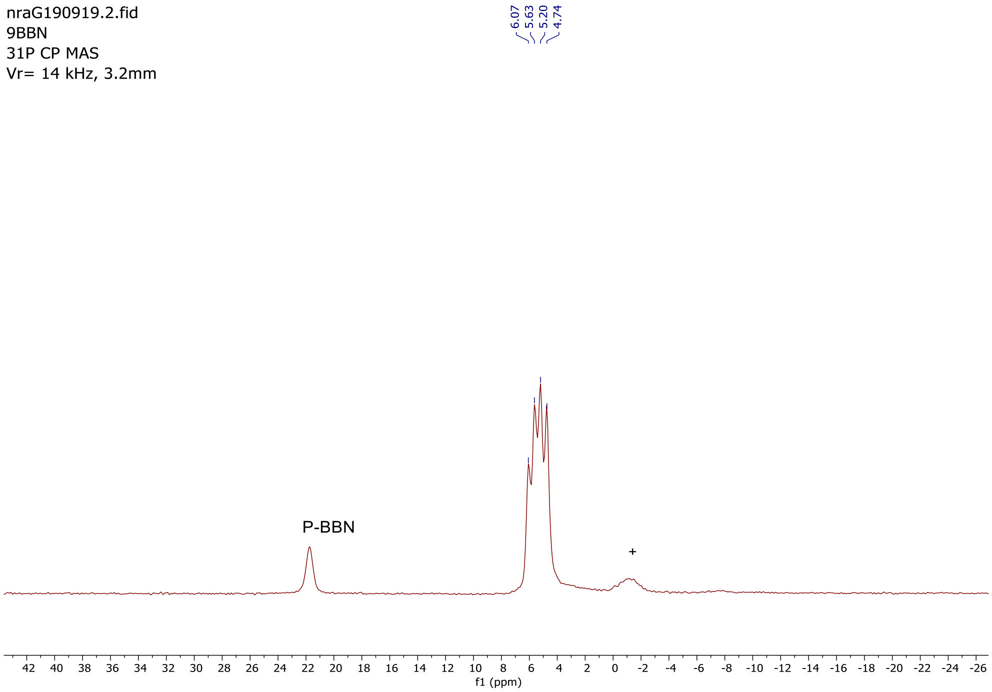

Figure S12. $^{31}P\{^1H\}$ CP MAS NMR spectrum of **1a** at 298 K. Peak marked '+' is arising due to decomposition of **1a**.

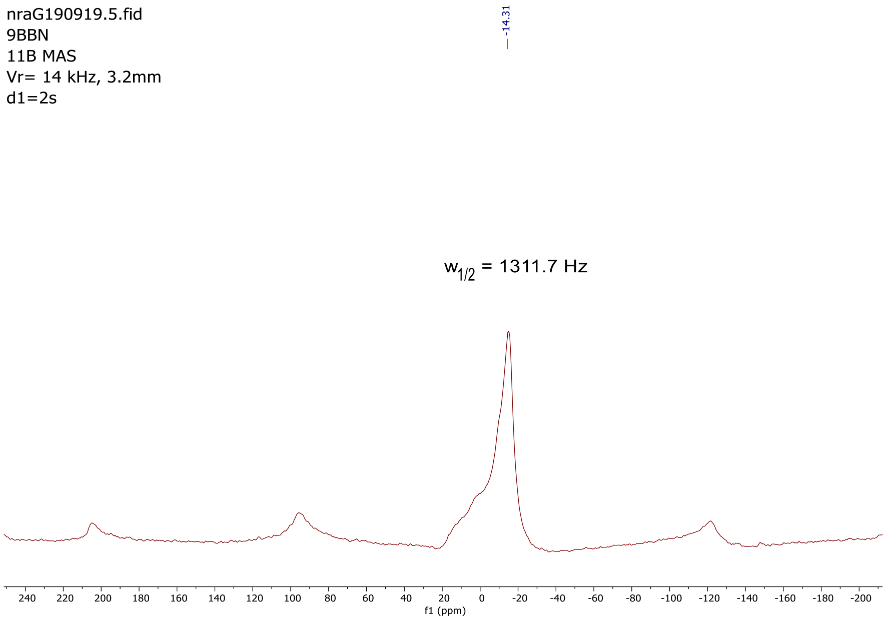

Figure S13. $^{11}B\{^{1}H\}$ MAS NMR spectrum of **1a** at 298 K.

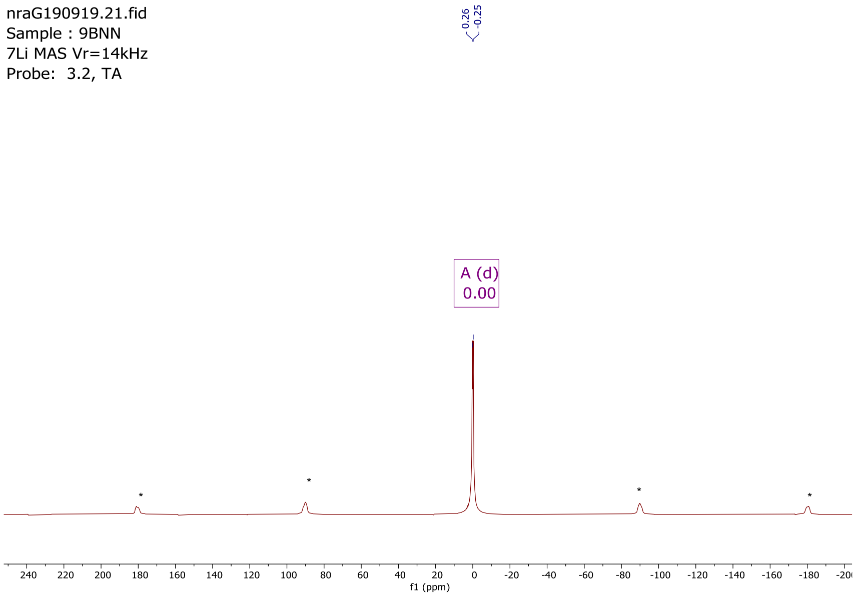

Figure S14. ^{7}Li MAS NMR spectrum of **1a** at 298 K. *-spinning side bands.

3. $[\mathrm{Li(THF)}]^+[o\text{-}{}^i\mathrm{Pr_2P\text{-}C_6H_4\text{-}B(Mes_2)\text{-}H}]^-$ (1b)

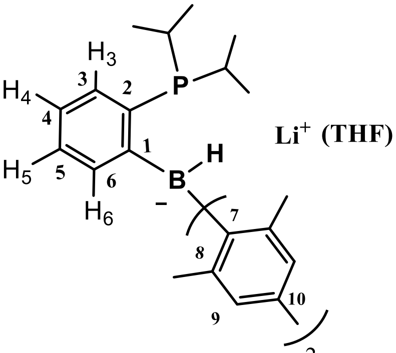

(1b)

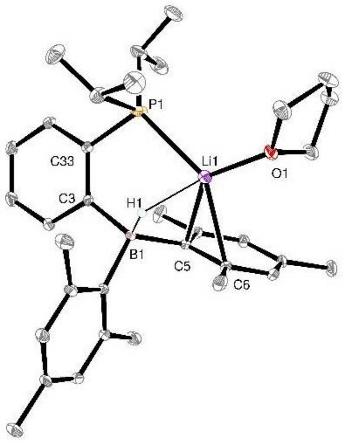

Mes$_2$B-H dimer (0.984 g, 1.97 mmol) and *o*-Li(0.9 Et$_2$O)-C$_6$H$_4$-P^{i}Pr$_2$ (1.05 g, 3.94 mmol) were stirred at rt in THF (20 mL) for 3 h under an argon atmosphere. Then the solvent volume was reduced to about 5 mL under vacuum. The product was precipitated by addition of *n*-pentane, and washed with *n*-pentane (3 x 10 mL). The solid was dried under vacuum before isolating it as a white powder (1.5 g, 2.87 mmol, 73 %). Monocrystals suitable for X-ray analysis were grown in n-pentane at –20 °C. Compound **1b** features one molecule of THF coordinated to Li$^+$ as shown in the crystal structure as well as by ^{1}H NMR.

^{1}H NMR (400.18 MHz, 298 K, THF-*d*$_8$): δ 7.08 (dd, $^3J_{\text{H-H}}$ = 7.6 Hz, $^3J_{\text{H-P}}$ = 1.6 Hz, 1H, H3), 7.06 (br d, overlapping with H3, $^3J_{\text{H-H}}$ = 7.4 Hz, 1H, H6), 6.68 (td, $^3J_{\text{H-H}}$ = 7.3 Hz, $^4J_{\text{H-H}}$ = 1.6 Hz, 1H, H4), 6.65 (td, $^3J_{\text{H-H}}$ = 7.2 Hz, $^4J_{\text{H-H}}$ = 1.3 Hz, 1H, H5), 6.34 (s, 4H, H$_{\text{aro}}$(Mes)), 4.05 (quart, $^1J_{\text{B-H}}$ = 77.9 Hz, 1H, B-H), 2.08 (s, 6H, *p*-CH$_3$(Mes)), 2.02 (dseptet, $^3J_{\text{H-H}}$ = 7.2 Hz, $^2J_{\text{H-P}}$ = 2.5 Hz, 2H, CH(iPr)), 1.89 (s, 12H, *o*-CH$_3$(Mes)), 0.99 (dd, $^3J_{\text{H-P}}$ = 9.5 Hz, $^3J_{\text{H-H}}$ = 6.9 Hz, 6H, CH$_3$(^{i}Pr)), 0.93 (dd, $^3J_{\text{H-P}}$ = 13.4 Hz, $^3J_{\text{H-H}}$ = 7.1 Hz, 6H, CH$_3$(^{i}Pr)).

^{1}H NMR (600.47 MHz, 298 K, C$_6$D$_6$): δ 7.82 (ddd, $^3J_{\text{H-H}}$ = 6.8 Hz, $^3J_{\text{H-P}}$ = 4.0 Hz, $^4J_{\text{H-H}}$ = 1.7 Hz, 1H, H6), 7.29 (ddd, $^3J_{\text{H-P}}$ = 6.8 Hz, $^3J_{\text{H-P}}$ = 4.8 Hz, $^4J_{\text{H-H}}$ = 1.7 Hz, 1H, H3), 7.14 (td, $^3J_{\text{H-H}}$ = 7.2 Hz, $^4J_{\text{H-H}}$ = 1.5 Hz, 2H, H4 & H5 overlapping with C$_6$D$_6$ signal), 7.05 (s, 1H, H$_{\text{aro}}$(Mes)), 6.72 (s, 1H, H$_{\text{aro}}$(Mes)), 6.66 (s, 1H, H$_{\text{aro}}$(Mes)), 3.68 (quart, $^1J_{\text{B-H}}$ = 65.0 Hz, 1H, B-H), 2.65 (s, 3H, *o*-CH$_3$(Mes)), 2.41 (s, 3H, *o*-CH$_3$(Mes)), 2.24 (s, 3H, *o*-CH$_3$(Mes)), 2.11 (s, 6H, *p*-CH$_3$(Mes)), 2.04 (s, 3H, *p*-CH$_3$(Mes)), 2.07 (m, $^3J_{\text{H-H}}$ & $^2J_{\text{H-P}}$ were not identified due to overlap with CH$_3$(Mes), 2H, CH(iPr)), 1.09 (s, 6H, overlap with THF, $J_{\text{H-P}}$ and $J_{\text{H-H}}$ could not identified), 0.98 (dd, $^3J_{\text{H-P}}$ = 15.1 Hz, $^3J_{\text{H-H}}$ = 7.0 Hz, 3H, CH$_3$(^{i}Pr)), 0.92 (dd, $^3J_{\text{H-P}}$ = 14.0 Hz, $^3J_{\text{H-H}}$ = 6.7 Hz, 3H, CH$_3$(^{i}Pr)).

Note: Among the four aromatic Mes protons, only three were identified. The last signal is overlapping with C$_6$D$_6$ signal.

^{31}P{^{1}H} NMR (162.01 MHz, 298 K, THF-*d*$_8$): δ 1.2 (quart, $J_{\text{B-P}}$ = 16.7 Hz)

^{31}P{^{1}H} NMR (243.07 MHz, 298 K, C$_6$D$_6$): δ 0.52 (quart, $^1J_{\text{P-Li}}$ = 74.9 Hz)

^{11}B NMR (128.39 MHz, 298 K, THF-d_8): δ –14.0 (dd, $^1J_{\text{B-H}}$ = 78.3, $J_{\text{B-P}}$ = 17.0 Hz)

^{11}B NMR (192.65 MHz, 298 K, C_6D_6): δ –12.2 (dd, $^1J_{\text{B-H}}$ = 67.0, $J_{\text{B-P}}$ = 11 Hz)

^{13}C{^{1}H} NMR (151.00, 298 K, THF-d_8): δ 174.2 (br quart, C1), 159.8 (quart, $^1J_{\text{C-B}}$ = 51.4 Hz, C7), 143.6 (d, $^1J_{\text{C-P}}$ = 13.9 Hz, C2), 143.4 (s, C8), 137.0 (d, $^2J_{\text{C-P}}$ = 9.4 Hz, C3), 129.2 (s, C10), 128.8 (s, C6), 127.8 (s, C9), 125.8 (s, C5), 121.6 (s, C4), 25.8 (s, *o*-CH_3(Mes)), 24.6 (d, $^1J_{\text{C-P}}$ = 20.8 Hz, CH(^{i}Pr)), 22.4 (d, $^2J_{\text{C-P}}$ = 21.9 Hz, CH_3(^{i}Pr)), 21.6 (s, *p*-CH_3(Mes)), 20.0 (d, $^2J_{\text{C-P}}$ = 13.5 Hz, CH_3(^{i}Pr)).

^{7}Li NMR (155.53, 298 K, THF-d_8): δ 0.5 (s)

^{7}Li NMR (233.37, 298 K, C_6D_6): δ –0.4 (d, $^1J_{\text{P-Li}}$ = 73.0 Hz, $^1J_{\text{Li-H}}$ = 5.0 Hz).

^{7}Li MAS NMR (155.53, 298 K): δ −0.9 (d, $^1J_{\text{P-Li}}$ = 72.1 Hz).

^{31}P{^{1}H} MAS (161.76 MHz, 298 K): δ 0.8 (quart, $^1J_{\text{P-Li}}$ = 72.2 Hz).

HRMS ESI: Calc: 443.3039 ($C_{30}H_{41}BP$), found: 443.3040.

Anal. cald. for $C_{30}H_{41}BLiP \cdot 2THF$: C, 76.76; H, 9.66. Found: C, 76.83; H, 9.05.

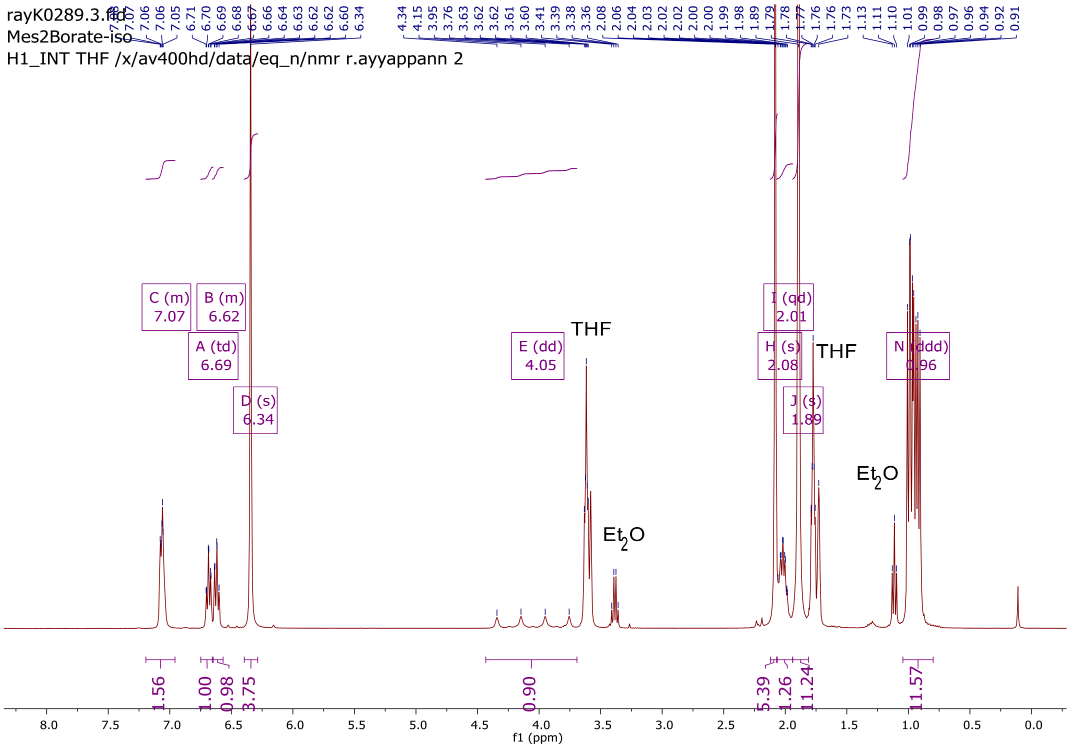

Figure S15. ^{1}H NMR spectrum of phosphine borate compound **1b** in THF-d_8 at 298 K.

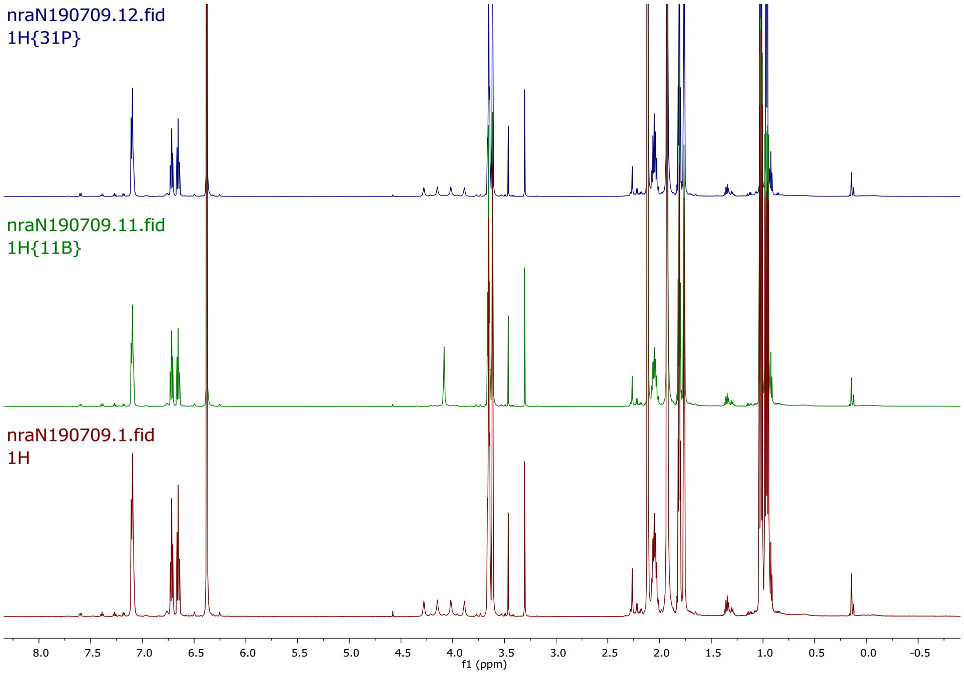

Figure S16. ^{1}H, ^{1}H{^{11}B} and ^{1}H{^{31}P} NMR spectral stack plot of **1b** in THF-d_8 at 298 K.

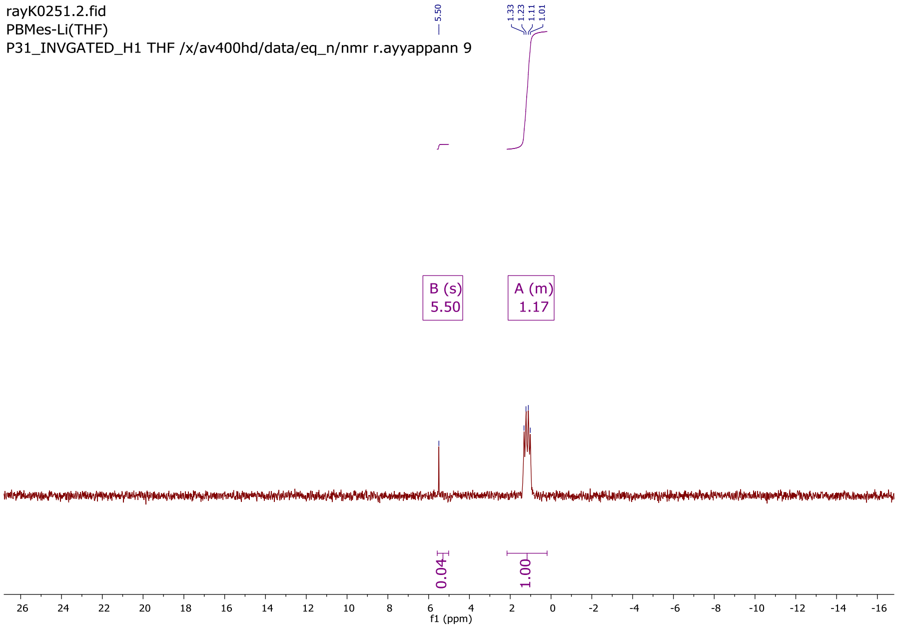

Figure S17. ^{31}P_INVAGATED_^{1}H NMR spectrum of **1b** at 298 K in THF-d_8 for the integration of the presence of **5b** **(**o-^{i}Pr$_2$P-C$_6$H$_4$-B(Mes$_2$)**)**.

Note: Low temperature NMR spectra recorded for **1b** at 213 K are the same as the 298 K spectra.

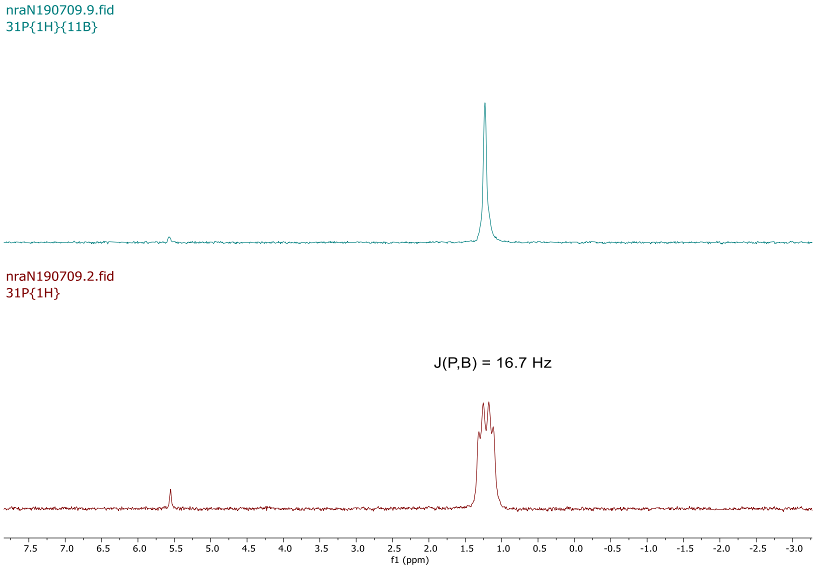

Figure S18. $^{31}P\{^{1}H\}$ and $^{31}P\{^{11}B\}\{^{1}H\}$ NMR spectral stack plot of **1b** in THF-d_8 at 298 K.

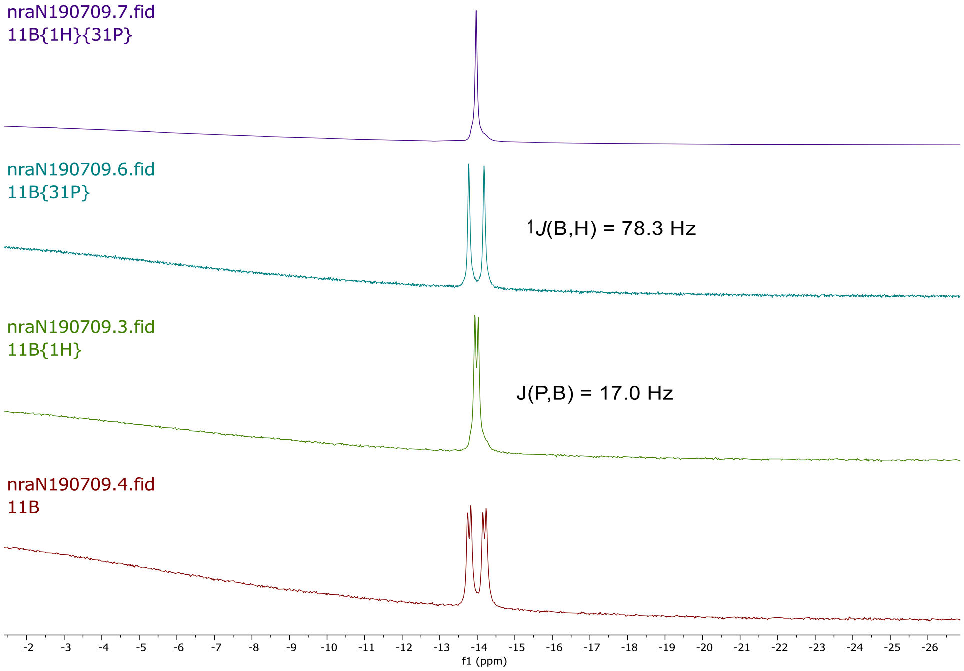

Figure S19. ^{11}B NMR spectral stack plot of **1b** upon decoupling ^{1}H and ^{31}P at 298 K in THF-d_8.

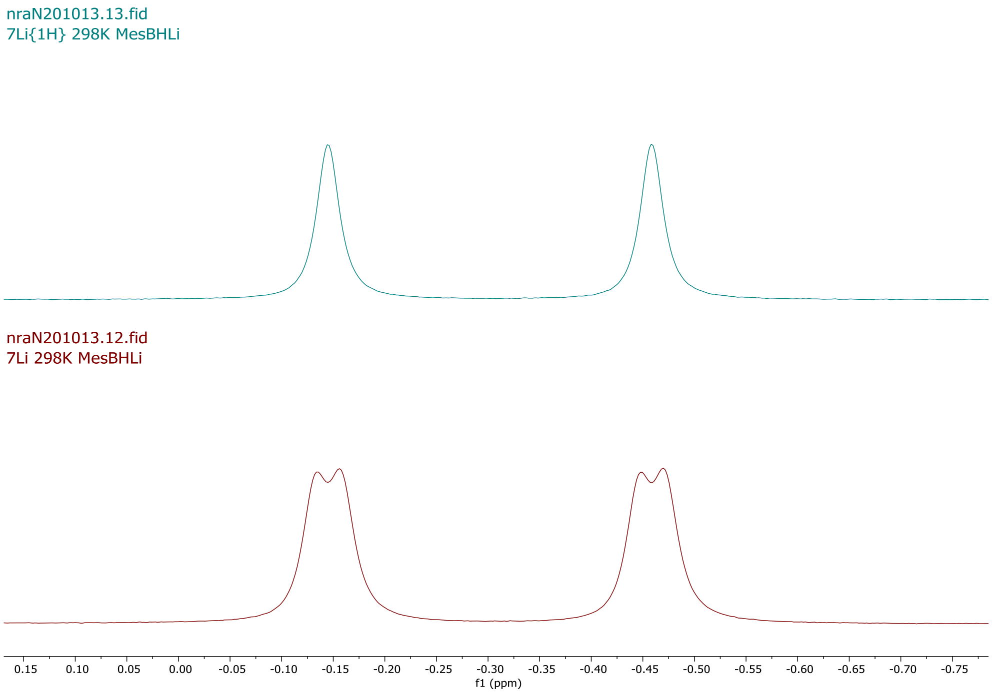

Figure S20. ^{7}Li and ^{7}Li{^{1}H} NMR spectral stack plot of **1b** at 298 K in tol-d_8.

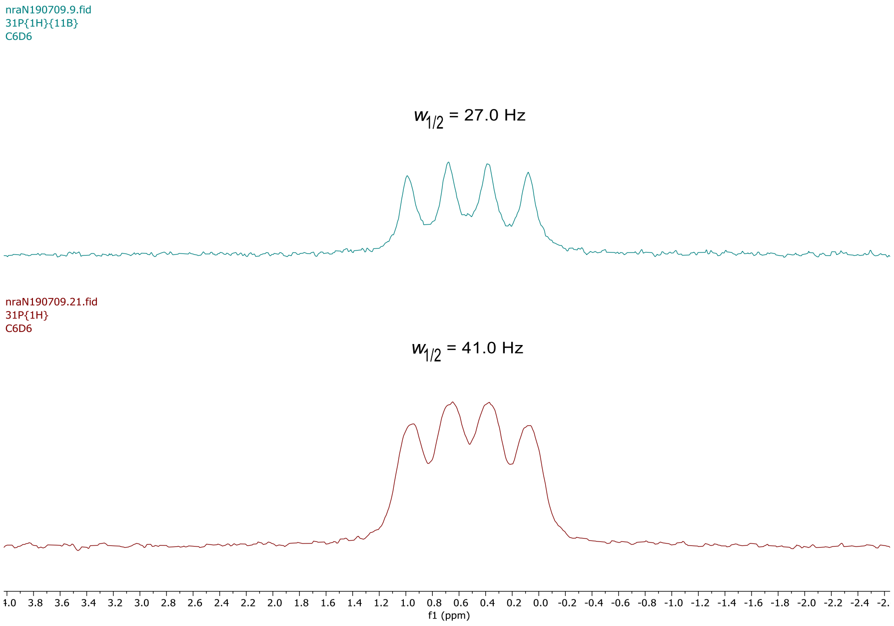

Figure S21. ^{31}P{^{1}H} and ^{31}P{^{1}H}{^{11}B} stack plot of spectra of **1b** in C_6D_6 at 298 K. The change in $w_{1/2}$ – 14.0 Hz.

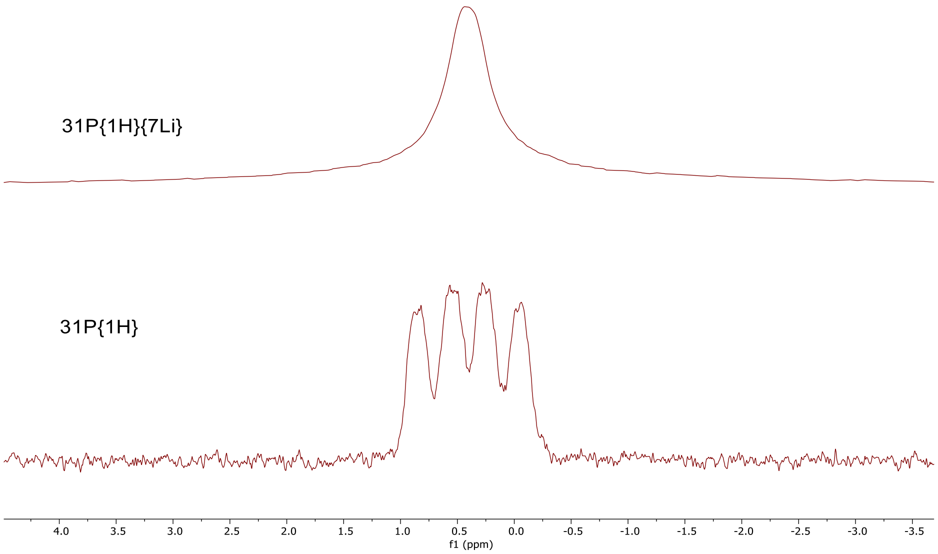

Figure S22. $^{31}P\{^{1}H\}$ and $^{31}P\{^{1}H\}\{^{7}Li\}$ stack plot of spectra of **1b** in C_6D_6 at 298 K.

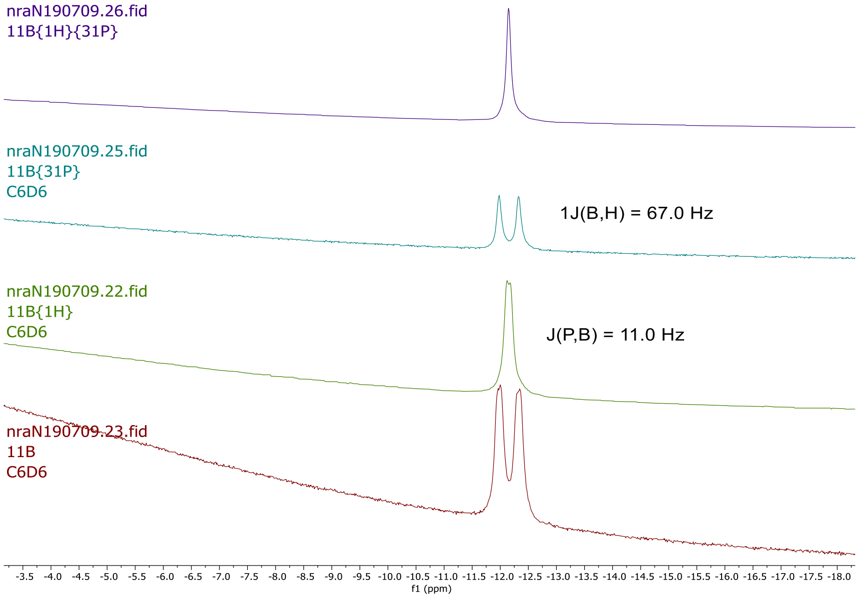

Figure S23. ^{11}B NMR spectral stack plot of **1b** upon decoupling ^{1}H and ^{31}P at 298 K in C_6D_6.

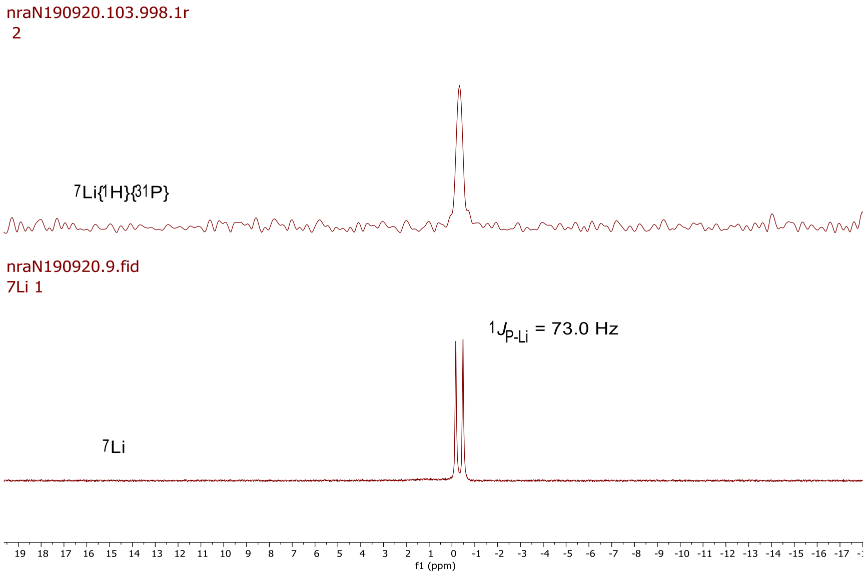

Figure S24. ^{7}Li and ^{7}Li{^{1}H}{^{31}P} stack plot of spectra of **1b** in tol-d_8 at 298 K.

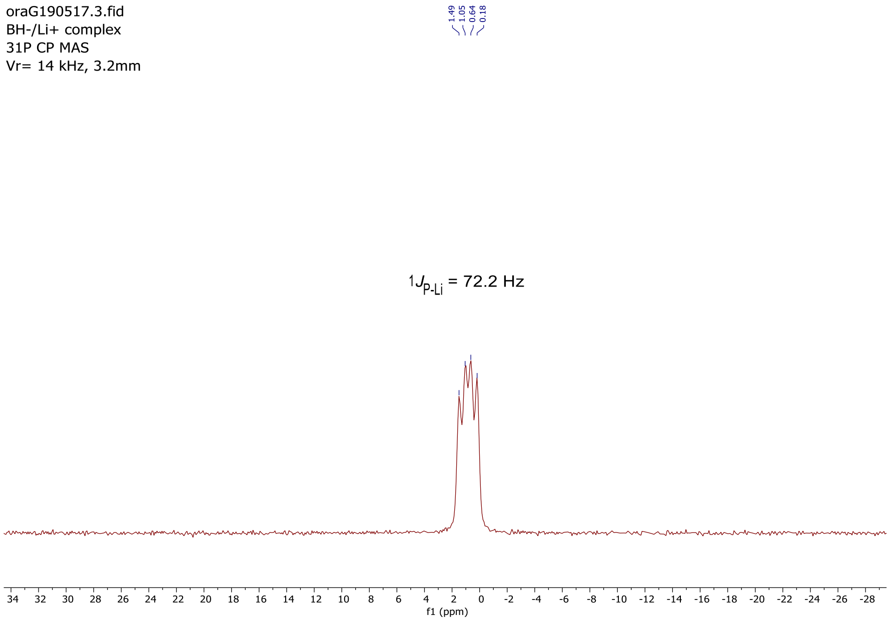

Figure S25. ^{31}P{^{1}H} CPMAS NMR spectrum of **1b** at 298 K.

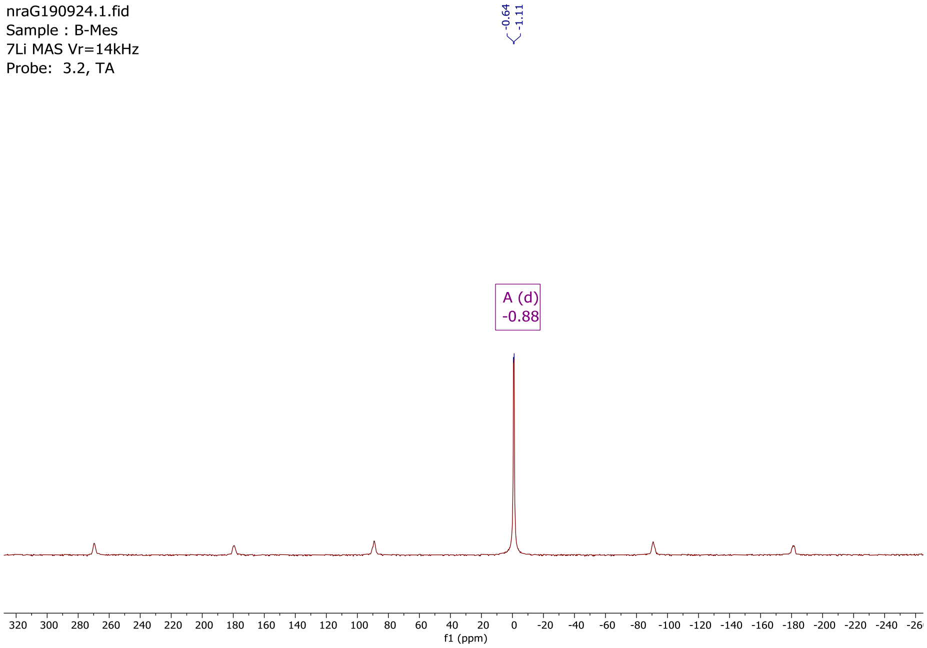

Figure S26. ^{7}Li MAS NMR spectrum of **1b** at 298 K.

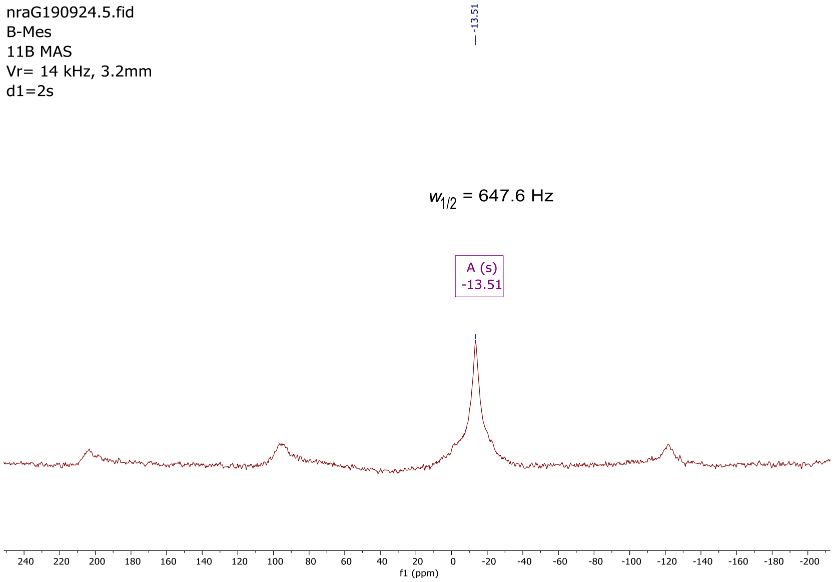

Figure S27. ^{11}B{^{1}H} MAS spectrum of **1b** at 298 K.

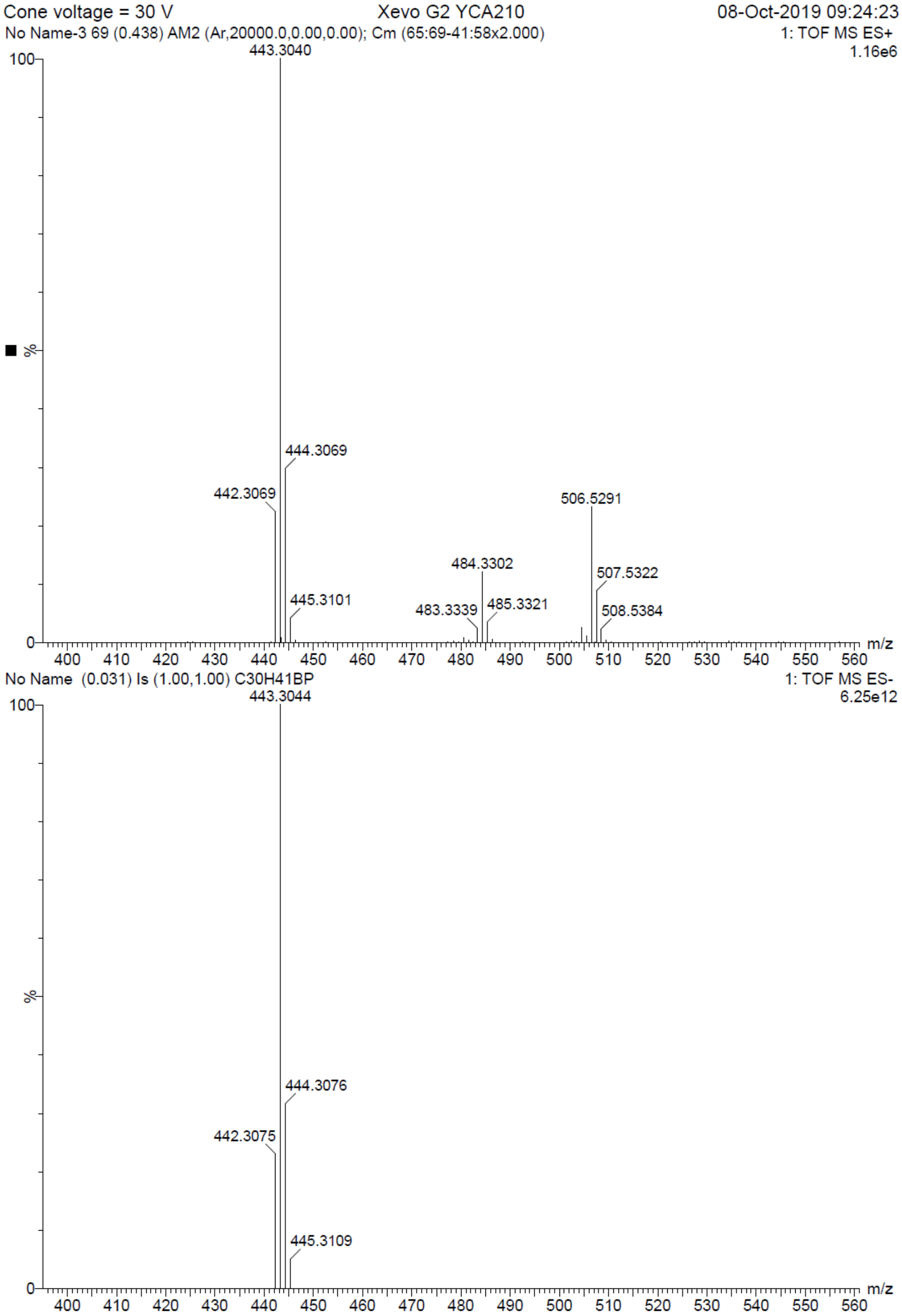

Figure S28. HRMS ESI spectrum of compound **1b**.

4. [Li$^+$(THF)$_2$][*o*-iPr$_2$P-C$_6$H$_4$-B(Ipc)$_2$-H]- (1c)

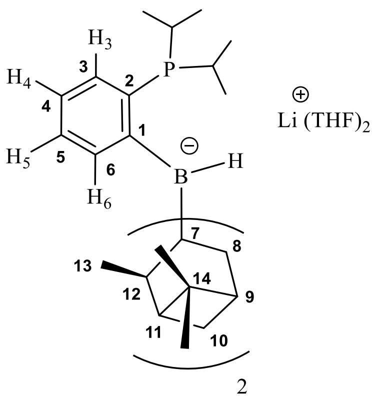

(**1c**)

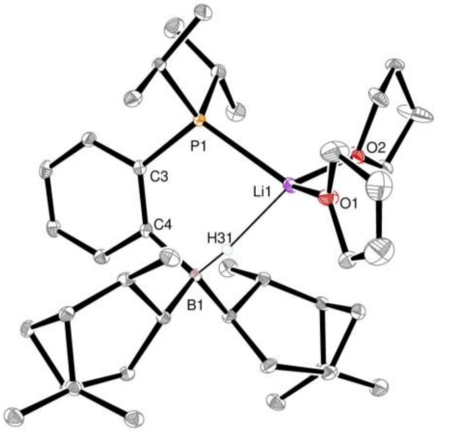

Diisopinocampheylborane (0.414 g, 1.45 mmol) and *o*-Li(0.9 Et$_2$O)-C$_6$H$_4$-P^{i}Pr$_2$ (0.386 g, 1.45 mmol) were stirred at 298 K in toluene (10 mL) for 2 h under an argon atmosphere. Toluene was removed under vacuum. THF (3 mL) was added. Slow evaporation of THF under an argon atmosphere resulted in the formation of an oil. The supernatant was carefully filtered. Storage of the oil at –35°C in n-pentane (20 mL) resulted in the formation of a white precipitate. The colourless precipitate was separated and dried under vacuum. (0.660 g, 73 %). Monocrystals suitable for X-ray diffraction were obtained in n-pentane at –35 °C upon standing for 72 h.

^{1}H NMR (600.47 MHz, 298 K, THF-*d*$_8$): δ 7.66 (ddd, $^3J_{H\text{-}H}$ = 7.4 Hz, $^4J_{H\text{-}P}$ = 3.4 Hz, $^4J_{H\text{-}H}$ = 1.6 Hz, 1H, H3), 7.07 (dt, $^3J_{H\text{-}H}$ = 7.7 Hz, $^4J_{H\text{-}H}$ = 1.7 Hz, 1H, H6), 6.76 (td, $^3J_{H\text{-}H}$ = 7.2 Hz, $^4J_{H\text{-}P}$ = 1.4 Hz, 1H, H4), 6.64 (td, $^3J_{H\text{-}H}$ = 7.3 Hz, $^4J_{H\text{-}H}$ = 1.5 Hz, 1H, H5), 2.44 (quart, $^1J_{B\text{-}H}$ = 81.3 Hz, 1H, B-H), 2.12 (m, $^3J_{H\text{-}H}$ = 6.0 Hz, $^4J_{H\text{-}H}$ = 2.9 Hz, 2H, CH + CH$_2$ (1H diastero)), 2.01 (m, 4H, $^2J_{H\text{-}P}$ = 15.9 Hz, $^3J_{H\text{-}H}$ = 7.2 Hz, $^4J_{H\text{-}H}$ = 2.9 Hz, CH(^{i}Pr) overlap with C-H(Ipc) + CH$_2$ (1H diastereo)), 1.91 (m, 2H, $^3J_{H\text{-}H}$ = 6.2 Hz, $^4J_{H\text{-}H}$ = 3.6 Hz, C-H(Ipc) + CH$_2$ (1H diastereo)), 1.78 (m, 2H, C-H(Ipc) + CH$_2$ (1H diastereo) overlapping), 1.61 (m, 2H, $^3J_{H\text{-}H}$ = 6.2 Hz, $^4J_{H\text{-}H}$ = 3.6 Hz, C-H(Ipc) + CH$_2$ (1H diastereo) overlapping), 1.44 (td, 1H, $^3J_{H\text{-}H}$ = 5.9 Hz, $^4J_{H\text{-}H}$ = 2.2 Hz, C-H(Ipc)), 1.37 (d, 1H, $^3J_{H\text{-}H}$ = 8.0 Hz, CH$_2$ (1H diastereo)), 1.36 (td, 1H, $^3J_{H\text{-}H}$ = 5.8 Hz, $^4J_{H\text{-}H}$ = 2.2 Hz, CH(Ipc)), 1.13 (d, 6H, $^3J_{H\text{-}H}$ = 3.9 Hz, CH$_3$(Ipc)), 1.09 (s, 3H, CH$_3$(Ipc)), 1.08 (s, 3H, CH$_3$(Ipc)), 1.07 (dd, 3H, $^3J_{H\text{-}P}$ = 12.0 Hz, $^3J_{H\text{-}H}$ = 7.0 Hz, CH$_3$(^{i}Pr)), 1.01 (s, 3H, CH$_3$(Ipc)), 1.01 (dd, 3H, $^3J_{H\text{-}P}$ = 10.5 Hz, $^3J_{H\text{-}H}$ = 7.2 Hz, CH$_3$(^{i}Pr)), 0.99 (dd, 3H, $^3J_{H\text{-}P}$ = 11.0 Hz, $^3J_{H\text{-}H}$ = 7.2 Hz, CH$_3$(^{i}Pr)), 0.93 (dd, 3H, $^3J_{H\text{-}P}$ = 12.2 Hz, $^3J_{H\text{-}H}$ = 7.0 Hz, CH$_3$(^{i}Pr)), 0.63 (d, 3H, $^3J_{H\text{-}H}$ = 7.2 Hz, CH$_3$(Ipc)), 0.24 (d, $^3J_{H\text{-}H}$ = 7.7 Hz, CH$_2$ (1H diastereo)).

Notes: one CH$_3$(^{i}Pr) and two CH$_3$(Ipc) signals are overlapping at δ 1.08 ppm: CH + CH$_2$(diastereo) signals are overlapping at δ 1.37 ppm: CH + CH$_2$(diastereo) signals are overlapping at δ 1.61: In total, all CH of CH$_2$ signals are diastereotopic, so eight different sets of signals were found: CH (chiral group) + CH$_2$ (diastero) accounting 2H is buried inside THF signal at δ 1.78 ppm.

^{1}H NMR (600.47 MHz, 298 K, C$_6$D$_6$): δ 8.20 (ddd, $^3J_{H\text{-}H}$ = 7.8 Hz, $^4J_{H\text{-}P}$ = 3.8 Hz, $^4J_{H\text{-}H}$ = 1.5 Hz, 1H, H3), 7.40 (tt, $^3J_{H\text{-}H}$ = 7.3 Hz, $^4J_{H\text{-}H}$ = 1.4 Hz, 1H, H4), 7.29 (ddd, $^3J_{H\text{-}H}$ = 7.8 Hz, $^4J_{H\text{-}P}$ = 4.6 Hz, $^4J_{H\text{-}P}$ = 1.4 Hz, 1H, H6), 7.18 (td, $^3J_{H-H}$ = 7.8 Hz, $^4J_{H-H}$ = 1.4 Hz, 1H, H5), 2.57 (t, $^3J_{H-H}$ = 10.7 Hz, 1H, CH), 2.39 (dd, 2H, $^3J_{H-H}$ = 7.6 Hz, $^4J_{H-H}$ = 2.8 Hz, C-H(Ipc)), 2.34 (m, 1H, $^3J_{H-H}$ = 8.3 Hz, $^4J_{H-H}$ = 1.8 Hz, C-H(Ipc)), 2.17 (m, 2H, $^3J_{H-H}$ = 8.3 Hz, C-H(Ipc)), 2.14 (m, 1H, $^3J_{H-H}$ = 5.8 Hz, C-H(Ipc)), 1.98 (dsept, 2H, $^2J_{H-P}$ = 9.2 Hz, $^3J_{H-H}$ = 4.6 Hz, C-H(iPr)), 1.92 (td, 2H, $^3J_{H-H}$ = 5.7 Hz, $^4J_{H-H}$ = 1.8 Hz, CH), 1.69 (m, 1H, CH(Ipc)), 1.51 (s, 3H, CH_3(Ipc)), 1.46 (s, 3H, CH_3(Ipc)), 1.39 (d, $^3J_{H-H}$ = 7.1 Hz, 3H, CH_3(Ipc)), 1.36 (s, 3H, CH_3(Ipc)), 1.34 (s, 3H, CH_3(Ipc)), 1.28 (d, 3H, $^3J_{H-H}$ = 7.1 Hz, CH_3(Ipc)), 1.05 (dd, 6H, $^3J_{H-P}$ = 15.5 Hz, $^3J_{H-H}$ = 6.8 Hz, two CH_3(^{i}Pr) group overlap), 0.99 (dd, 6H, $^3J_{H-P}$ = 11.6 Hz, $^3J_{H-H}$ = 7.2 Hz, two CH_3(^{i}Pr) group overlap), 0.82 (d, 1H, $^3J_{H-H}$ = 8.5 Hz, CH_2 (1H diastereo)), 0.76 (d, $^3J_{H-H}$ = 8.5 Hz, CH_2 (1H diastereo)).

Notes: B-H signal was not identified: 8 C-H and 4 CH_2 signals of chiral group are inequivalent. The CH_2 hydrogens are diastereotopic and overlapping with CH signals.

$^{31}P\{^1H\}$ NMR (243.07 MHz, 298.1 K, THF-d_8): δ 1.4 (quart, J_{P-B} = 14.5 Hz)

$^{31}P\{^1H\}$ NMR (243.08 MHz, 298 K, C_6D_6): 2.7 (quart, $^1J_{P-Li}$ = 72.8 Hz)

$^{31}P\{^1H\}$ CPMAS NMR (161.76 MHz, 298 K): δ 0.6 (br s, $w_{1/2}$ – 1400 Hz)

Note: The two signals were attributed to two different orientation of the molecule in the solid state.

^{11}B NMR (192.65 MHz, 298 K, THF-d_8): δ –9.4 (d, $^1J_{B-H}$ = 81.4 Hz)

$^{11}B\{^1H\}$ NMR (192.65 MHz, 298 K, THF-d_8): δ –9.4 (d, J_{B-P} = 13.0 Hz)

$^{11}B\{^1H\}$ NMR (192.65 MHz, 298 K, C_6D_6): δ –4.6 (d, $^1J_{B-H}$ = 64.7 Hz)

$^{13}C\{^1H\}$ NMR (151.00 MHz, 298 K, THF-d_8): δ 175.3 (quart, $^1J_{B-C}$ = 48.1 Hz, C1), 144.3 (d, $^1J_{P-C}$ = 11.2 Hz, C2), 137.6 (d, $^2J_{C-P}$ = 9.3 Hz, C3), 129.1 (s, C6), 124.1 (s, C4), 121.0 (s, C5), 52.6 (s, CH), 51.1 (s, CH), 45.1 (s, CH), 44.9 (s, CH_2), 44.2 (s, CH), 41.5 (s, overlapping CH), 41.0 (s, CH), 40.4 (s, quaternary carbon (Ipc)), 36.6 (s, CH_2), 33.3 (s, CH_2), 33.1 (s, CH_2), 32.8 (s, CH_2), 31.4 (s, quaternary carbon (Ipc)), 29.6 (s, CH_3(Ipc)), 29.4 (s, CH_3(Ipc)), 26.9 (d, $^1J_{P-C}$ = 22.4 Hz, CH(^{i}Pr)), 26.6 (s, CH_3(Ipc)), 24.7 (d, $^1J_{P-C}$ = 21.6 Hz, CH(^{i}Pr)), 24.1 (s, CH_3(Ipc)), 23.8 (s, CH_3(Ipc)), 22.3 (d, $^2J_{P-C}$ = 19.9 Hz, CH_3(^{i}Pr)), 22.0 (d, $^2J_{P-C}$ = 18.0 Hz, CH_3(^{i}Pr)), 21.2 (d, $^2J_{P-C}$ = 21.2 Hz, CH_3(^{i}Pr)), 20.1 (d, $^2J_{P-C}$ = 11.7 Hz, CH_3(^{i}Pr)),

Notes: 2 CH(^{i}Pr) and 4 CH_3(^{i}Pr) carbons on isopropyl group are inequivalent: 8 CH and 4 CH_2 carbons are inequivalent.

^7Li (155.53, 298 K, THF-d_8): δ –0.5 (s)

^7Li NMR (233.37, 298 K, C_6D_6): δ 1.5 (dd, $^1J_{P-Li}$ = 73.0 Hz, $^1J_{Li-H}$ = 11.0 Hz)

^7Li MAS NMR (155.30, 298 K): δ 0.9 (br s, $w_{1/2}$ = 271.0 Hz)

$^{13}C\{^1H\}$ NMR (151.00 MHz, 298 K, C_6D_6): δ 169.3 (br, C1), 138.3 (d, $^1J_{P-C}$ = 11.2 Hz, C3),134.7 (d, $^2J_{C-P}$ = 16.0 Hz, C2), 131.0 (s, C6), 127.4 (s, C4), 123.3 (d, $^4J_{P-C}$ = 3.3 Hz, C5), 51.8 (s, CH), 50.4 (s, CH), 43.8 (s, CH), 43.6 (s, CH), 43.3 (s, CH), 41.3 (s, CH), 40.2 (s, CH), 39.9 (s, C-H), 36.6 (s, CH_2), 34.3 (s, CH2), 33.3 (s, CH_2), 31.7 (s, CH_2), 28.8 (s, CH), 28.6 (s, CH), 25.6 (s, CH), 24.7 (s, CH), 24.6 (d, $^1J_{\text{P-C}}$ = 6.5 Hz, CH(^{i}Pr)), 23.6 (s, CH), 23.5 (s, CH), 21.0 (d, $^2J_{\text{P-C}}$ = 14.2 Hz, CH_3(^{i}Pr)), 20.8 (d, $^2J_{\text{P-C}}$ = 13.4 Hz, CH_3(^{i}Pr)), 20.3 (d, $^2J_{\text{P-C}}$ = 6.9 Hz, CH_3(^{i}Pr)), 20.2 (d, $^2J_{\text{P-C}}$ = 6.8 Hz, CH_3(^{i}Pr)).

Anal. cald. for $C_{32}H_{53}BLiP{\cdot}4THF$: C, 74.40; H, 11.06. Found: C, 74.44; H, 10.58. The presence of four THF molecules was confirmed by ^{1}H NMR spectroscopy.

Specific optical rotation $[\alpha]_D^{25}$ = + 48.0°

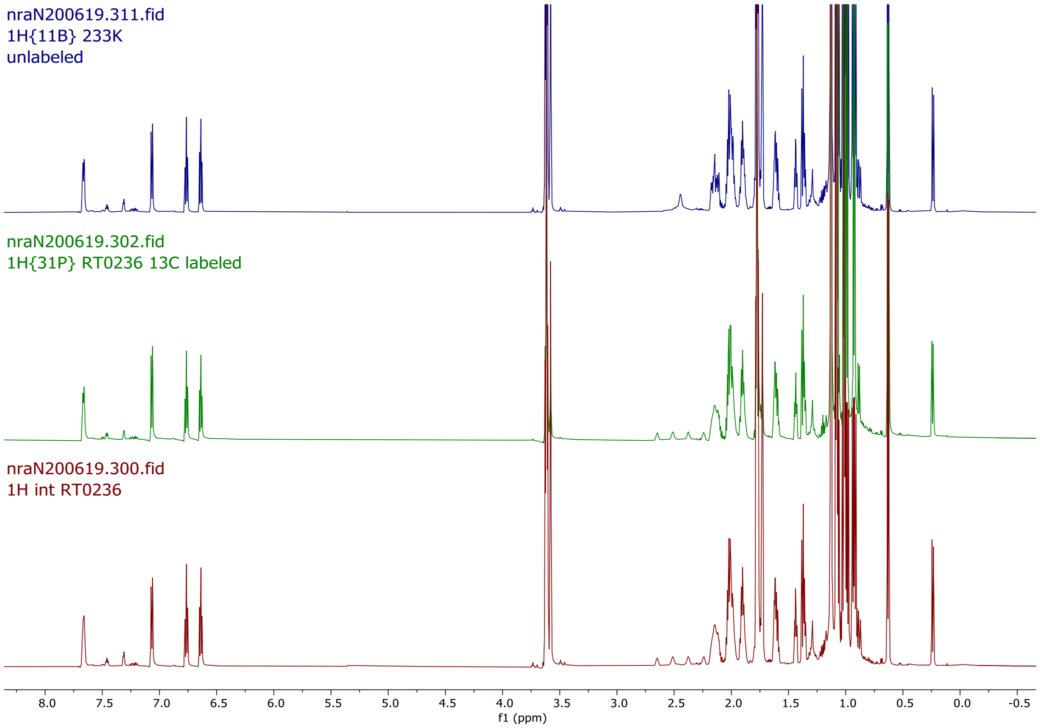

Figure S29. Stack plot spectra of ^{1}H, ^{1}H {^{11}P} and ^{1}H {^{31}B} NMR of **1c** in THF-d_8 at 298 K.

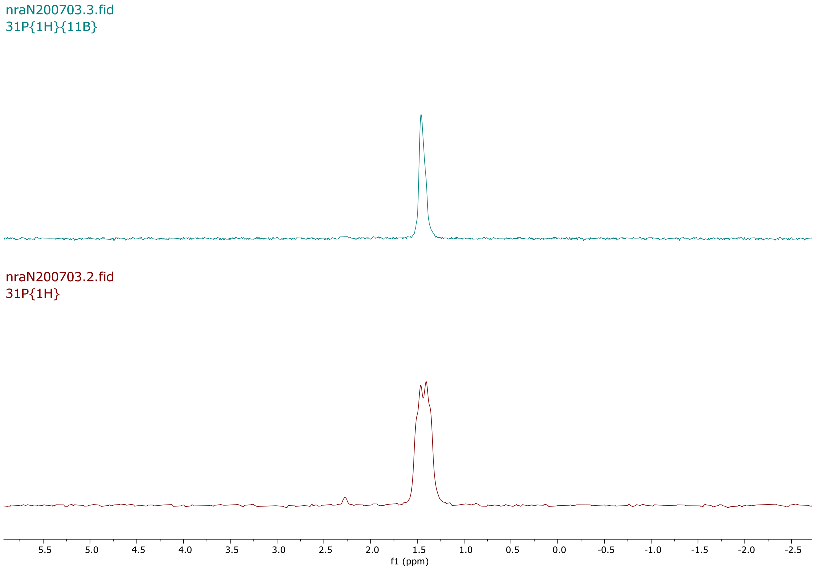

Figure S30. $^{31}P\{^{1}H\}$ and $^{31}P\{^{11}B\}\{^{1}H\}$ NMR spectral stack plot of **1c** in THF-d_8 at 298 K.

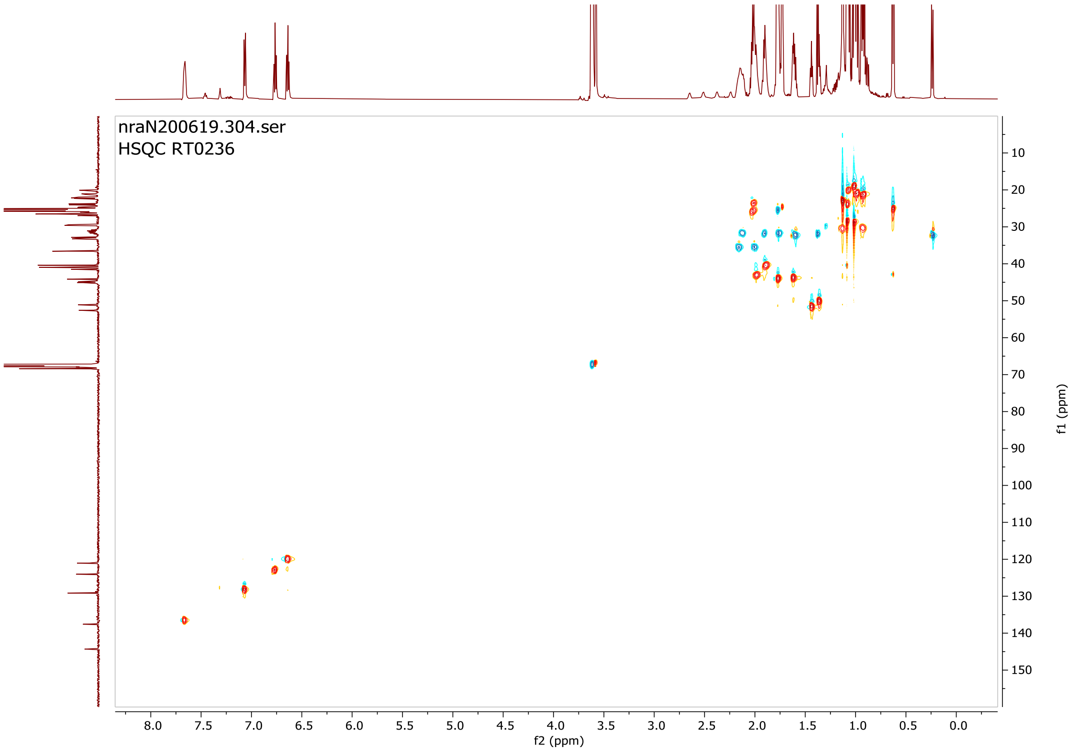

Figure S31. ^{1}H-$^{13}C\{^{1}H\}$ HSQC spectrum of **1c** at 298 K in THF-d_8.

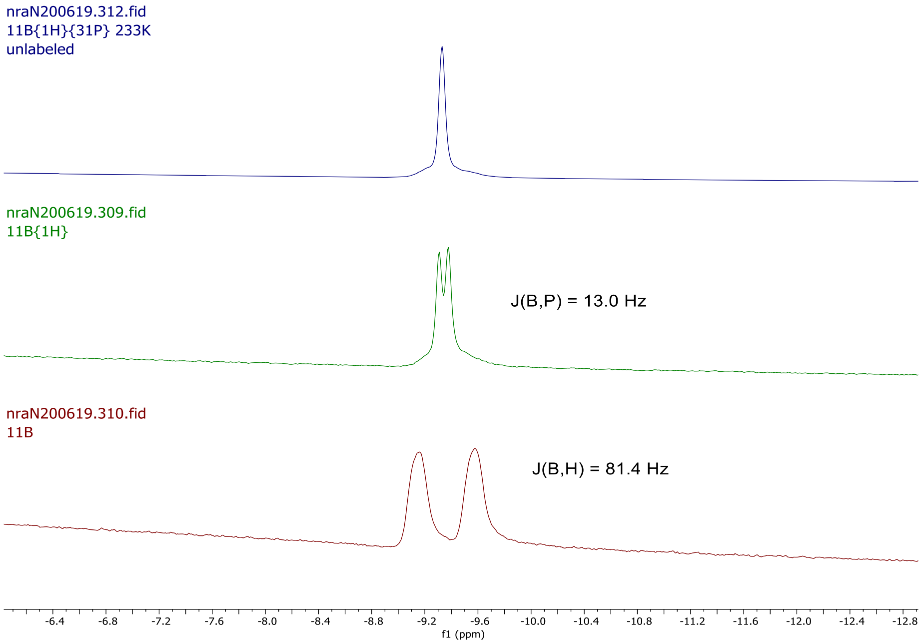

Figure S32. ^{11}B NMR spectral stack plot of **1c** upon decoupling ^{1}H and ^{31}P at 298 K in THF-d_8.

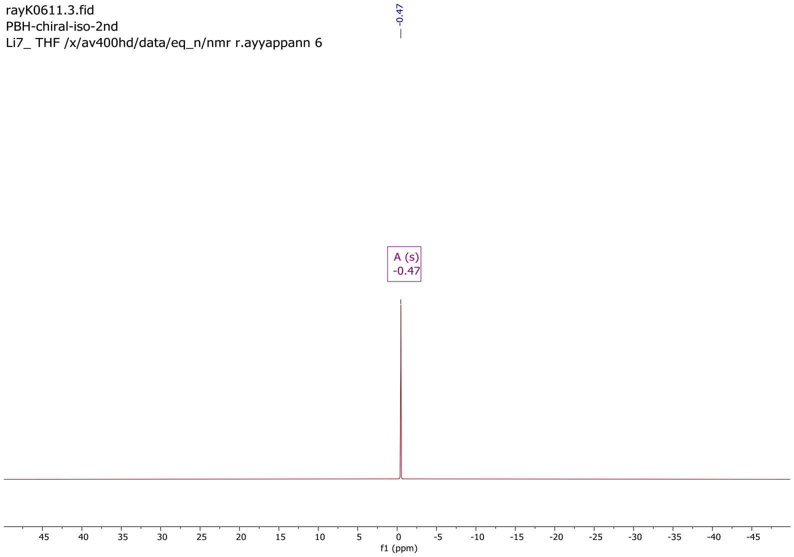

Figure S33. ^{7}Li NMR spectrum of **1c** at 298 K in THF-d_8.

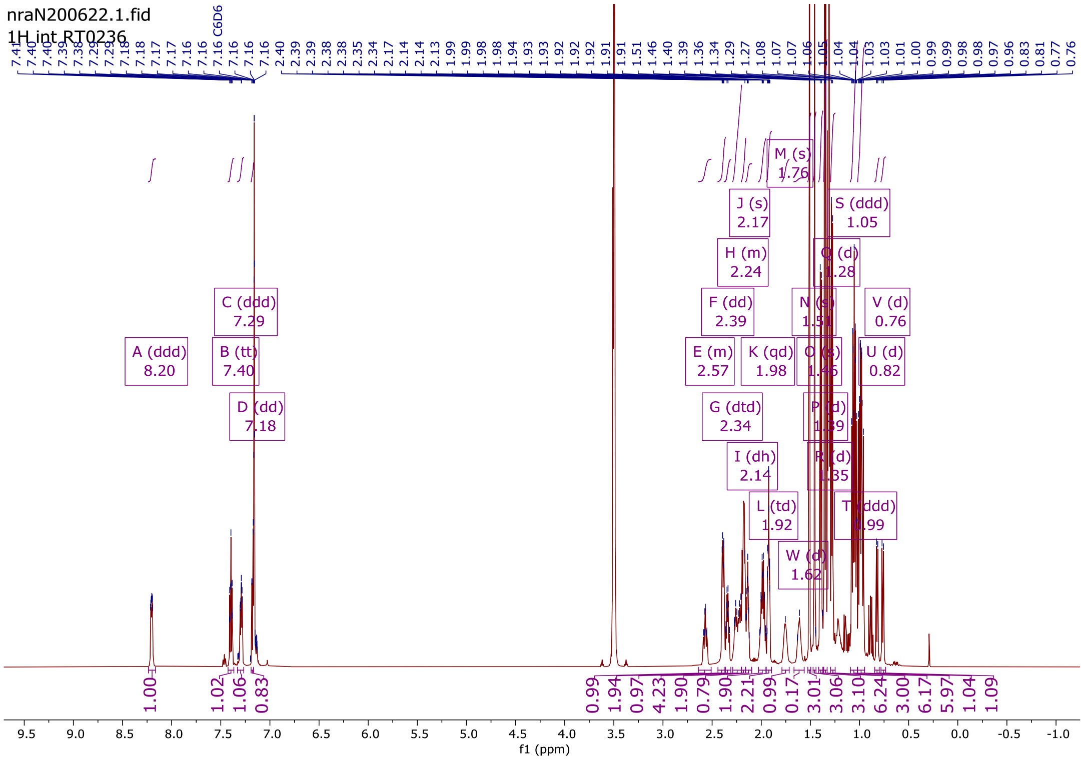

Figure S34. ^{1}H NMR spectrum of compound **1c** in C_6D_6 at 298 K.

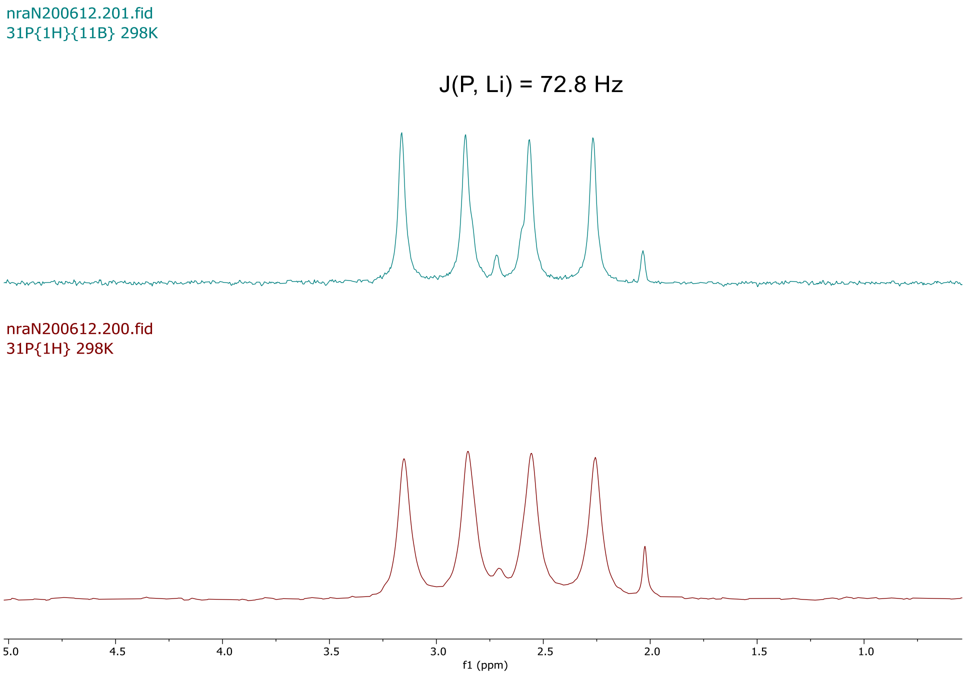

Figure S35. ^{31}P{^{1}H} and ^{31}P{^{1}H}{^{11}B} stack plot of spectra of **1c** in C_6D_6 at 298 K. Change in $w_{1/2}$ is 9.0 Hz.

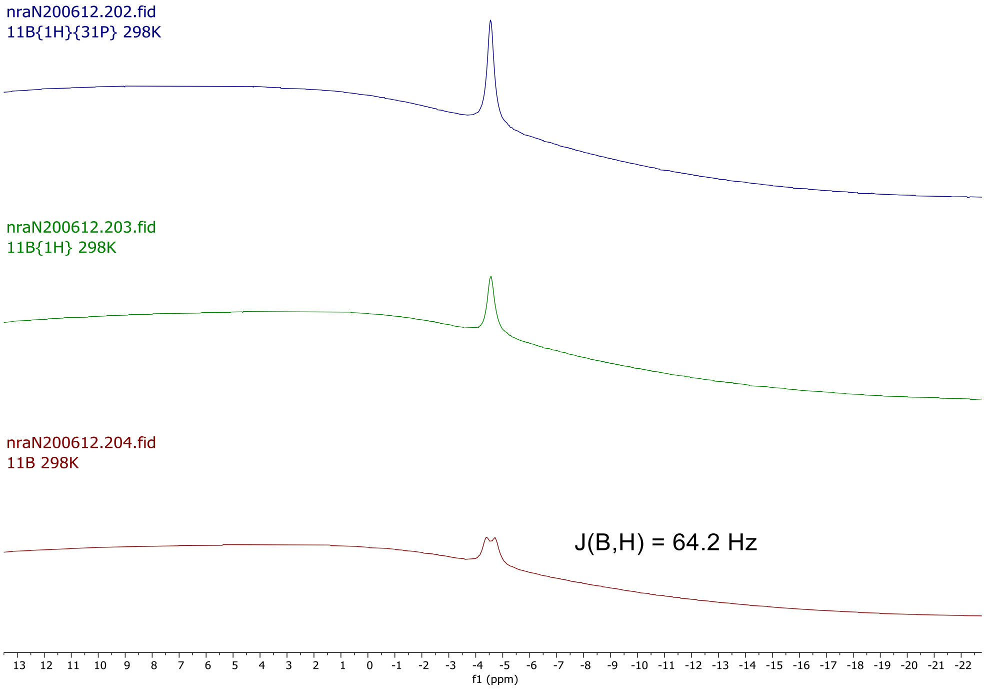

Figure S36. ^{11}B, $^{11}B\{^{1}H\}$ and $^{11}B\{^{1}H\}\{^{31}P\}$ stack plot of spectra of **1c** in C_6D_6 at 298 K.

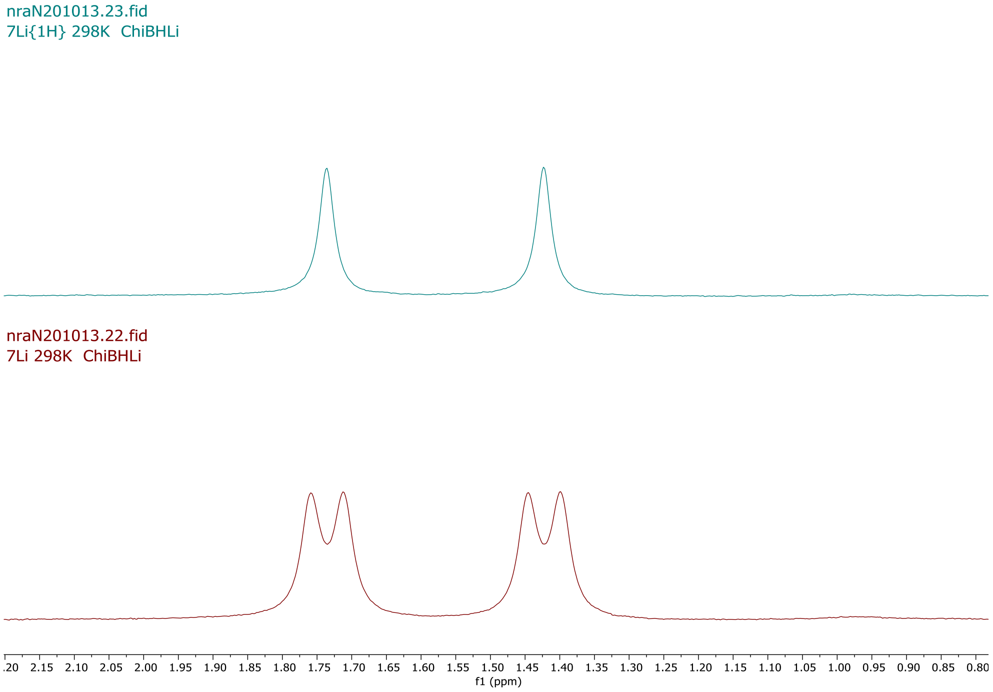

Figure S37. ^{7}Li and $^{7}Li\{^{1}H\}$ NMR spectral stack plot of **1c** at 298 K in tol-d_8.

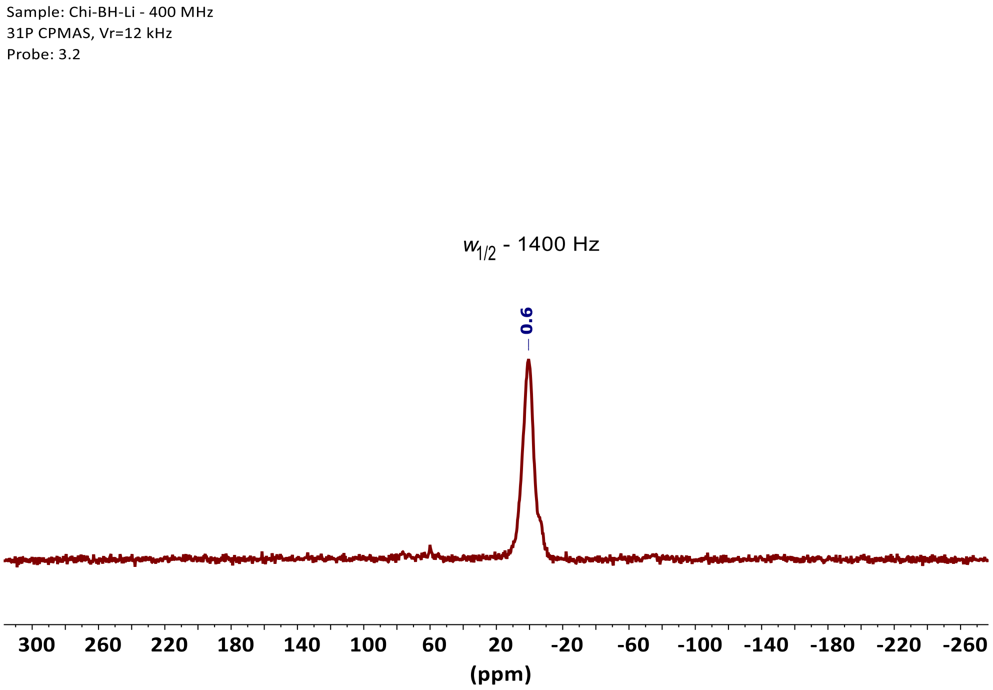

Figure S38. $^{31}P\{^{1}H\}$ CP MAS NMR spectrum of **1c** at 298 K. The P-Li coupling is not resolved probably due to the crystallinity of the sample.

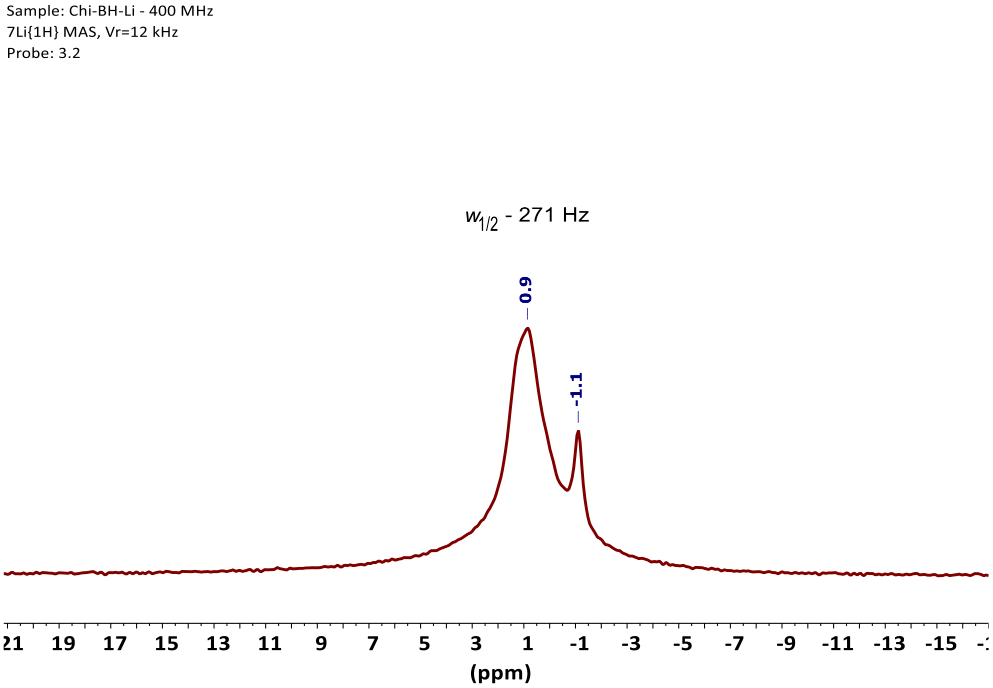

Figure S39. ^{7}Li MAS NMR spectrum of **1c** at 298 K. Due to the broadness of the signal, $^{1}J_{P\text{-}Li}$ is not resolved. The sharp signal at –1.1 ppm could be due to a different crystalline arrangement.

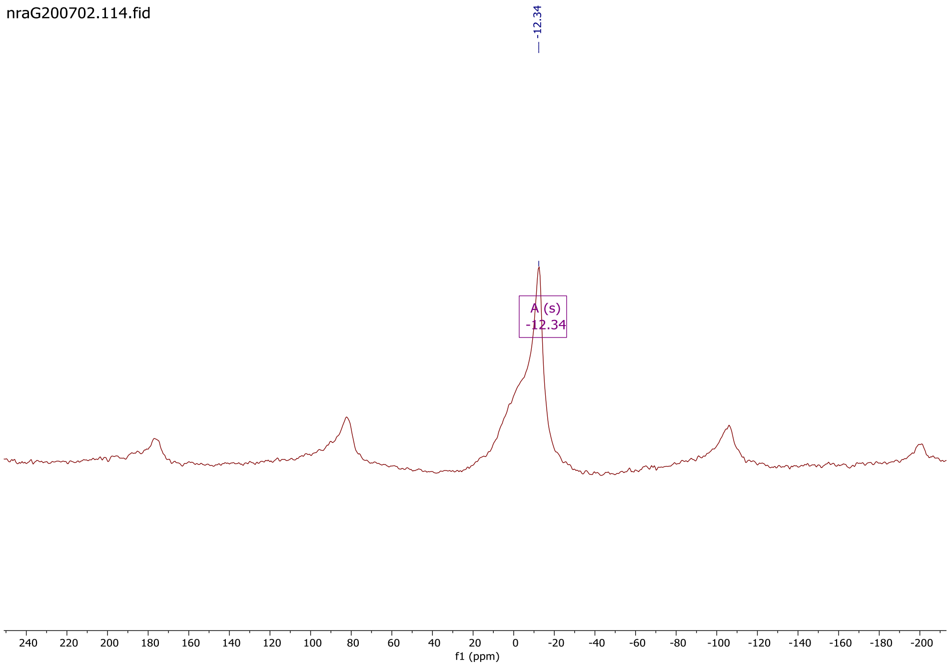

Figure S40. $^{11}B\{^1H\}$ MAS NMR spectrum of **1c** at 298 K.

5. [*o*-iPr$_2$P(CH$_3$)-C$_6$H$_4$-B(Mes$_2$)-H] (2)

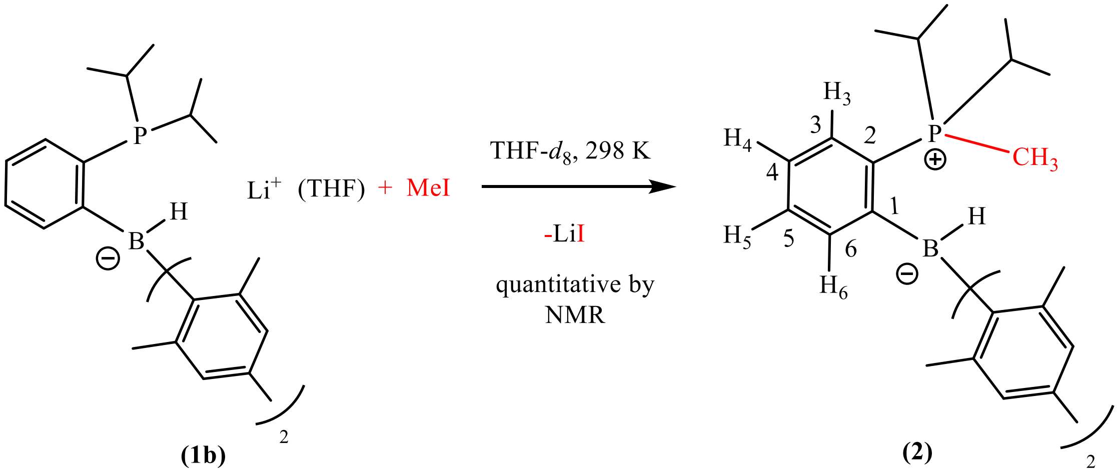

Lithium phosphine borohydride **1b** (20 mg, 0.04 mmol) was dissolved in a J. Young NMR tube in THF-*d*$_8$ at 298 K. Then, four equivalents of methyl iodide (21.6 mg, 0.15 mmol) were added. NMR spectroscopy revealed the complete formation of **2**.

^{1}H NMR (600.47 MHz, 233 K, THF-*d*$_8$): δ 7.55 (dd, $^3J_{H\text{-}P}$ = 12.1 Hz, $^3J_{H\text{-}H}$ = 7.7 Hz, 1H, H3), 7.49 (ddd, $^3J_{H\text{-}H}$ = 7.5 Hz, $^4J_{H\text{-}P}$ = 4.5 Hz, $^4J_{H\text{-}H}$ = 1.7 Hz, 1H, H6), 7.13 (td, $^3J_{H\text{-}H}$ = 7.3 Hz, $^4J_{H\text{-}H}$ = 1.4 Hz, 1H, H4), 7.09 (td, $^3J_{H\text{-}H}$ = 7.4 Hz, $^4J_{H\text{-}H}$ = 1.6 Hz, 1H, H5), 6.53 (s, 2H, H$_{aro}$(Mes)), 6.48 (s, 1H, H$_{aro}$(Mes)), 6.36 (s, 1H, H_{aro}(Mes)), 3.64 (quart, $^1J_{B\text{-}H}$ = 76.8 Hz, 1H, B-H), 3.58 (dseptet, $^3J_{H\text{-}H}$ = 7.0 Hz, $^2J_{H\text{-}P}$ = 4.2 Hz, 1H, CH(^{i}Pr)), 3.43 (septet, $^3J_{H\text{-}H}$ = 7.5 Hz, 1H, CH(iPr)), 2.13 (s, 3H, *o*-CH_3(Mes)), 2.10 (s, 6H, *o*-CH_3(Mes)), 1.92 (s, 3H, *o*-CH_3(Mes)), 1.78 (s, 3H, *p*-CH_3(Mes)), 1.69 (d, $^2J_{H\text{-}P}$ = 12.9 Hz 3H, P-CH_3), 1.59 (s, 3H, *p*-CH_3(Mes)), 1.31 (dd, $^3J_{H\text{-}P}$ = 15.6 Hz, $^3J_{H\text{-}H}$ = 6.9 Hz, 3H, CH_3(^{i}Pr)), 1.18 (dd, $^3J_{H\text{-}P}$ = 17.2 Hz, $^3J_{H\text{-}H}$ = 7.3 Hz, 3H, CH_3(^{i}Pr)), 1.13 (dd, $^3J_{H\text{-}P}$ = 17.0 Hz, $^3J_{H\text{-}H}$ = 8.1 Hz, 3H, CH_3(^{i}Pr)), 1.07 (dd, $^3J_{H\text{-}P}$ = 16.2 Hz, $^3J_{H\text{-}H}$ = 7.0 Hz, 3H, CH_3(^{i}Pr)).

Comments: B-H signal partially overlapped with THF signal at δ 3.58. Two CH(iPr) signals are inequivalent and one of them overlap with THF signal at δ 3.58. Two mesityl CH_3 singlets overlap at δ 2.10, thus appearing as a doublet, and one of the CH_3(Mes) overlap with THF signal at δ 1.78.

$^{31}P\{^1H\}$ NMR (243.09 MHz, 233 K, THF-*d*$_8$): δ 37.9 (s, $w_{1/2}$ = 21.3 Hz)

$^{31}P\{^1H\}\{^{11}B\}$ NMR (243.09 MHz, 233 K, THF-*d*$_8$): δ 37.9 (s, $w_{1/2}$ = 11.4 Hz)

With ^{13}C labelled compound. $^{31}P\{^1H\}$ NMR (243.07 MHz, 233 K, C_6D_6): δ 37.7 (d, $^1J_{P\text{-}C}$ = 49.5 Hz).

^{11}B NMR (192.65 MHz, 233 K, THF-*d*$_8$): δ –13.2 (d, $^1J_{B\text{-}H}$ = 75.4 Hz).

$^{11}B\{^1H\}$ NMR (192.65 MHz, 233 K, THF-*d*$_8$): δ –13.2 (d, $w_{1/2}$ = 21.0 Hz, $J_{P\text{-}B}$ = 3 Hz).

$^{11}B\{^1H\}\{^{31}P\}$ NMR (192.65 MHz, 233 K, THF-*d*$_8$): δ –13.2 (s, $w_{1/2}$ = 16.7 Hz).

$^{13}C\{^1H\}$ NMR (151.00, 233 K, THF-*d*$_8$): δ 176.0 (quart, $^1J_{C\text{-}B}$ = 44.8 Hz, C-1), 157.4 (quart, $^1J_{C\text{-}B}$ = 49.1 Hz, quaternary), 155.5 (quart, $^1J_{C\text{-}B}$ = 52.7 Hz, quaternary), 143.2 (s, Mes(quaternary)), 142.7 (s, Mes(quaternary)), 142.4 (s, Mes(quaternary)), 142.0 (s, Mes(quaternary)), 140.3 (d, $^2J_{C\text{-}P}$ = 16.3 Hz, C-3), 131.7 (s, Mes(quaternary)), 132.1 (d, $^2J_{C\text{-}P}$ = 14.0 Hz, C-6), 131.6 (s, C-5), 129.4 (s, Mes(aromatic)), 128.9 (s, Mes(aromatic)), 128.3 (s, Mes(aromatic)), 124.8 (d, $^3J_{C\text{-}P}$ = 12.6 Hz, C-4), 122.5 (d, $^1J_{C\text{-}P}$ = 82.2 Hz, C-2), 27.1 (s, CH_3(Mes)), 26.6 (s, CH_3(Mes)), 26.5 (s, CH_3(Mes)), 24.6 (s, CH_3(Mes)), 24.7 (d, $^1J_{C\text{-}P}$ = 46.8 Hz, CH(^{i}Pr)), 21.8 (d, $^1J_{C\text{-}P}$ = 47.3 Hz, CH(^{i}Pr)), 21.5 (s, CH_3(Mes)), 21.4 (s, CH_3(Mes)), 17.9 (s, CH_3(^{i}Pr)), 17.0 (d, $^2J_{C\text{-}P}$ = 2.6 Hz, CH_3(^{i}Pr)), 16.9 (s, CH_3(^{i}Pr)), 15.8 (s, CH_3(^{i}Pr)), 1.4 (d, $^1J_{C\text{-}P}$ = 45.7 Hz, P-CH_3).

Comments: Surprisingly, no $^3J_{C\text{-}P}$ was found for three CH_3(^{i}Pr) and very large $^1J_{C\text{-}P}$ found for CH(^{i}Pr).

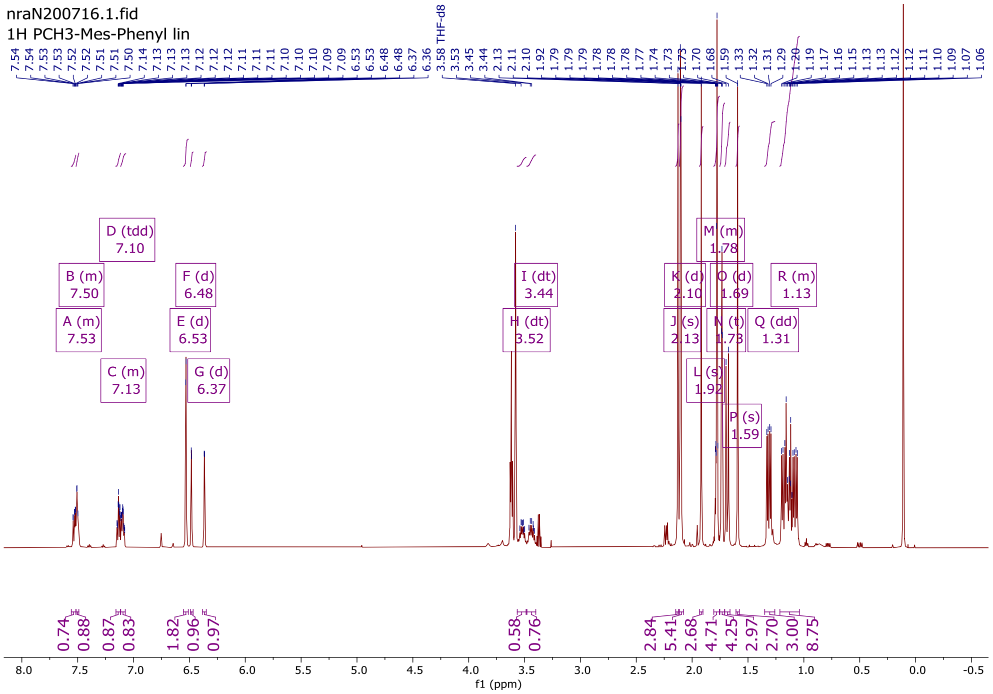

Figure S41. ^{1}H NMR spectrum of **2** at 233 K in THF-d_8.

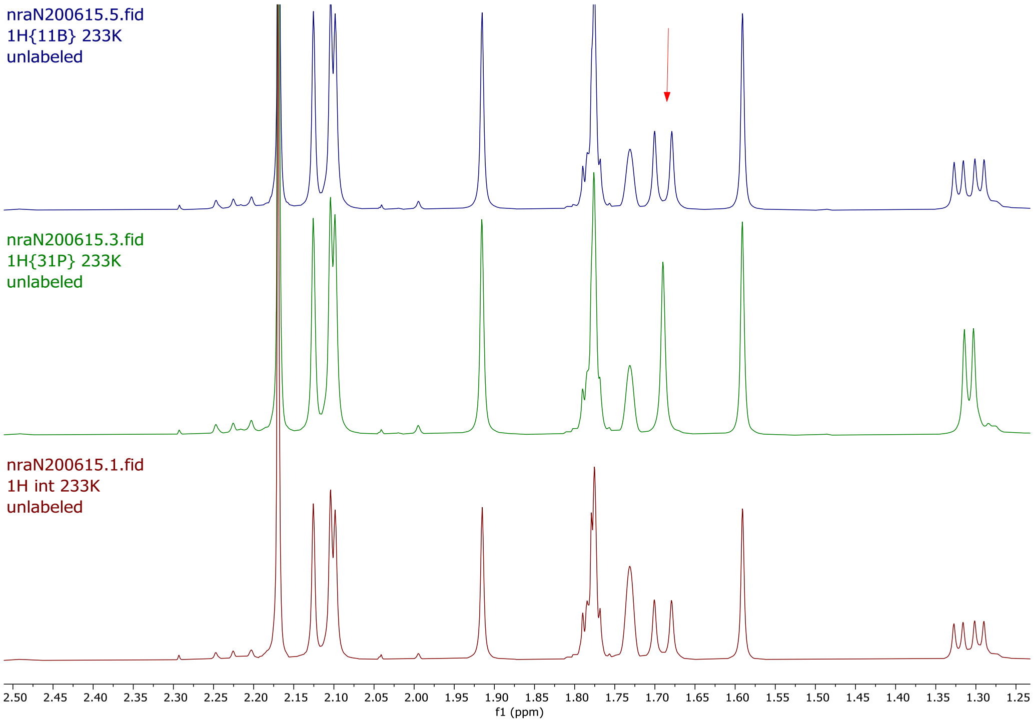

Figure S42. ^{1}H, ^{1}H{^{31}P} and ^{1}H{^{11}B} NMR spectral stack plot of methyl phosphonium borate **2** in THF-d_8 at 233 K. The doublet centred at δ 1.69 ppm with $^{2}J_{\mathrm{P\text{-}H}}$ = 12.9 Hz become a singlet after ^{1}H{^{31}P} decoupling.

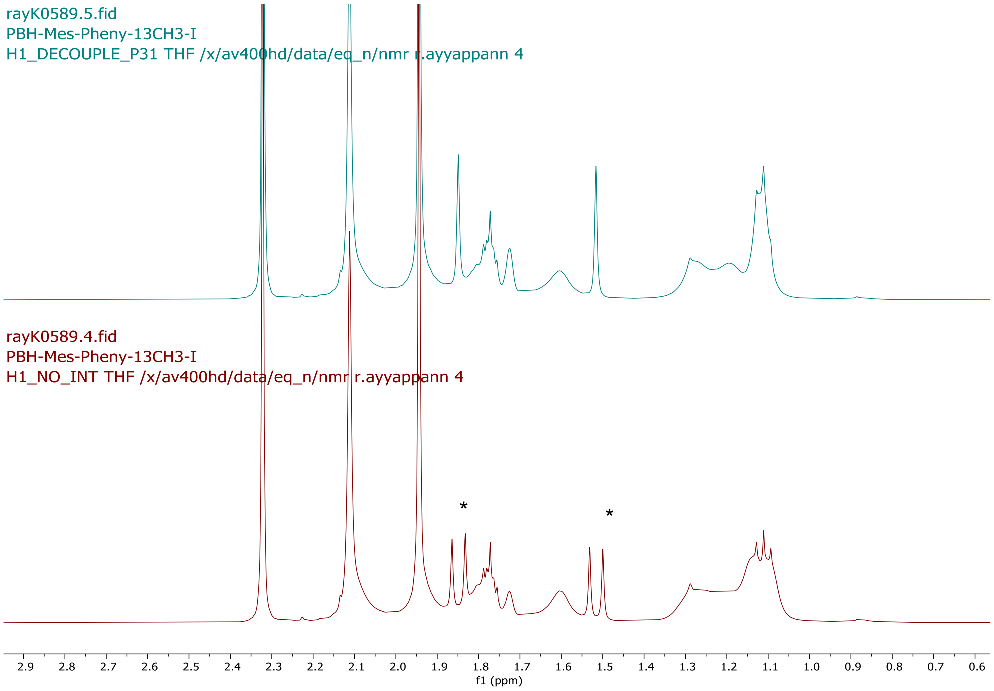

Figure S43. ^{1}H and ^{1}H{^{31}P} NMR spectral stack plot of ^{13}C labelled methyl phosphonium borate **2** in THF-d_8 at 298 K. The doublet of doublet (**) centred at δ 1.7 ppm with $^2J_{\text{P-H}}$ = 12.7 Hz and $^1J_{\text{C-H}}$ = 134.0 Hz can be assigned to P-CH_3.

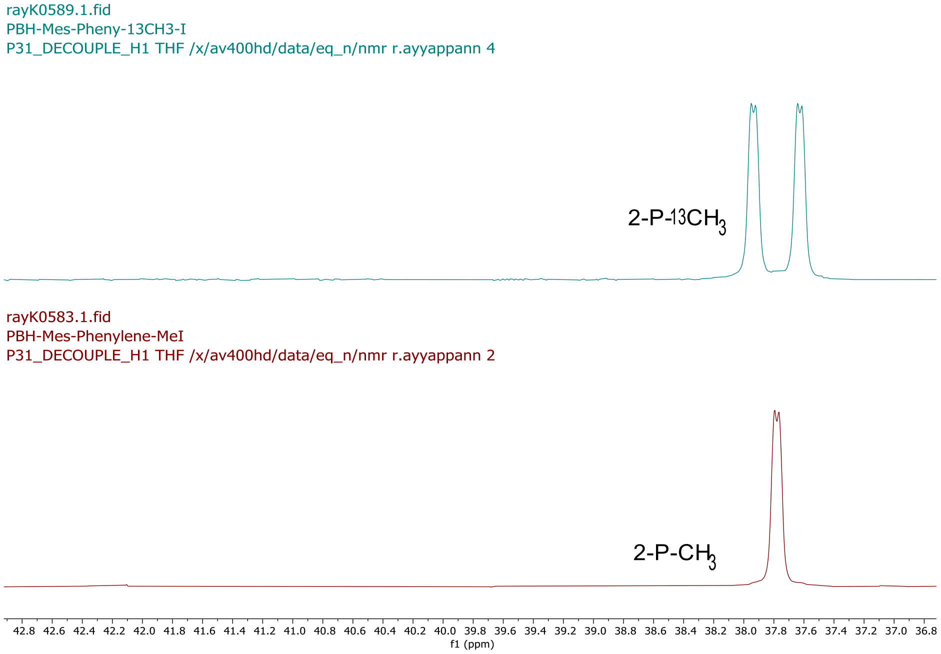

Fig S44. ^{31}P{^{1}H} NMR spectral stack plot of **2** at 298 K in THF-d_8: bottom trace (**2-P-CH$_3$)** and top trace (**2-P-^{13}CH$_3$)**. It shows $^1J_{\text{P-C}}$ = 50.0 Hz.

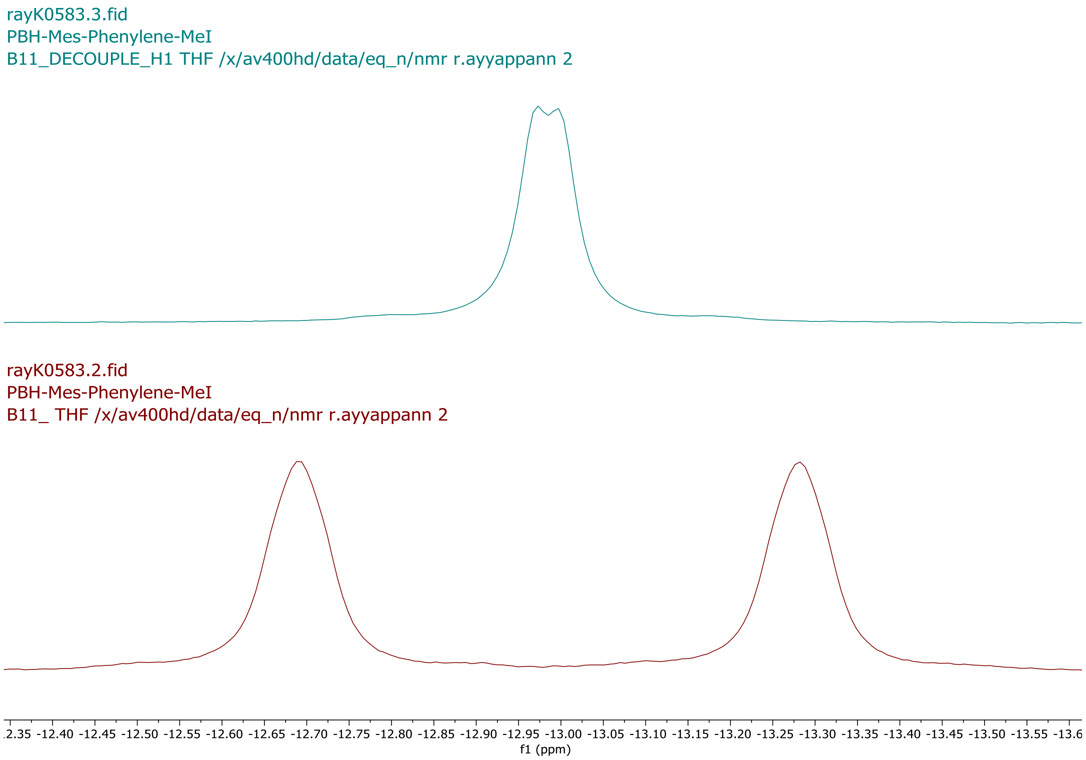

Figure S45. ^{11}B and ^{11}B{^{1}H} NMR spectral stack plot of **2** at 298 K in THF-d_8, giving $J_{\text{P-B}}$ = 3 Hz.

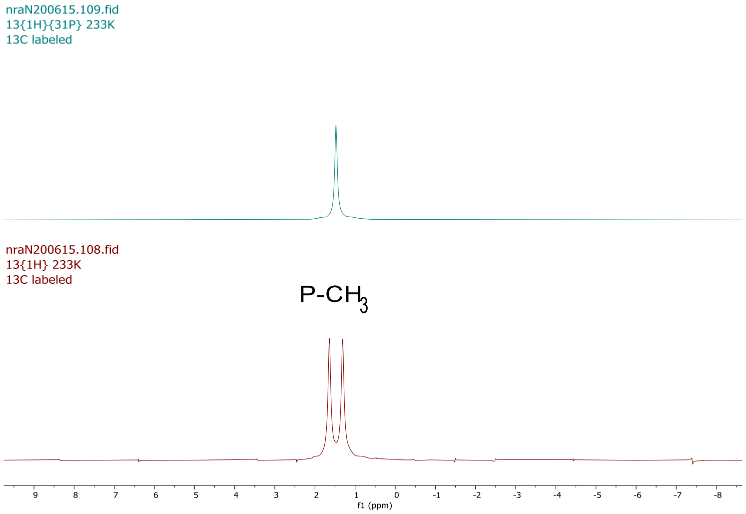

Figure S46. ^{13}C{^{1}H} and ^{13}C{^{1}H}{^{31}P} superimposed NMR stack plot of the ^{13}CH$_3$ labelled **2**. The doublet due to P-C coupling at δ 1.6 ppm become singlet upon decoupling.

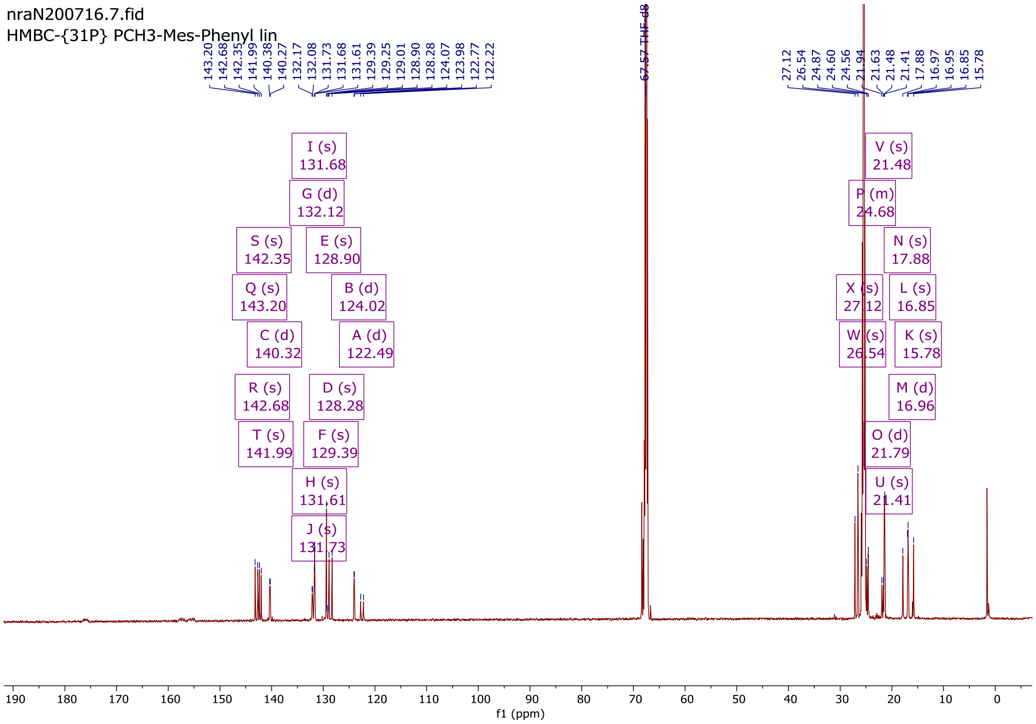

Figure S47. $^{13}C\{^{1}H\}$ NMR spectrum of **2** in THF-d_8 at 233 K.

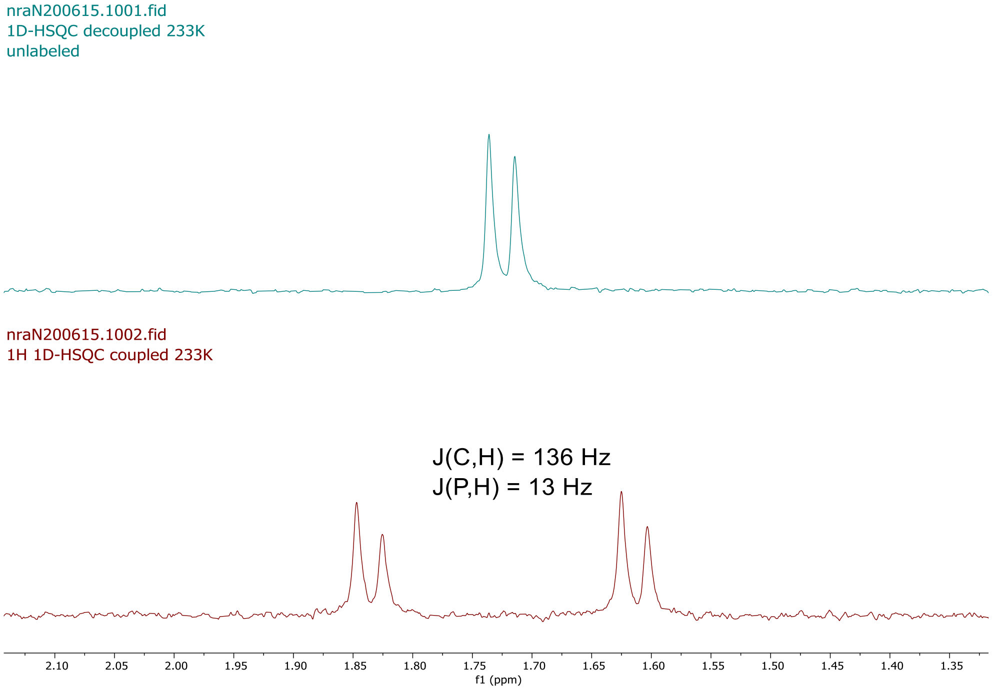

Figure S48. Selective 1D ^{1}H-^{13}C HSQC experiment on **2** to prove P-CH_3 bond formation.

6. $Li^+(THF)[1\text{-}B((Mes_2)\text{-}H)\text{-}(C_{10}H_6)\text{-}8\text{-}(P^iPr_2)]^-$ (3)

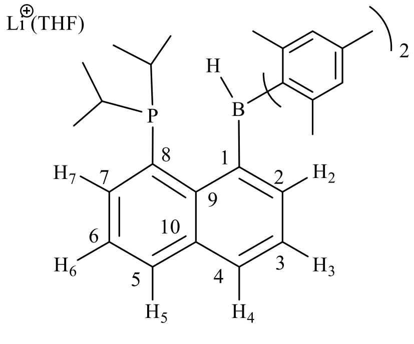

(**3**)

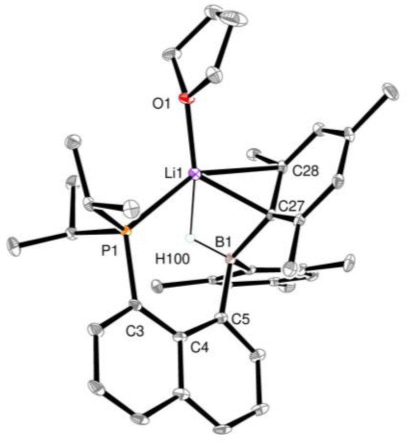

Dimesitylborane dimer (0.392 g, 0.78 mmol) and *o*-Li(0.9 Et_2O)-$C_{10}H_6$-P^iPr_2 (0.508 g, 1.57 mmol) were stirred together at 298 K in THF (10 mL) for 2 h under argon atmosphere. Then, THF was completely removed under vacuum. Diethyl ether (5 mL) was added to precipitate the product at –35°C. The pale-yellow precipitate was washed with n-pentane (3 x 3 mL) and dried under vacuum. The pale yellow solid **3** was isolated (0.820 g, 1.04 mmol, 66 %). Monocrystals suitable for X-ray diffraction were obtained in n-pentane at –35°C upon standing for a week.

^{1}H NMR (600.47 MHz, 233 K, THF-d_8): δ 7.54 (d, $^3J_{H\text{-}H}$ = 7.8 Hz, 1H, H5), 7.48 (d, $^3J_{H\text{-}H}$ = 7.0 Hz, 1H, H7), 7.33 (d, $^3J_{H\text{-}H}$ = 7.0 Hz, 1H, H4), 7.22 (d, $^3J_{H\text{-}H}$ = 7.7 Hz, 1H, H2), 7.10 (t, $^3J_{H\text{-}H}$ = 7.4 Hz, 1H, H6), 6.83 (t, $^3J_{H\text{-}H}$ = 7.4 Hz, 1H, H3), 6.45 (s, 1H, H_{aro}Mes), 6.39 (s, 2H, H_{aro}Mes), 6.11 (s, 1H, H_{aro}Mes), 4.51 (quart, $^1J_{B\text{-}H}$ = 71.4 Hz, 1H, B-H), 2.12 (s, 6H, *p*-CH_3(Mes)), 2.07 (s, 3H, *o*-CH_3(Mes)), 2.00 (s, 3H, *o*-CH_3(Mes)), 1.82 (s, 3H, *o*-CH_3(Mes)), 1.78 (m, 1H, CH(iPr) overlapping with THF signal), 1.63 (sept, 2H, $^3J_{H\text{-}H}$ = 6.8 Hz), 1.35 (s, 3H, *o*-CH_3(Mes)), 1.04 (overlapping dd, 6H, $^3J_{H\text{-}H}$ = 6.5 Hz, CH_3(iPr)), 0.72 (dd, 3H, $^3J_{H\text{-}P}$ = 14.8 Hz, $^3J_{H\text{-}H}$ = 6.5 Hz, CH_3(iPr)), 0.32 (dd, 3H, $^3J_{H\text{-}P}$ = 10.6 Hz, $^3J_{H\text{-}H}$ = 6.8 Hz, CH_3(iPr)).

^{31}P{^{1}H} NMR (243.07 MHz, 298 K, THF-d_8): δ 5.37 (quart, $J_{P\text{-}B}$ = 22.3 Hz).

^{31}P{^{1}H} NMR (162.01 MHz, 298 K, C_6D_6): 4.2 (quart, $^1J_{P\text{-}Li}$ = 73.0 Hz).

^{11}B NMR (192.65 MHz, 298 K, THF-d_8): δ –11.8 (dd, $^1J_{B\text{-}H}$ = 79.7 Hz, $J_{B\text{-}P}$ = 20 Hz).

^{11}B{^{1}H} NMR (192.65 MHz, 298 K, THF-d_8): δ –11.8 (d, $J_{B\text{-}P}$ = 20 Hz).

^{11}B NMR (128.39 MHz, 298 K, C_6D_6): δ –10.8 (dd, $^1J_{B\text{-}H}$ = 68.8 Hz, $J_{B\text{-}P}$ = 9 Hz).

^{11}B{^{1}H} NMR (128.39 MHz, 298 K, C_6D_6): δ –10.8 (d, $J_{B\text{-}P}$ = 9 Hz).

^{13}C{^{1}H} NMR (151.00 MHz, 233 K, THF-d_8): δ 167.9 (br, ipso-C(Mes)), 161.4 (br, C-8), 145.6 (d, $^1J_{C\text{-}P}$ = 22.6 Hz, C-1), 143.9 (s, quaternary), 143.5 (s, quaternary), 143.4 (s, quaternary), 143.24 (s, quaternary), 143.23 (s, quaternary), 143.20 (s, quaternary overlapping), 135.8 (d, ${}^{2}J_{\text{C-P}}$ = 5.8 Hz, C-2), 135.1 (s, C-4), 131.2 (s, C-7), 130.7 (s, C-5), 129.4 (s, C_{aro}Mes), 128.7 (s, C_{aro}Mes), 128.2 (s, C_{aro}Mes), 127.8 (s, C_{aro}Mes), 127.63 (s, C_{aro}Mes), 127.56 (s, C_{aro}Mes), 125.1 (s, C_{aro}Mes), 124.6 (s, C-3), 122.3 (s, C6), 32.0 (d, ${}^{1}J_{\text{C-P}}$ = 27.4 Hz, CH(^{i}Pr)), 28.6 (d, ${}^{1}J_{\text{P-C}}$ = 29.9 Hz, CH(^{i}Pr)), 27.3 (s, CH_3(Mes)), 25.9 (s, CH_3(iPr)), 23.3 (d, ${}^{2}J_{\text{P-C}}$ = 17.9 Hz, CH_3(^{i}Pr)), 22.1 (d, ${}^{2}J_{\text{P-C}}$ = 36.8 Hz, CH_3(^{i}Pr)), 21.8 (s, CH_3(Mes)), 21.0 (d, ${}^{2}J_{\text{P-C}}$ = 15.6 Hz, CH_3(^{i}Pr)), 20.8 (d, ${}^{2}J_{\text{P-C}}$ = 19.3 Hz, CH_3(^{i}Pr)).

Notes: All the quaternary carbons were identified by ^{1}H-^{13}C{^{1}H} HSQC NMR spectrum. ^{1}H-^{13}C{^{1}H} HMBC NMR spectrum was also used to assign quaternary signals.

^{7}Li (233.37, 298 K, THF-d_8): δ –0.1 (s)

^{7}Li NMR (155.53, 298 K, C_6D_6): δ –0.2 (d, ${}^{1}J_{\text{P-Li}}$ = 71.3 Hz)

Anal. cald. for $C_{42}H_{59}BLiO_2P{\cdot}2THF$: C, 78.25; H, 9.23. Found: C, 77.68; H, 8.52. The presence of two THF molecules was confirmed by ^{1}H NMR spectroscopy.

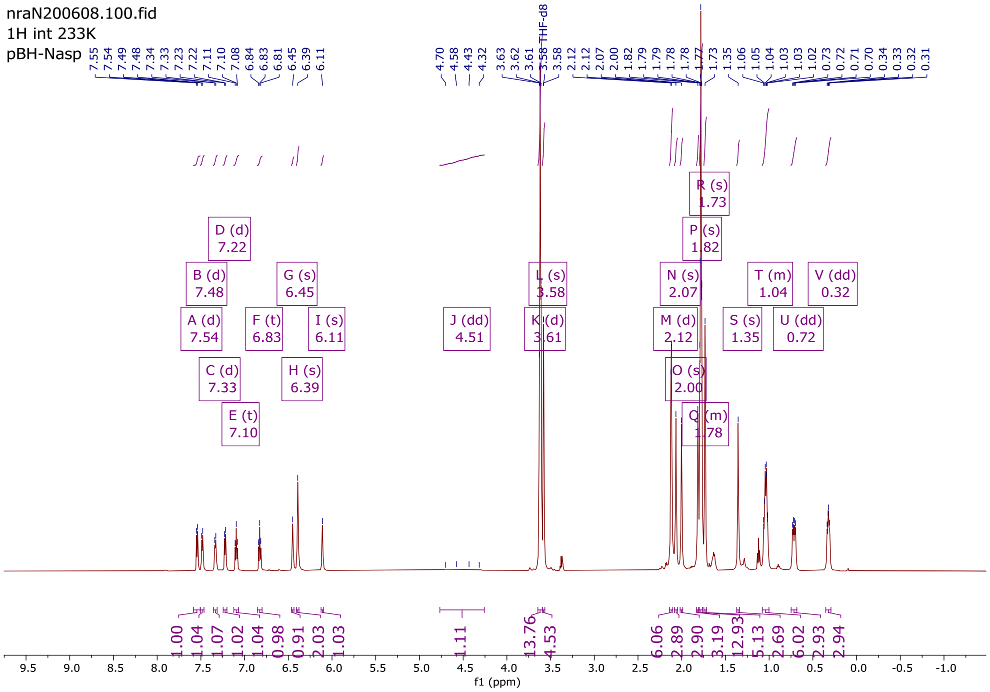

Figure S49.^{1}H NMR spectrum of naphtyl borate **3** at 233 K in THF-d_8. At 298 K, the isopropyl region is broad, overlapping and multiplicity are not well resolved.

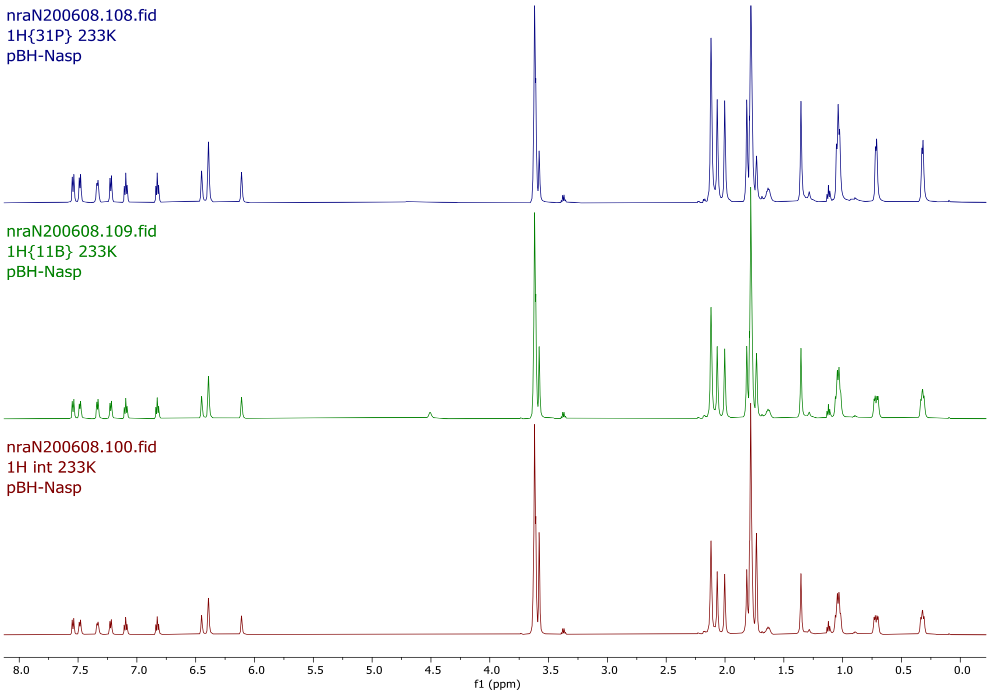

Figure S50. ^{1}H, ^{1}H{^{11}B} and ^{1}H{^{31}P} stack plot of **3** at 233 K in THF-d_8.

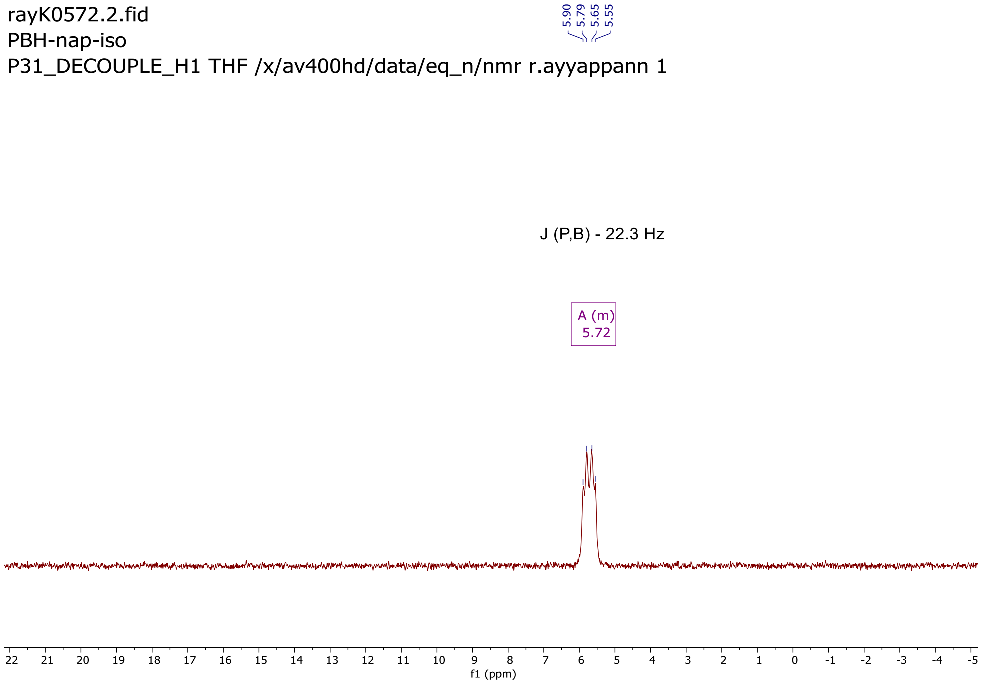

Figure S51. ^{31}P{^{1}H} NMR spectrum of naphtyl borate **3** in THF-d_8 at 298 K.

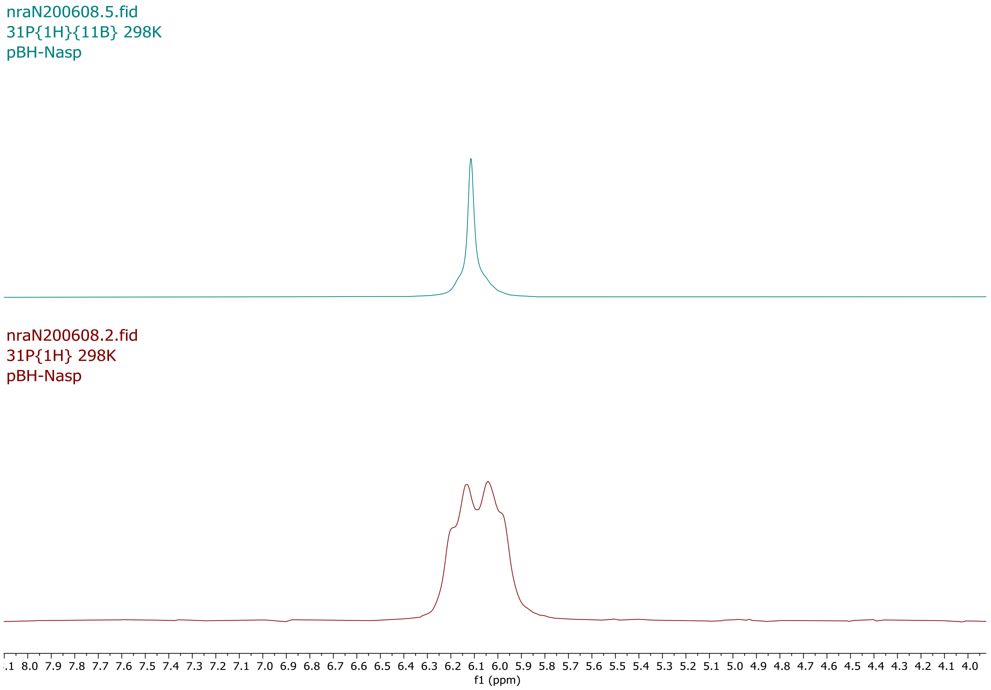

Figure S52. ${}^{31}P\{{}^{1}H\}$ and ${}^{31}P\{{}^{1}H\}\{{}^{11}B\}$ NMR spectra of naphtyl borate **3** at 233 K in THF-d_8.

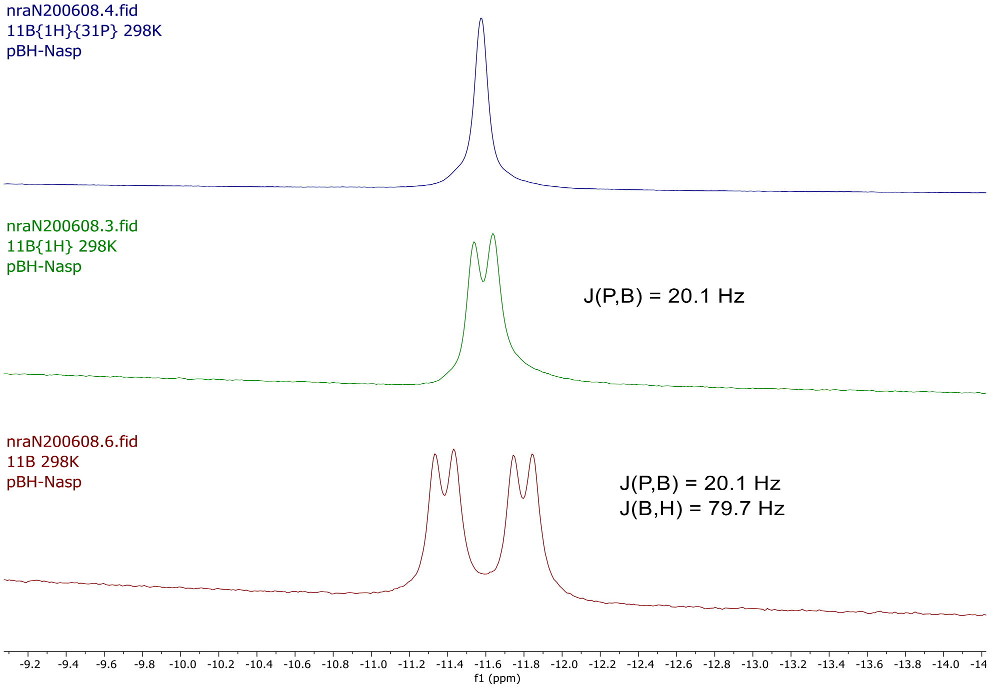

Figure S53. ${}^{11}B$, ${}^{11}B\{{}^{1}H\}$ and ${}^{11}B\{{}^{1}H\}\{{}^{31}P\}$ NMR spectral stack plot of naphtyl borate **3** at 298 K in THF-d_8.

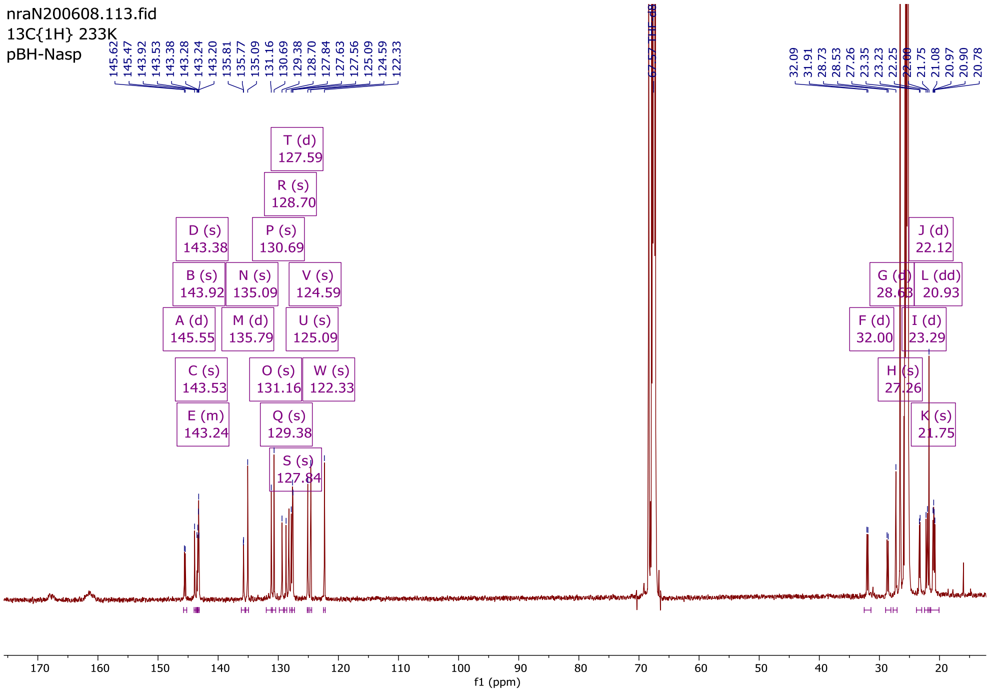

Figure S54. $^{13}C\{^{1}H\}$ NMR spectrum of naphtyl borate **3** at 233 K in THF-d_8.

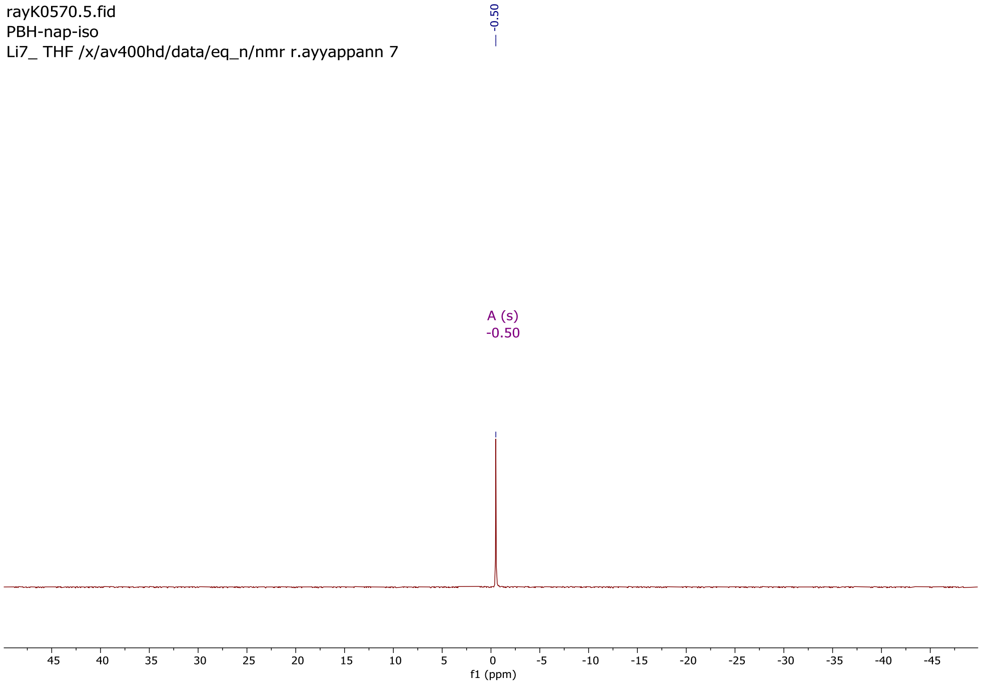

Figure S55. ^{7}Li NMR spectrum of naphtyl borate **3** at 233 K in THF-d_8.

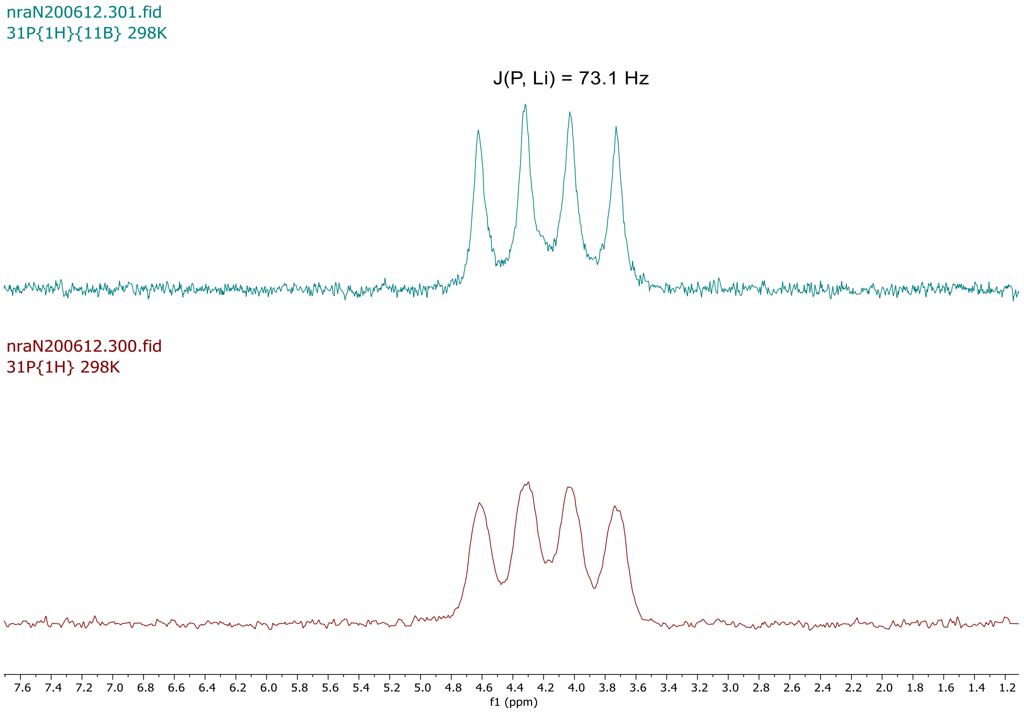

Figure S56. $^{31}P\{^{1}H\}$ and $^{31}P\{^{1}H\}\{^{11}B\}$ Decoupling experiment of naphtyl borate **3** in C_6D_6 at 298 K.

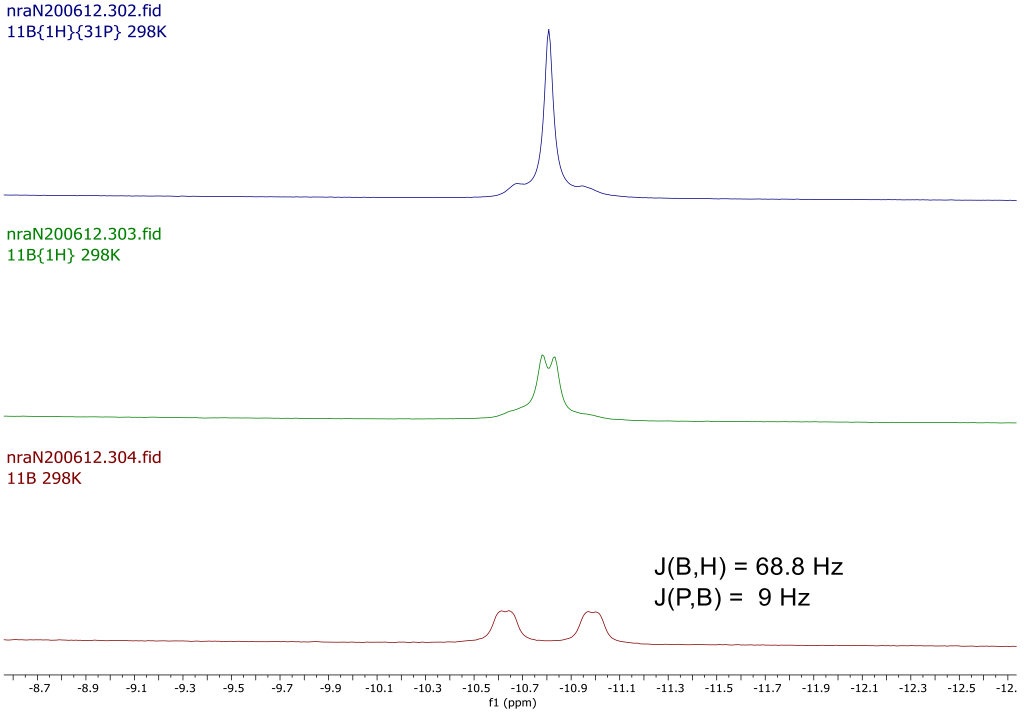

Figure S57. ^{11}B, $^{11}B\{^{1}H\}$ and $^{11}B\{^{1}H\}\{^{31}P\}$ decoupling experiment of naphtyl borate **3** in C_6D_6 at 298 K. In the $^{11}B\{^{1}H\}\{^{31}P\}$ spectrum (top), the broadness at the base line could indicate a not complete ^{31}P decoupling.

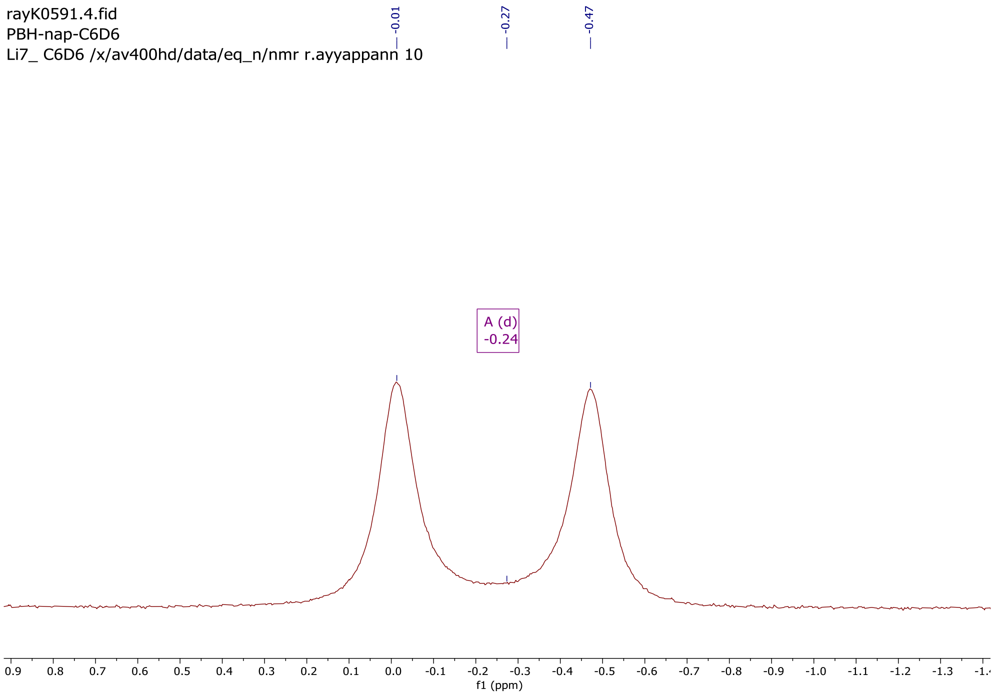

Figure S58. ^{7}Li NMR spectrum of napthyl borate **3** in C_6D_6 at 298 K.

7. Characterization of methyl phosphonium naphtyl borate [1-B(Mes$_2$)-H)-(C$_{10}$H$_6$)-8-P(iPr$_2$)(CH$_3$)]- (4)

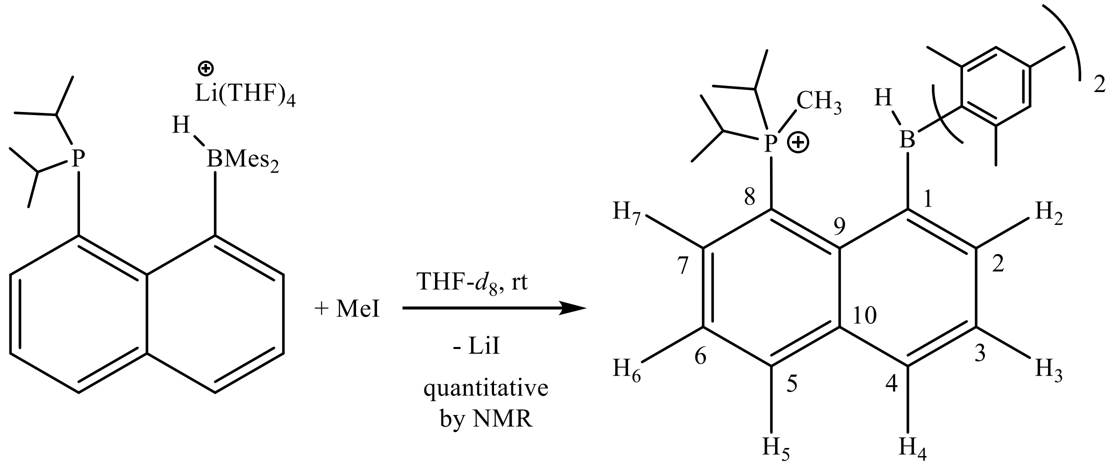

(**3**) (**4**)

Lithium napthyl phosphine borohydride **3** (20 mg, 0.254 mmol) was dissolved in a J. Young NMR tube in THF-d_8 at 298 K. Then, four equivalents of methyl iodide (14.4 mg, 1.016 mmol) were added. NMR spectroscopy revealed the complete formation of **4**.

^{1}H NMR (600.47 MHz, 233 K, THF-d_8): δ 8.03 (d, $^3J_{H\text{-}H}$ = 8.0 Hz, 1H, H4), 7.70 (dd, $^3J_{H\text{-}P}$ = 16.8 Hz, $^3J_{H\text{-}H}$ = 7.2 Hz, 1H, H2), 7.57 (d, $^3J_{H\text{-}H}$ = 7.8 Hz, 1H, H5), 7.54 (d, $^3J_{H\text{-}H}$ = 7.0 Hz, 1H, H7), 7.40 (td, $^3J_{H\text{-}H}$ =

7.6 Hz, $^3J_{H\text{-}P}$ = 1.8 Hz, 1H, H3), 7.15 (t, $^3J_{H\text{-}H}$ = 7.4 Hz, 1H, H6), 6.67 (s, 1H, H_{aro}Mes), 6.47 (s, 2H, H_{aro} Mes), 6.43 (s, 1H, H_{aro}Mes), 6.10 (s, 1H, H_{aro}Mes), 4.59 (dsept, $^2J_{H\text{-}P}$ = 14.5 Hz, $^3J_{H\text{-}H}$ = 7.2 Hz, 1H, CH(^{i}Pr)), 4.10 (quart, $^1J_{B\text{-}H}$ = 73.3 Hz, 1H, B-H), 3.76 (dsept, $^2J_{H\text{-}P}$ = 14.3 Hz, $^3J_{H\text{-}H}$ = 7.2 Hz, 1H, CH(^{i}Pr)), 2.50 (s, 3H, *p*-CH_3(Mes)), 2.17 (s, 3H, *o*-CH_3(Mes)), 2.01 (s, 3H, *o*-CH_3(Mes)), 1.89 (s, 3H, *o*-CH_3(Mes)), 1.77 (d, $^2J_{H\text{-}P}$ = 10.9 Hz, 3H, P-CH_3), 1.48 (dd, $^3J_{H\text{-}P}$ = 17.1 Hz, $^3J_{H\text{-}H}$ = 7.3 Hz, 3H, CH_3(^{i}Pr)), 1.42 (s, 3H, *o*-CH_3(Mes)), 1.20 (dd, 3H, $^3J_{H\text{-}P}$ = 17.1 Hz, $^3J_{H\text{-}H}$ = 7.1 Hz, CH_3(^{i}Pr)), 0.45 (overlapping dd, 6H, $^3J_{H\text{-}P}$ = 12.9 Hz, $^3J_{H\text{-}H}$ = 7.0 Hz, CH_3(^{i}Pr)), 0.35 (s, 3H, CH_3(Mes)).

^{31}P{^{1}H} NMR (243.09 MHz, 233 K, THF-d_8): δ 43.6 (s).

With labelled $^{13}CH_3$; ^{31}P{^{1}H} NMR (162.01 MHz, 233 K, THF-d_8): 43.7 (d, $^1J_{P\text{-}C}$ = 54.1 Hz).

^{11}B NMR (192.65 MHz, 233 K, THF-d_8): δ –11.8 (d, $^1J_{B\text{-}H}$ = 73.8 Hz).

^{11}B{^{1}H} NMR (192.65 MHz, 233 K, THF-d_8): δ –11.8 (s).

^{13}C{^{1}H} NMR (151.00 MHz, 233 K, THF-d_8): δ 161.3 (quart, $^1J_{C\text{-}B}$ – 47.5 Hz, C-8), 156.5 (quart, $^1J_{C\text{-}B}$ – 56.2 Hz, *ipso*-C(Mes)), 143.8 (s, C_{aro}Mes quaterary), 143.7 (s, C_{aro}Mes quaternary), 142.4 (s, C_{aro}Mes quaternary), 137.8 (s, C-7), 137.0 (d, $^3J_{C\text{-}P}$ = 3.8 Hz, C-4), 136.9 (d, $^2J_{C\text{-}P}$ = 11.2 Hz, C-2), 136.7 (d, $^2J_{C\text{-}P}$ = 6.9 Hz, C-9), 131.6 (s, C_{aro}Mes quaternary), 131.4 (s, C_{aro}Mes quaternary), 129.7 (s, C_{aro}Mes quaternary), 129.4 (s, C_{aro}Mes quaternary), 129.1 (s, C_{aro}Mes quaternary), 128.1 (s, C_{aro}Mes quaternary), 127.3 (s, C6), 126.5 (s, C5), 122.2 (d, $^3J_{C\text{-}P}$ = 13.8 Hz, C3), 117.8 (d, $^1J_{C\text{-}P}$ = 78.8 Hz, C1), 26.3 (s, CH_3(Mes)), 24.7 (d, $^1J_{C\text{-}P}$ = 42.4 Hz, CH(^{i}Pr)), 24.5 (s, CH_3(Mes)), 21.5 (s, CH_3(Mes)), 21.2 (s, CH_3(Mes)), 17.9 (s, CH_3(^{i}Pr)), 17.8 (s, CH_3(iPr)), 17.5 (s, CH_3(iPr)), 1.5 (d, $^1J_{P\text{-}C}$ = 54.2 Hz, P-CH_3).

Note: All the quaternary carbons were identified by ^{1}H-^{13}C{^{1}H} HSQC and HMBC NMR spectra. One of the CH_3(Mes) and CH(^{i}Pr) signals are overlapping with THF at δ 25.5 ppm. Surprisingly, no $^2J_{C\text{-}P}$ was observed for CH_3(^{i}Pr).

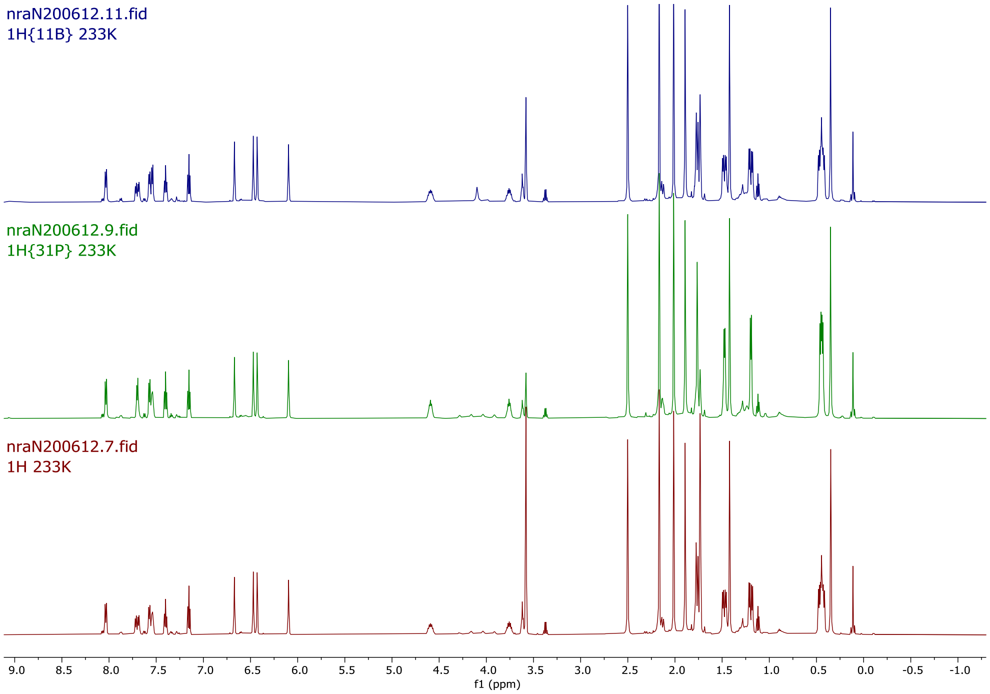

Figure S59. ^{1}H, $^{1}H\{^{31}P\}$ and $^{1}H\{^{11}B\}$ NMR spectral stack plot of the methyl phosphonium zwitterionic product **4** at 233 K in THF-d_8. The doublet (P-CH_3) centred at δ 1.76 ppm become singlet upon $^{1}H\{^{31}P\}$ decoupling.

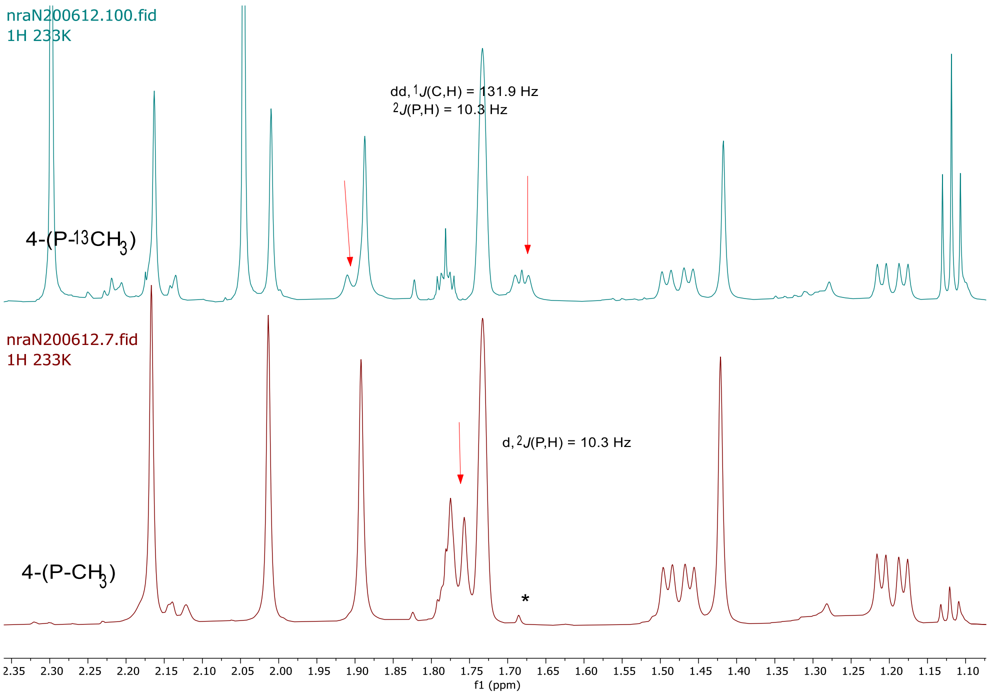

Figure S60. ^{1}H NMR spectral stack plot of unlabelled methyl phosphonium naphtyl borate (**4**-P(CH_3)) stacked with labelled (**4**-P$^{13}CH_3$) in THF-d_8 at 233 K. P-$^{13}CH_3$ appeared at δ 1.77 ppm as doublet of doublet (dd) with $^{1}J_{CH}$ = 131.86 Hz, $^{2}J_{P\text{-}H}$ = 10.30 Hz. * - impurity.

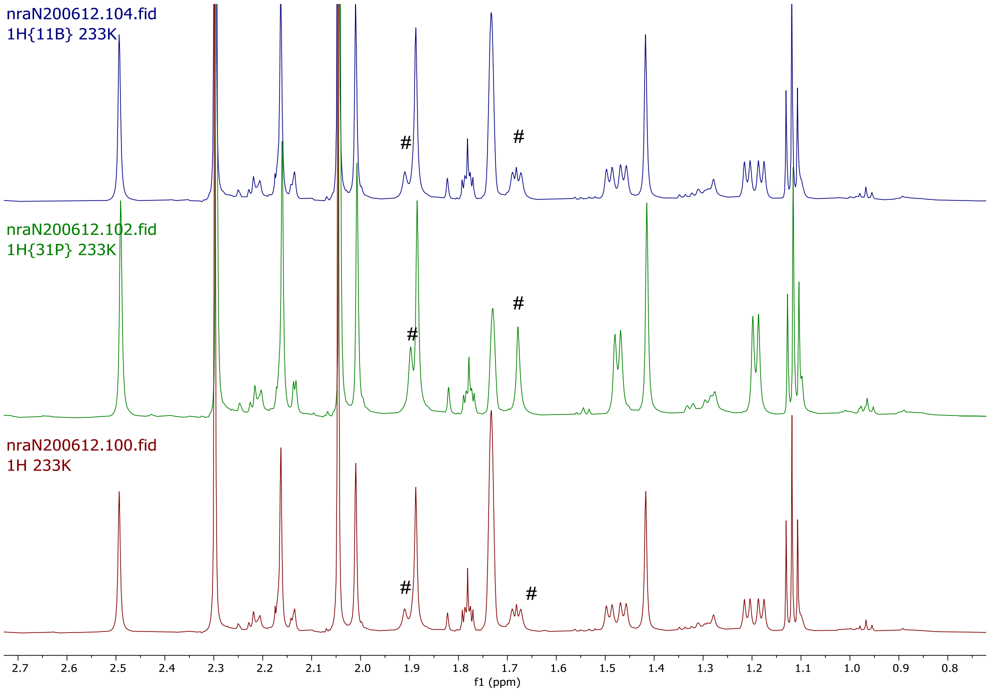

Figure S61. Expansion of ^{1}H NMR decoupling experiments with ^{31}P and ^{11}B of methyl phosphonium naphtyl borate **4** at 233 K with labelled ^{13}CH$_3$-I. - doublet of doublet with $^{1}J_{C\text{-}H}$ = 131.9 Hz, $^{2}J_{P\text{-}H}$ = 10.3 Hz noted. # for the P-^{13}CH$_3$ resonance at δ 1.77 ppm. In the middle of the right doublet, an impurity is present leading to a triplet appearance.

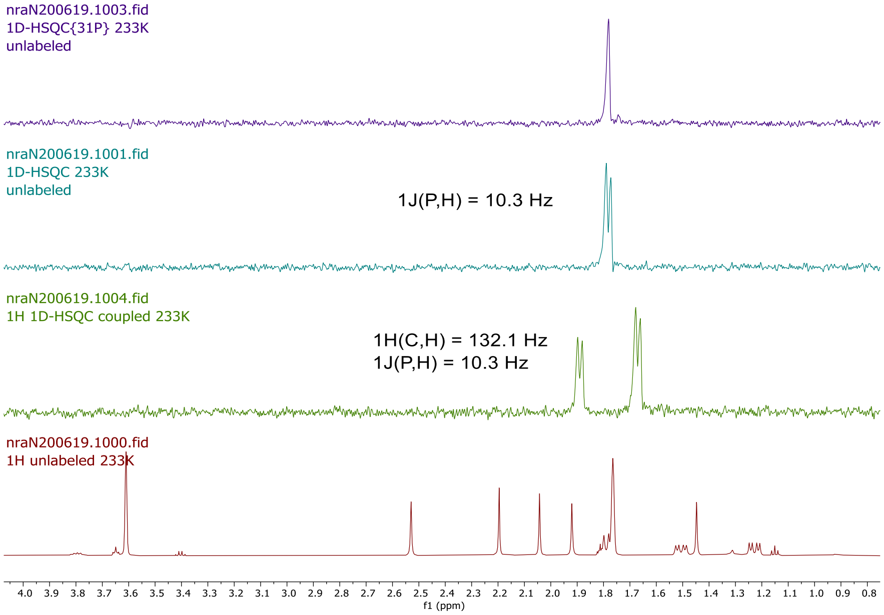

Figure S62. 1D-^{1}H-^{13}C HSQC transfer experiments to identify only P-CH$_3$ signal in **4** in the ^{1}H NMR spectrum at 233 K in THF-d_8. Actual signal is overlapping with THF δ 1.78 ppm.

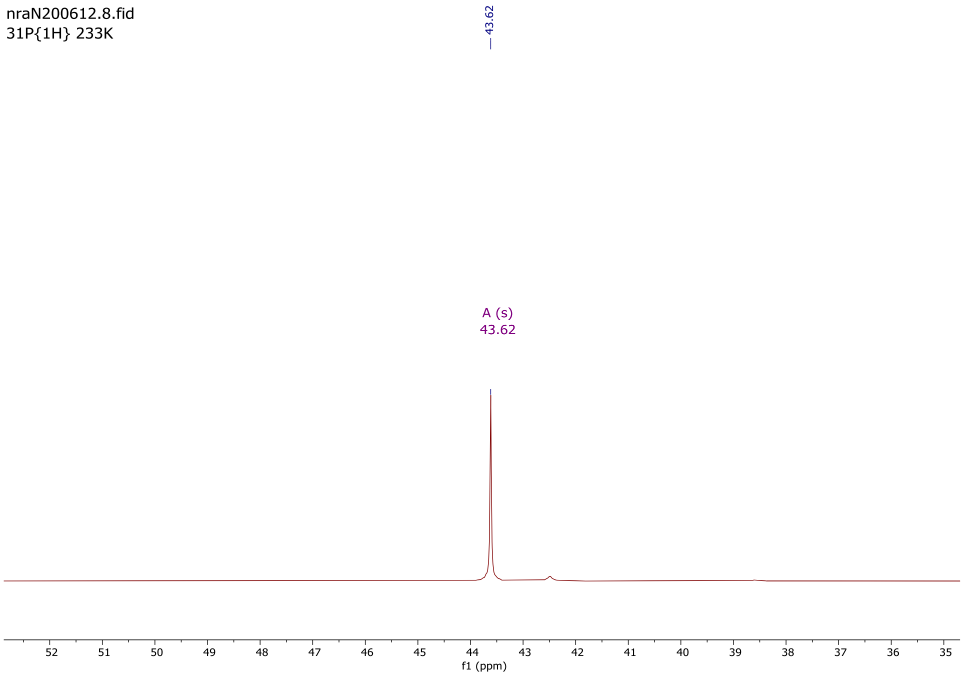

Figure S63. $^{31}P\{^{1}H\}$ NMR spectrum of methyl phosphonium naphtyl borate **4** at 233 K in THF-d_8.

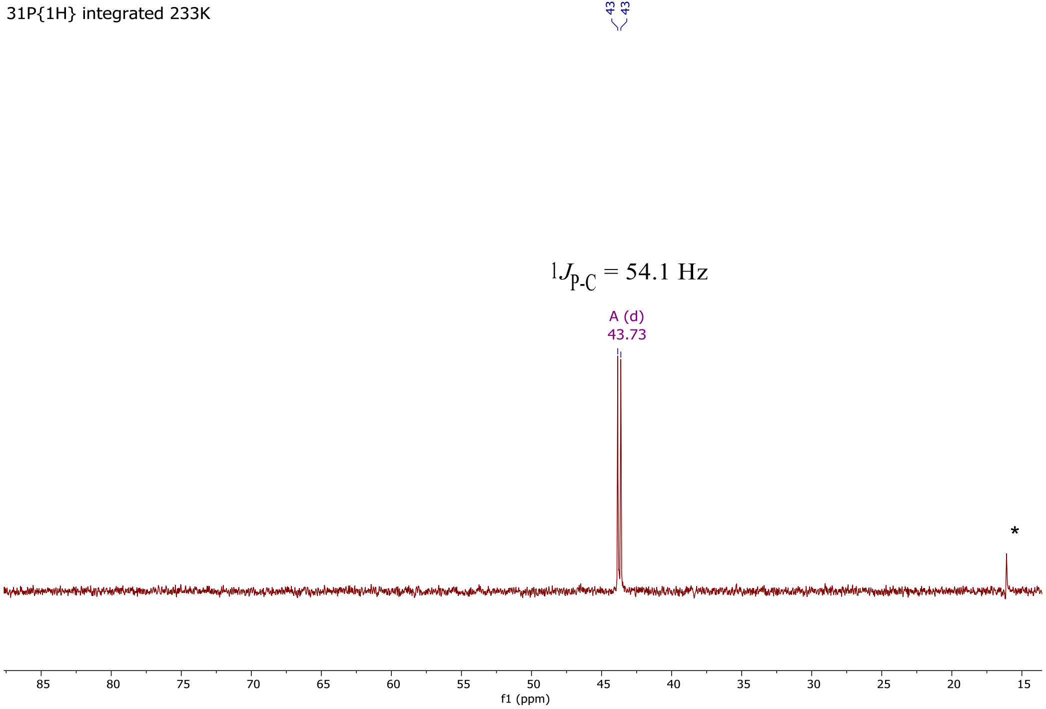

Figure S64. $^{31}P\{^{1}H\}$ NMR spectrum of ^{13}C-methyl phosphonium naphtyl borate **4** at 233 K. * - due to [1-B(Mes$_2$)-C$_{10}$H$_6$)-8-P^{i}Pr$_2$].

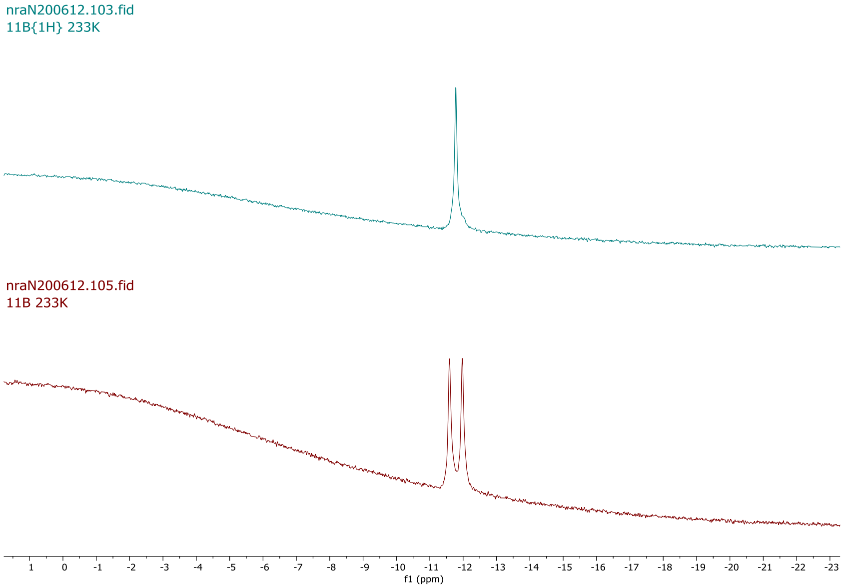

Figure S65. ^{11}B and ^{11}B{^{1}H} NMR spectral stack plot of methyl phosphonium naphtyl borate **4** at 233 K in THF-d_8.

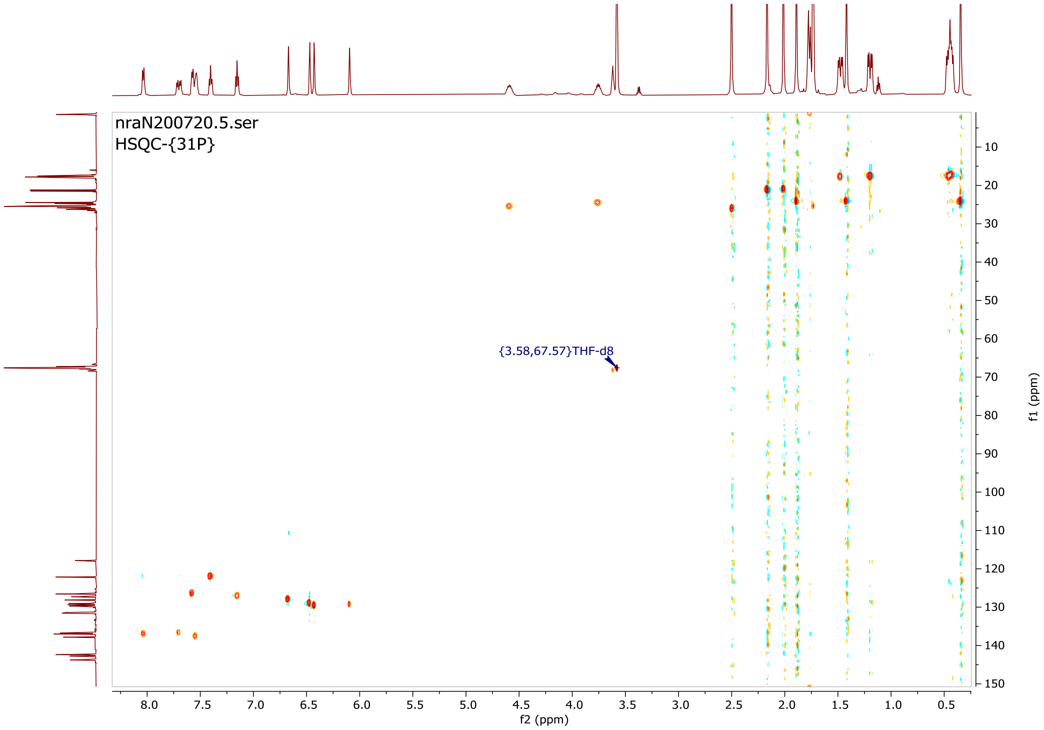

Figure S66. HSQC: ^{1}H / ^{13}C{^{1}H} NMR spectrum of **4** at 233 K in THF-d_8.

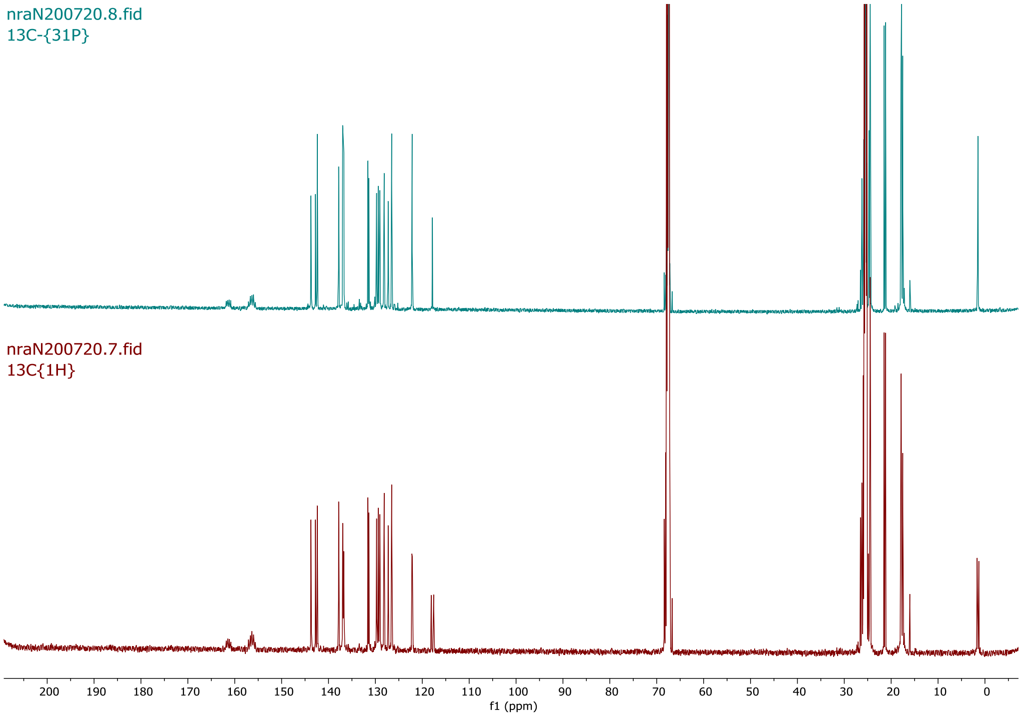

Figure S67. $^{13}C\{^{1}H\}$ and $^{13}C\{^{1}H\}\{^{31}P\}$ NMR spectral stack plot of methyl phosphonium naphtyl borate **4** at 233 K in THF-d_8. Doublet with $^{1}J_{P\text{-}C}$ = 54.1 Hz at δ 1.16 ppm became singlet upon ^{31}P decoupling.

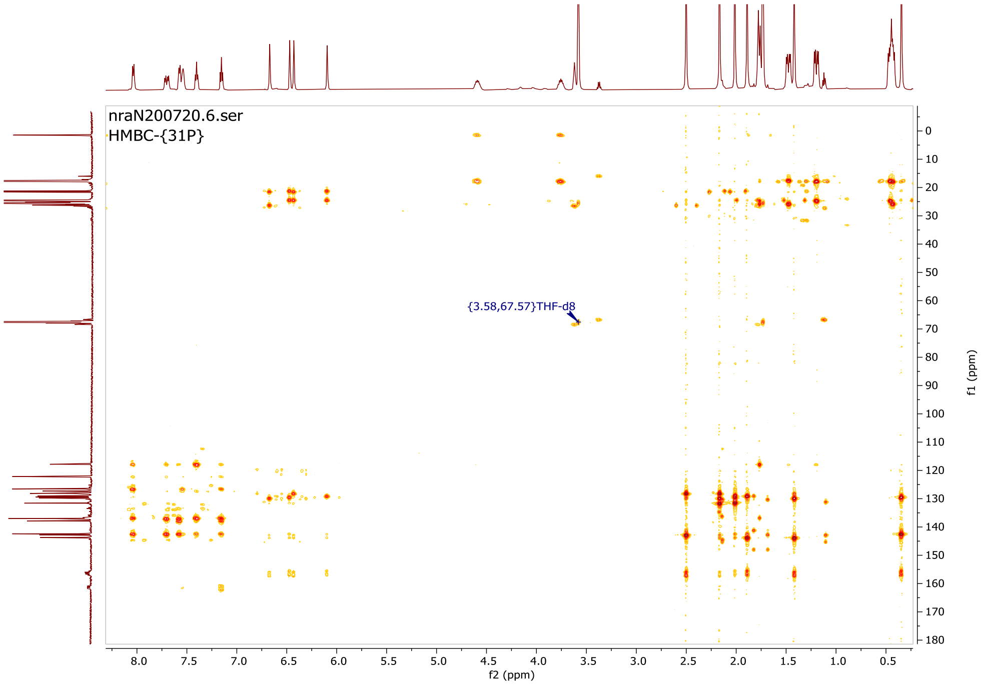

Fig S68. HMBC: ^{1}H / $^{13}C\{^{1}H\}$ NMR spectrum of **4** at 233 K in THF-d_8.

8. [*o*-iPr$_2$P-C$_6$H$_4$-B(C$_8$H$_{14}$)] (5a)

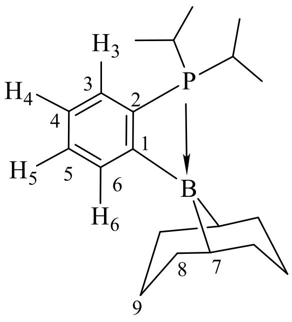

(5a)

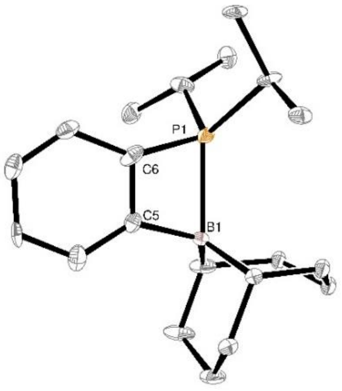

Li$^+$(Et$_2$O)[*o*-^{i}Pr$_2$P-C$_6$H$_4$-B(C$_8$H$_{14}$)-H]$^-$ (**1a**) (0.500 g, 1.26 mmol) was treated with CO$_2$ (1 atm) at rt for 1 h in toluene in a Fischer Porter bottle. Then, all solvent was removed under vacuum. The product was extracted in Et$_2$O through filter cannula leaving HCOOLi as a precipitate. The combined filtrates were reduced under vacuum to afford **1a** as a white solid. (0.380 g, 1.21 mmol, 96 %). Monocrystals suitable for X-ray diffraction were obtained by cooling a saturated n-pentane solution to –35 °C.

^{1}H NMR (400.13 MHz, 298 K, C$_6$D$_6$): δ 7.59 (dt, $^3J_{\text{H-H}}$ = 7.4 Hz, $^4J_{\text{H-H}}$ = 1.1 Hz, 1H, H6), 7.31 (td, $^3J_{\text{H-H}}$ = 7.1 Hz, $^4J_{\text{H-P}}$ = 1.0 Hz, $^4J_{\text{H-H}}$ = 1.9 Hz, 1H, H4), 7.12 (tdd, $^3J_{\text{H-H}}$ = 7.5 Hz, $^4J_{\text{H-P}}$ =3.2 Hz, $^4J_{\text{H-H}}$ = 1.2 Hz, 1H, H5), 7.10 (dd, $^3J_{\text{H-H}}$ = 7.6 Hz, $^4J_{\text{H-H}}$ = 1.0 Hz, 1H, H3), 2.26 (m, 10H, CH$_2$(9-BBN)), 1.95 (sept, $^3J_{\text{H-H}}$ = 7.2 Hz, $^2J_{\text{H-P}}$ = not found, 2H, CH(^{i}Pr), 1.91 (dt, $^3J_{\text{H-H}}$ = 10.5 Hz, $^3J_{\text{H-H}}$ = 3.3 Hz, 2H, CH$_2$(9-BBN) overlapping with CH(^{i}Pr)), 1.58 (dquint, $^3J_{\text{H-H}}$ = 3.5 Hz, $^2J_{\text{H-P}}$ = 3.2 Hz, 2H, CH(9-BBN)), 0.94 (dd, $^3J_{\text{H-P}}$ = 15.2 Hz, $^3J_{\text{H-H}}$ = 7.1 Hz, 12H, CH$_3$(^{i}Pr)).

^{31}P{^{1}H} NMR (161.99 MHz, 297.8 K, C$_6$D$_6$): δ 22.1 (s)

^{11}B NMR (128.38 MHz, 298 K, C$_6$D$_6$): δ 28.7 (s)

^{13}C{^{1}H} NMR (100.64 MHz, 298 K, C$_6$D$_6$): δ 172.7 (br s, C1), 131.0 (d, $^1J_{\text{C-P}}$ = 35.5 Hz, C2), 130.9 (d, $^3J_{\text{C-P}}$ = 1.9 Hz, C4), 129.4 (d, $^3J_{\text{C-P}}$ = 39.6 Hz, C6), 128.6 (s, C5), 126.0 (d, $^2J_{\text{C-P}}$ = 5.3 Hz, C3), 33.4 (d, $^3J_{\text{C-P}}$ = 9.2 Hz, CH$_2$(9-BBN)), 28.1 (br s, CH(9-BBN)), 25.0 (s, CH$_2$(9-BBN)), 23.7 (s, $^2J_{\text{C-P}}$ = not found, CH(^{i}Pr)), 19.0 (s, $^2J_{\text{C-P}}$ = not found, CH$_3$(^{i}Pr)), 18.6 (d, $^2J_{\text{C-P}}$ = 5.6 Hz, CH$_3$(^{i}Pr)).

Anal. cald. for C$_{20}$H$_{32}$BP: C, 76.44; H, 10.26. Found: C, 75.79; H, 10.19

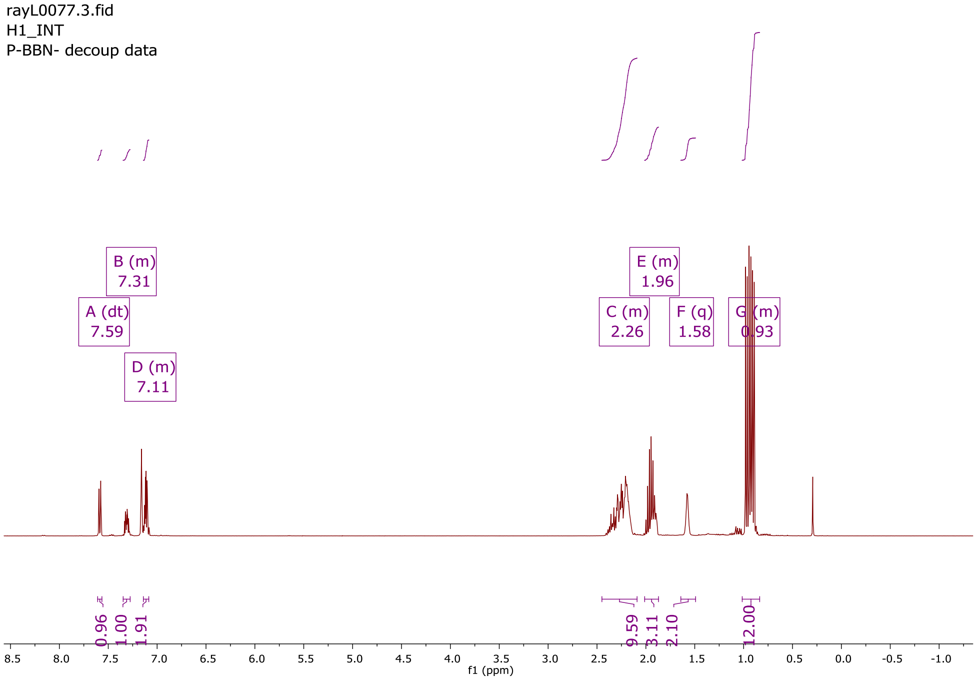

Figure S69. ^{1}H NMR spectrum of **5a** in C_6D_6 at 298 K.

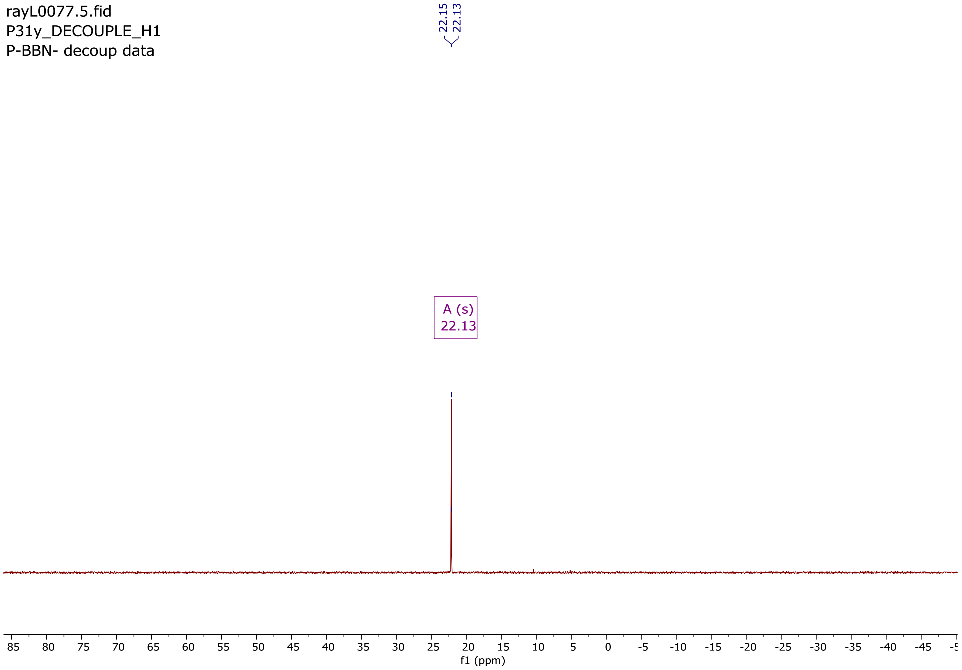

Figure S70. ^{31}P NMR spectrum of **5a** in C_6D_6 at 298 K.

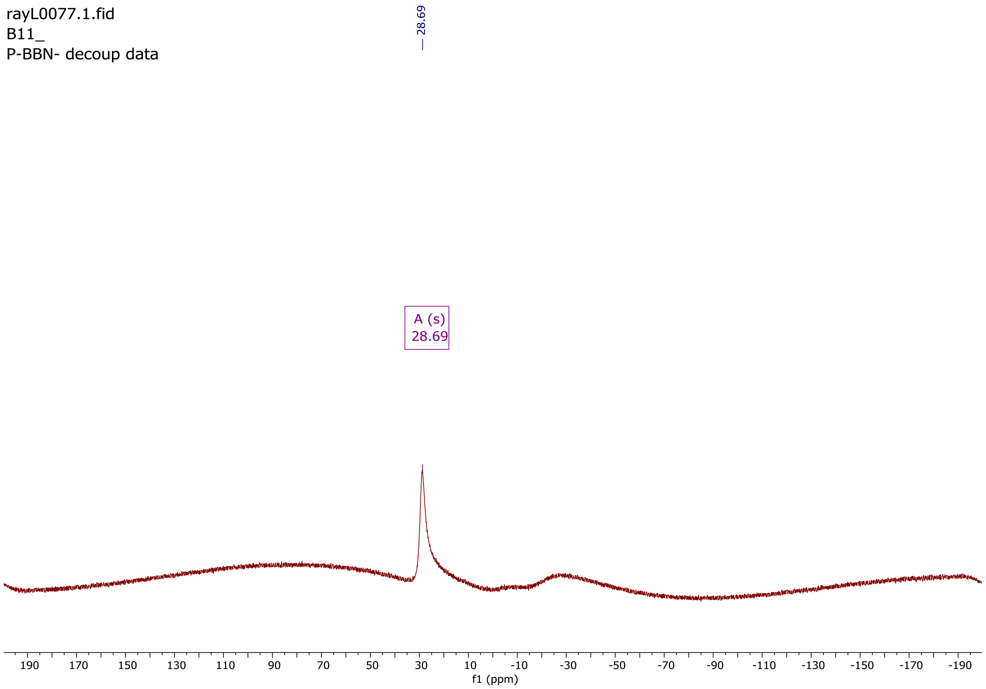

Figure S71. ^{11}B NMR spectrum of **5a** in C_6D_6 at 298 K.

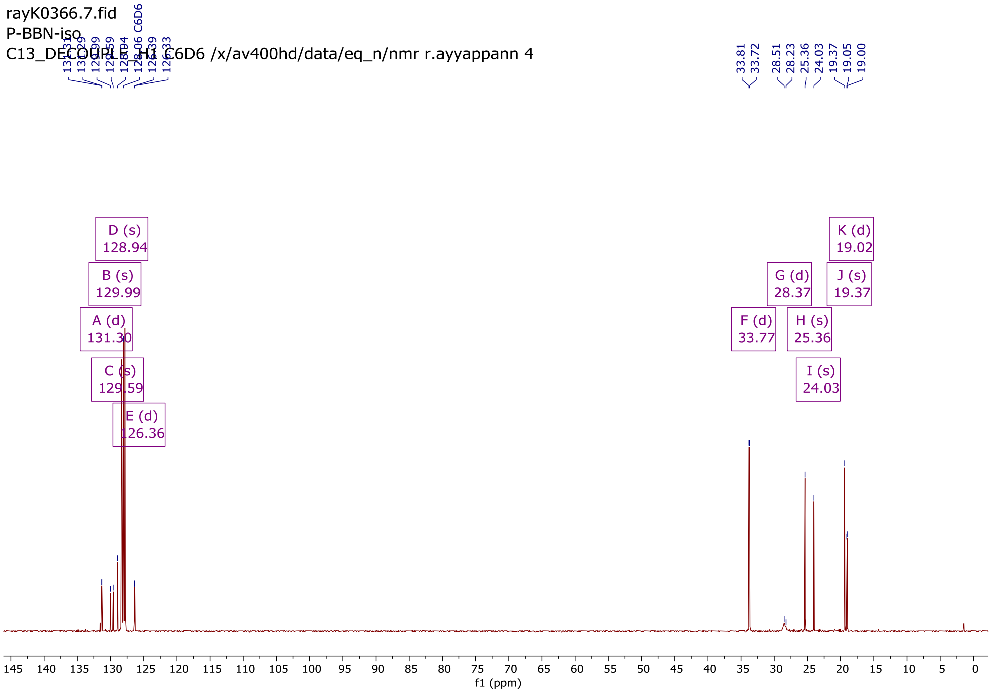

Figure S72. $^{13}C\{^1H\}$ NMR spectrum of **5a** in C_6D_6 at 298 K.

9. $[o\text{-}{}^{i}\mathrm{Pr_2P\text{-}C_6H_4\text{-}B(Ipc)_2}]$ (5c)

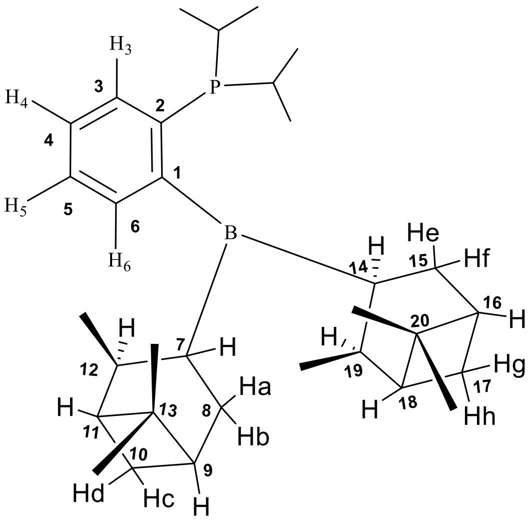

(5c)

$\mathrm{Li^+(THF)_2[\text{-}}o\mathrm{\text{-}P^iPr_2\text{-}C_6H_4\text{-}B(Ipc)_2H]^-}$ (**1c**) (0.500 g, 0.80 mmol) was dissolved in toluene (5 mL) in a Fischer-Porter bottle, followed by the admission of CO_2 (1 atm) at 298 K. The reaction contents were stirred for 10 min. During the course of the reaction, the solution became turbid. Toluene was removed under vacuum. The product was extracted in n-pentane (3 x 10 mL) leaving HCOOLi precipitated. The combined filtrates were reduced under vacuum to afford **5c** as a sticky solid. (0.360 g, 0.75 mmol, 94 %).

^{1}H NMR (600.47 MHz, 233 K, THF-d_8): δ 7.51 (ddd, $^3J_{\mathrm{H\text{-}H}}$ = 7.0 Hz, $^4J_{\mathrm{H\text{-}P}}$ = 2.7 Hz, 1H, H3), 7.26 (m, 3H, H4, H5, H6), 2.48 (quintet, $^3J_{\mathrm{H\text{-}H}}$ = 7.1 Hz, 1H, CH), 2.32 (m, $^3J_{\mathrm{H\text{-}H}}$ = 7.3 Hz, 3H, CH(^{i}Pr) + CH), 1.94 (m, 11H, CH + CH_2), 1.57 (t, $^3J_{\mathrm{H\text{-}H}}$ = 5.6 Hz, 1H, CH), 1.19 (m, 12H, CH_3(^{i}Pr) + CH_3(Ipc)), 1.16 (s, 3H, CH_3), 1.15 (s, 3H, CH_3), 1.10-1.07 (overlapping dd, $^3J_{\mathrm{H\text{-}H}}$ = 7.4 Hz, 9H, CH_3(^{i}Pr) + CH_3(Ipc)), 0.96 (dd, $^3J_{\mathrm{H\text{-}P}}$ = 13.3 Hz, $^3J_{\mathrm{H\text{-}H}}$ = 7.0 Hz, CH_3(^{i}Pr)), 0.76 (d, 1H, $^3J_{\mathrm{H\text{-}H}}$ = 9.1 Hz, CH_2 (1H diastereo)), 0.62 (d, $^3J_{\mathrm{H\text{-}H}}$ = 9.1 Hz, CH_2 (1H diastereo)).

^{31}P{^{1}H} NMR (243.07 MHz, 233 K, THF-d_8): δ –0.17 (s).

^{11}B NMR (192.65 MHz, 298 K, THF-d_8): δ 78.1 (s)

^{13}C{^{1}H} NMR (151.00 MHz, 233 K, THF-d_8): δ 156.6 (quart, $^1J_{\mathrm{B\text{-}C}}$ = 44.1 Hz, C1), 137.7 (d, $^1J_{\mathrm{P\text{-}C}}$ = 5.2 Hz, C3), 131.5 (s, C4), 130.6 (d, $^1J_{\mathrm{P\text{-}C}}$ = 20.8 Hz, C2), 128.4 (s, C5), 127.1 (s, C6), 49.1 (s, CH), 48.5 (s, CH), 42.5 (s, CH), 41.9 (s, CH), 40.6 (s, CH), 40.1 (s, CH), 40.0 (s, CH_2), 38.3 (s, CH), 37.1 (s, CH), 35.4 (s, CH_2), 33.5 (s, CH_2), 32.2 (s, CH_2), 31.3 (s, CH_2), 29.1 (s, CH_3(Ipc)), 28.5 (s, CH_3(Ipc)), 26.5 (s, 1C, CH_2), 25.6 (d, $^1J_{\mathrm{P\text{-}C}}$ = 13.2 Hz, 1C, CH(^{i}Pr), 24.7 (d, $^1J_{\mathrm{P\text{-}C}}$ = 12.1 Hz, CH(^{i}Pr)), 24.4 (s, CH_3(Ipc)), 23.4 (s, CH_3(Ipc)), 23.2 (s, CH_3(Ipc)), 22.3 (d, $^2J_{\mathrm{P\text{-}C}}$ = 14.4 Hz, CH_3(^{i}Pr)), 21.3 (d, $^2J_{\mathrm{P\text{-}C}}$ = 12.5 Hz, CH_3(^{i}Pr)), 21.0 (d, $^2J_{\mathrm{P\text{-}C}}$ = 18.7 Hz, CH_3(^{i}Pr)), 19.5 (d, $^2J_{\mathrm{P\text{-}C}}$ = 8.4 Hz, CH_3(^{i}Pr)).

Note: Assignment of C4, C5 and C6 signals are arbitrary. Because in ^1H-$^{13}C\{^1H\}$ HSQC spectrum, they all correlate with the multiplet appearing at the same chemical shift in ^1H NMR spectrum.

HRMS ESI: Calc: 494.3849 ($C_{32}H_{52}BPO$), Found: $[M+1]^+$ = 495.3929.

Specific optical rotation: $[\alpha]_D^{25}$ = –25.2°

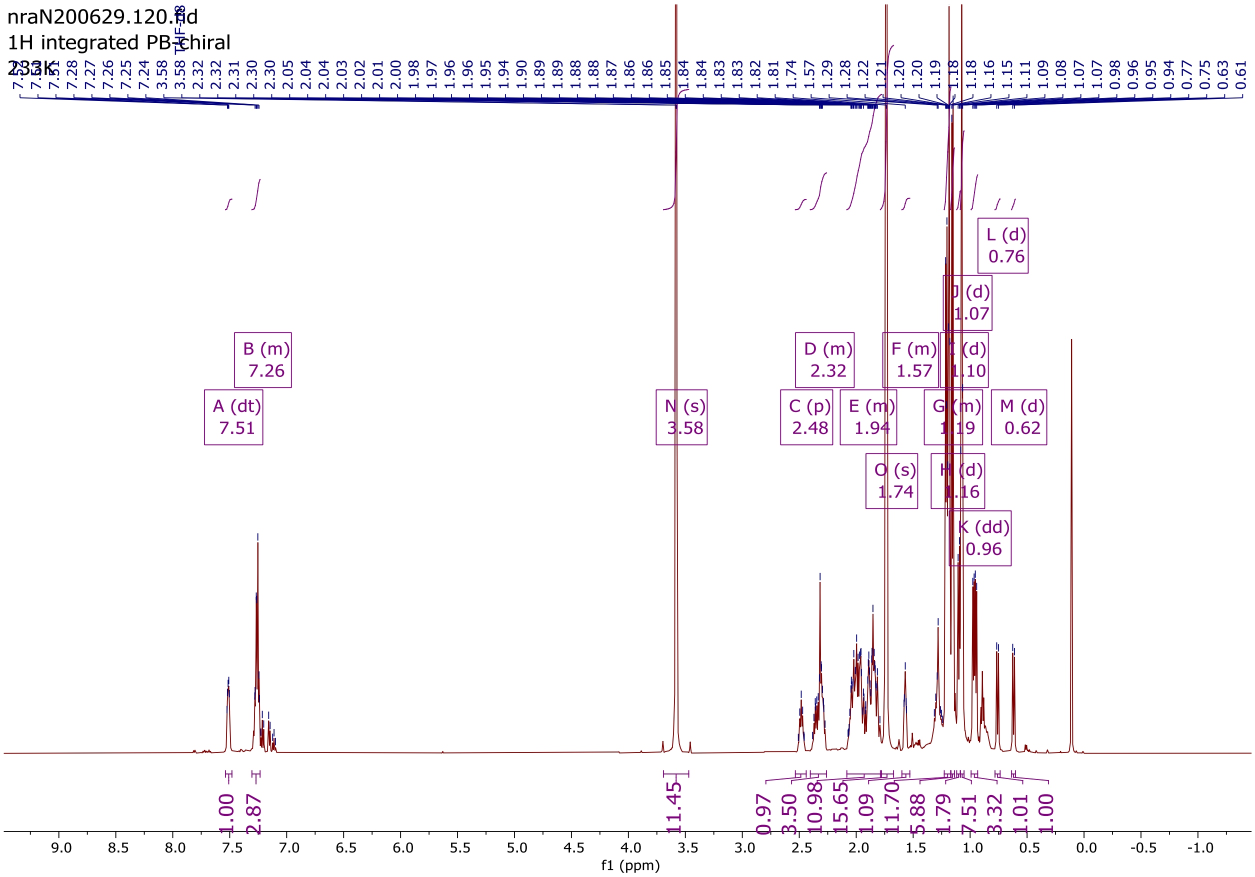

Figure S73. ^1H NMR spectrum of **5c** at 233 K in THF-d_8.

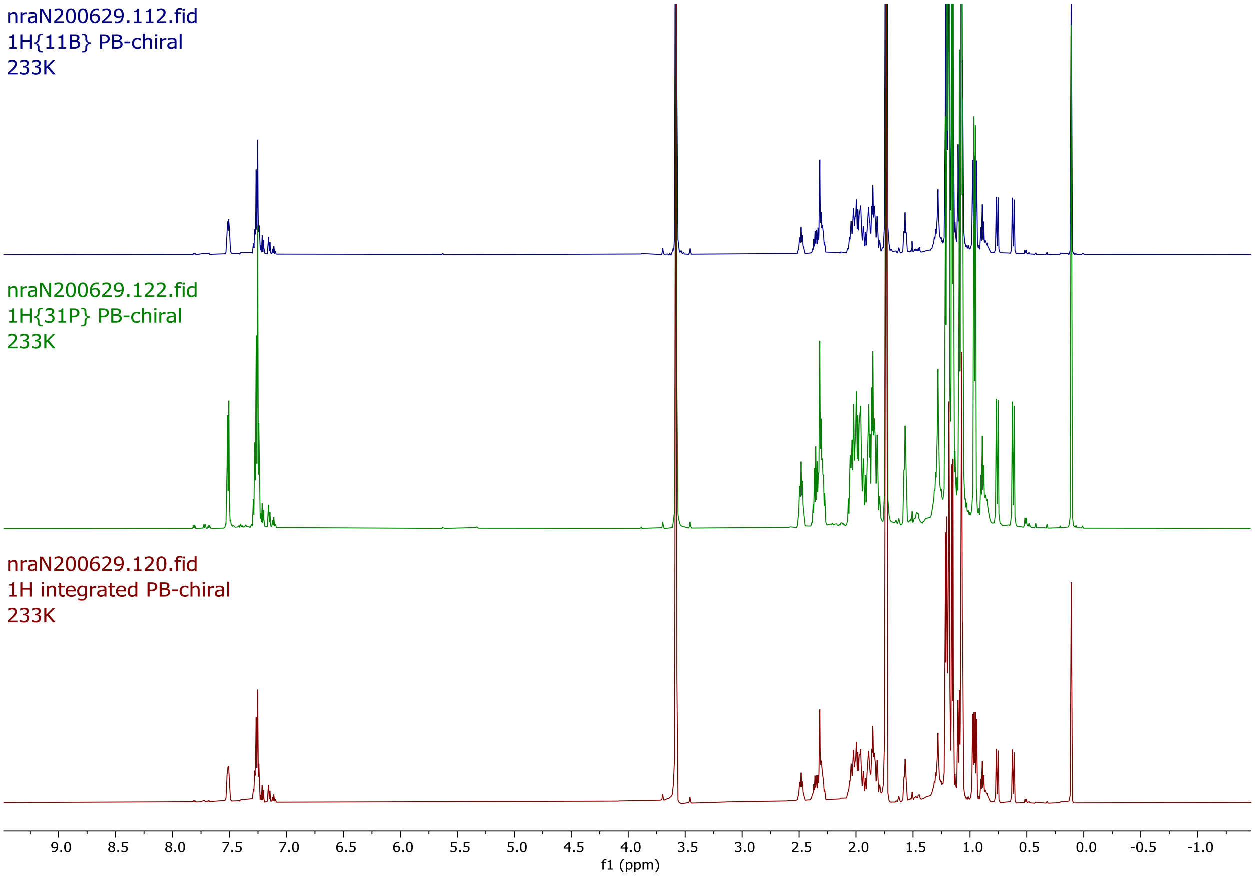

Figure S74. Stack plot spectra of ^{1}H, ^{1}H{^{31}P} and ^{1}H{^{11}B} NMR of **5c** at 233 K in THF-d_8.

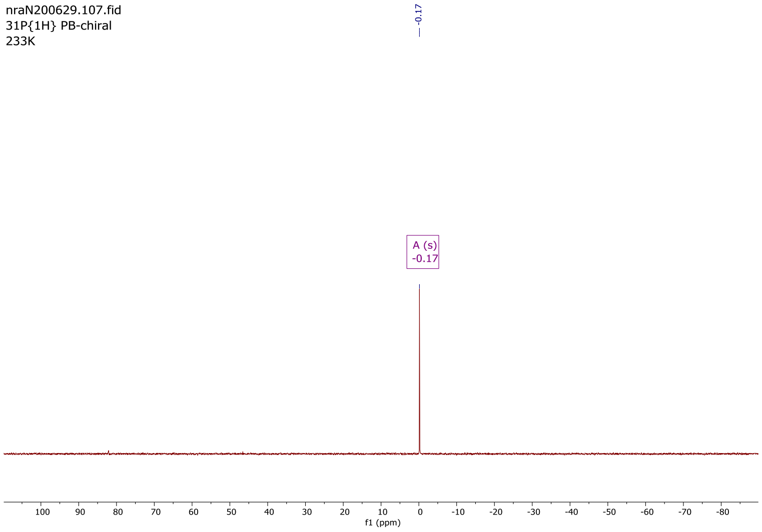

Figure S75. ^{31}P{^{1}H} NMR spectrum of **5c** at 233 K in THF-d_8.

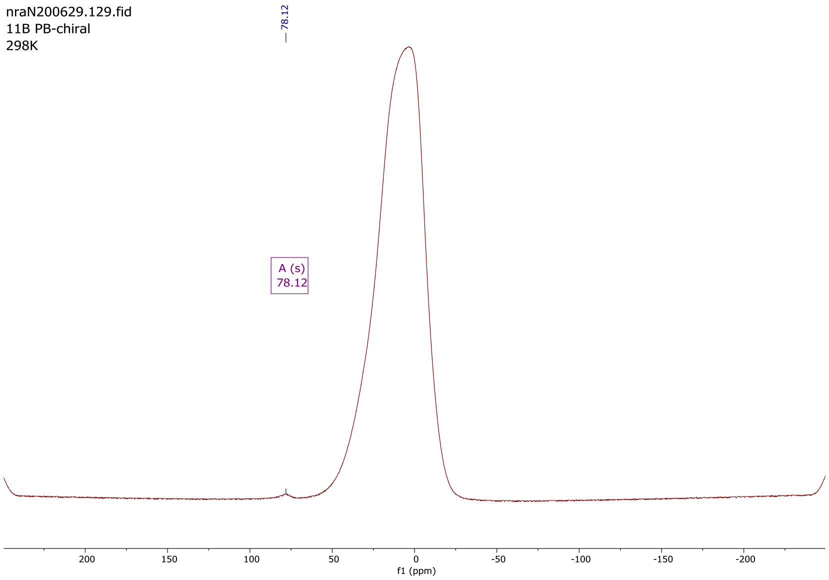

Figure S76. ^{11}B NMR spectrum of **5c** at 233 K in THF-d_8.

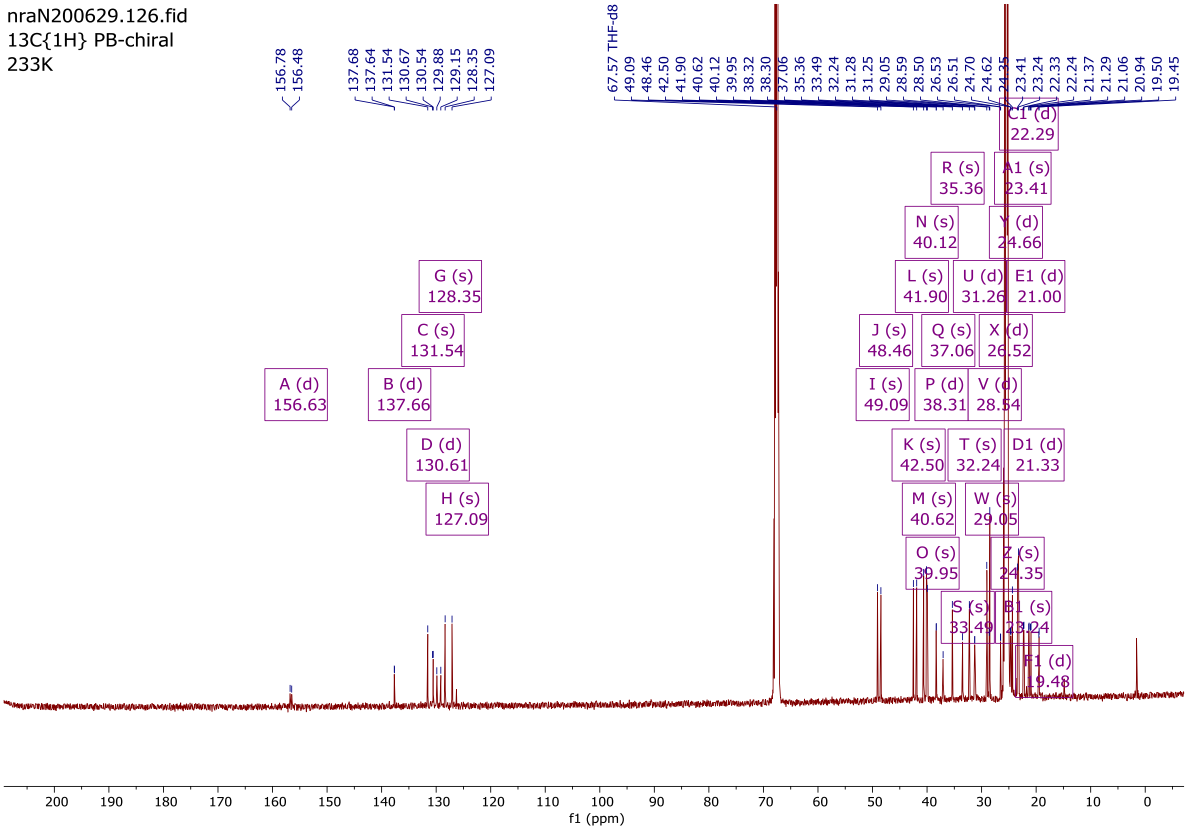

Figure S77. ^{13}C{^{1}H} NMR spectrum of **5c** at 233 K in THF-d_8.

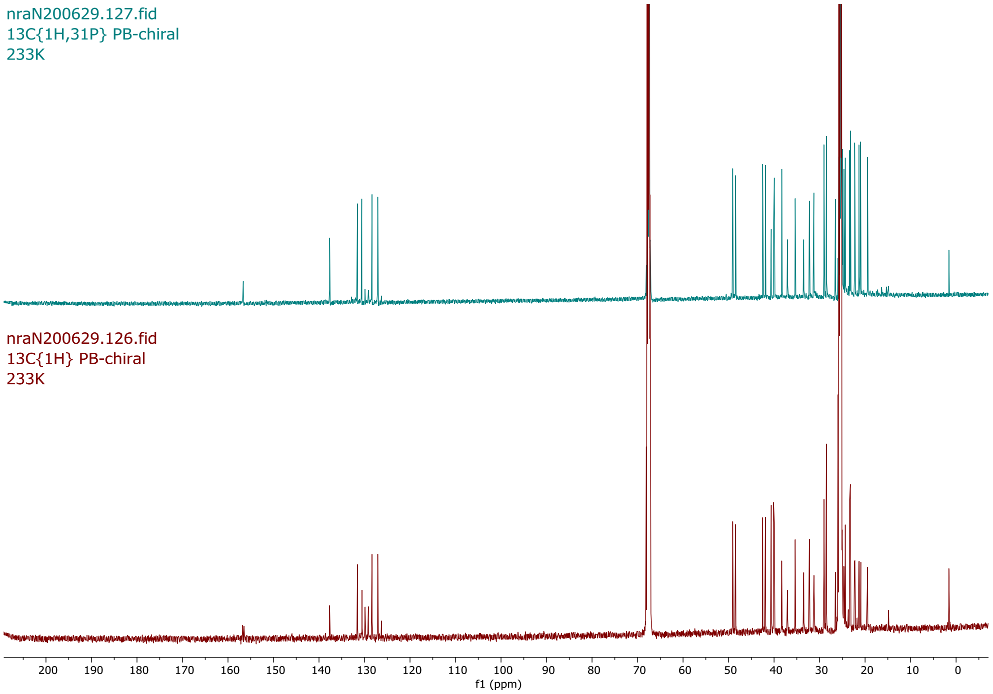

Figure S78. $^{13}C\{^1H\}$ and $^{13}C\{^1H\}\{^{31}P\}$ NMR stack spectra of **5c** at 233 K in THF-d_8.

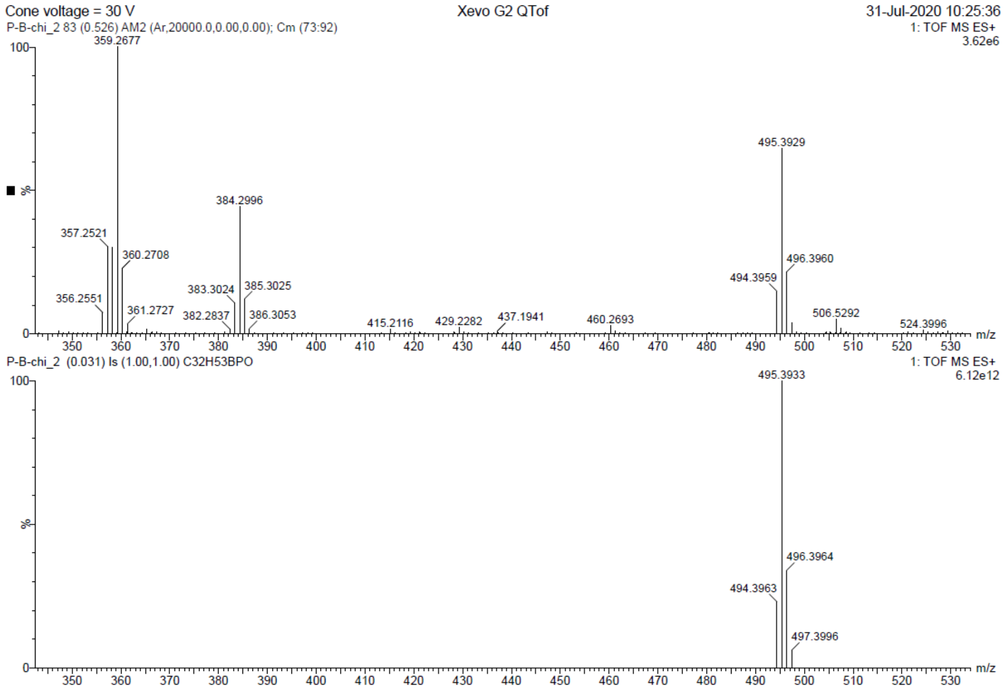

Fig S79. HRMS ESI spectrum of **5c**.

10. Table S1: Selected NMR data in solution and solid state for compounds 1-4.

Compound	^{1}H	^{31}P{^{1}H}	^{11}B{^{1}H}	^{7}Li
1a (tol-d_8, 253 K)	1.51	–1.6 (quart, $^1J_{\text{P-Li}}$ = 69.4 Hz) at 233 K	–13.5 (s, $w_{1/2}$ = 33.0 Hz)	0.5 (dd, $^1J_{\text{P-Li}}$ = 70.0 Hz, $^1J_{\text{Li-H}}$ = 7.0 Hz) at 233 K
1a (THF-d_8, 298 K)	signal not found	-0.4 (quart, $J_{\text{P-B}}$ = 10.7 Hz)	-13.7 (d, $J_{\text{P-B}}$ = 11 Hz)	-0.2 (sharp singlet, $w_{1/2}$ = 3.3 Hz)
1a (SS, 298 K)	-	5.4 (quart, $^1J_{\text{P-Li}}$ = 72.9 Hz)	-14.3 (br s, $w_{1/2}$ = 1311.7 Hz)	-1.0 (d, $^1J_{\text{P-Li}}$ = 72.9 Hz)
1b (THF-d_8, 298 K)	4.05	1.2 (quart, $J_{\text{P-B}}$ = 16.7 Hz)	-14.0 (d, $J_{\text{P-B}}$ = 17 Hz)	0.5 (sharp singlet, $w_{1/2}$ = 3.6 Hz)
1b (C_6D_6, 298 K)	3.68	0.5 (quart, $^1J_{\text{P-Li}}$ = 74.9 Hz),	-12.1 (d, $J_{\text{P-B}}$ = 11 Hz)	-0.4 (d, $^1J_{\text{P-Li}}$ = 73.0 Hz, $^1J_{\text{Li-H}}$ = 5.0 Hz)
1b (SS, 298 K)	-	0.8 (quart, $^1J_{\text{P-Li}}$ = 72.2 Hz)	-13.5 (br s, $w_{1/2}$ = 647.6 Hz)	-0.9 (d, $^1J_{\text{P-Li}}$ = 72.1 Hz)
1c (THF-d_8, 298 K)	2.44	1.4 (quart, $J_{\text{P-B}}$ = 14.5 Hz)	-9.4 (d, $J_{\text{P-B}}$ = 13 Hz)	-0.5 (sharp singlet, $w_{1/2}$ = 3.6 Hz)
1c (C_6D_6, 298 K)	-	2.7 (quart, $^1J_{\text{P-Li}}$ = 72.8 Hz)	-4.6 (s, $w_{1/2}$ – 59.0 Hz)	1.5 (dd, $^1J_{\text{P-Li}}$ = 73.0 Hz, $^1J_{\text{Li-H}}$ = 11.0 Hz)
1c[a] (SS, 298 K)	-	0.6 (v br, $w_{1/2}$ = 1400.0 Hz)	–12.3 (br s, $w_{1/2}$ = 1154.0 Hz)	0.9 (br s, $w_{1/2}$ = 271.0 Hz)
2 (THF-d_8, 233 K)	3.64	37.9 (br s)	-13.2 (d, $J_{\text{P-B}}$ = 3 Hz)	-
3 (THF-d_8, 233 K)	4.51	5.4 (quart, $J_{\text{P-B}}$ = 22.3 Hz)	-11.8 (d, $J_{\text{P-B}}$ = 20 Hz)	-0.1 (sharp singlet, $w_{1/2}$ = 6.9 Hz)
3(C_6D_6, 298 K)	-	4.2 (quart, $^1J_{\text{P-Li}}$ = 73.0 Hz)	-10.8 (d, $J_{\text{P-B}}$ = 9 Hz)	–0.2 (d, $^1J_{\text{P-Li}}$ = 71.3 Hz)
4 (THF-d_8, 233 K)	4.10	43.6 (s)	-11.8	-

$w_{1/2}$ is the line width of a signal at half its maximum intensity.

11. Hydrolithiation of benzophenone using stoichiometric quantity of 1a

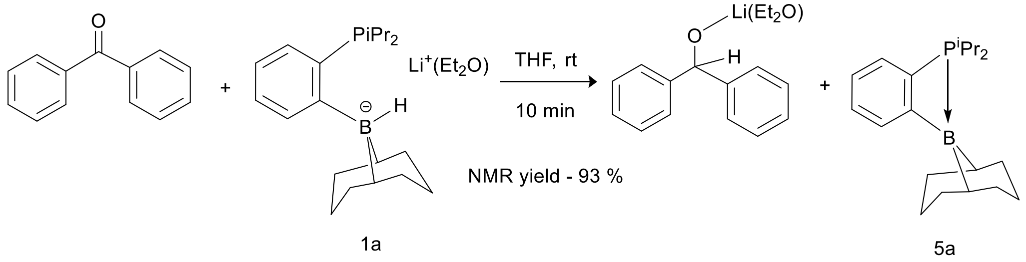

Stoichiometric quantities of Li$^+$[P-B(9-BBN)-H] (**1a**) (24.6 mg, 0.06 mmol) and benzophenone (11.3 mg, 0.06 mmol) were taken together in a J.Young NMR tube in THF-*d*$_8$ (0.5 mL). The reaction was completed in less than 10 minutes. The conversion into the product Ph$_2$CHOLi (15.1 mg, 0.06 mmol, 93 %) was calculated using an internal standard hexamethylbenzene (8.4 mg, 0.05 mmol) by ^{1}H NMR spectroscopy (T1 = 30 s).

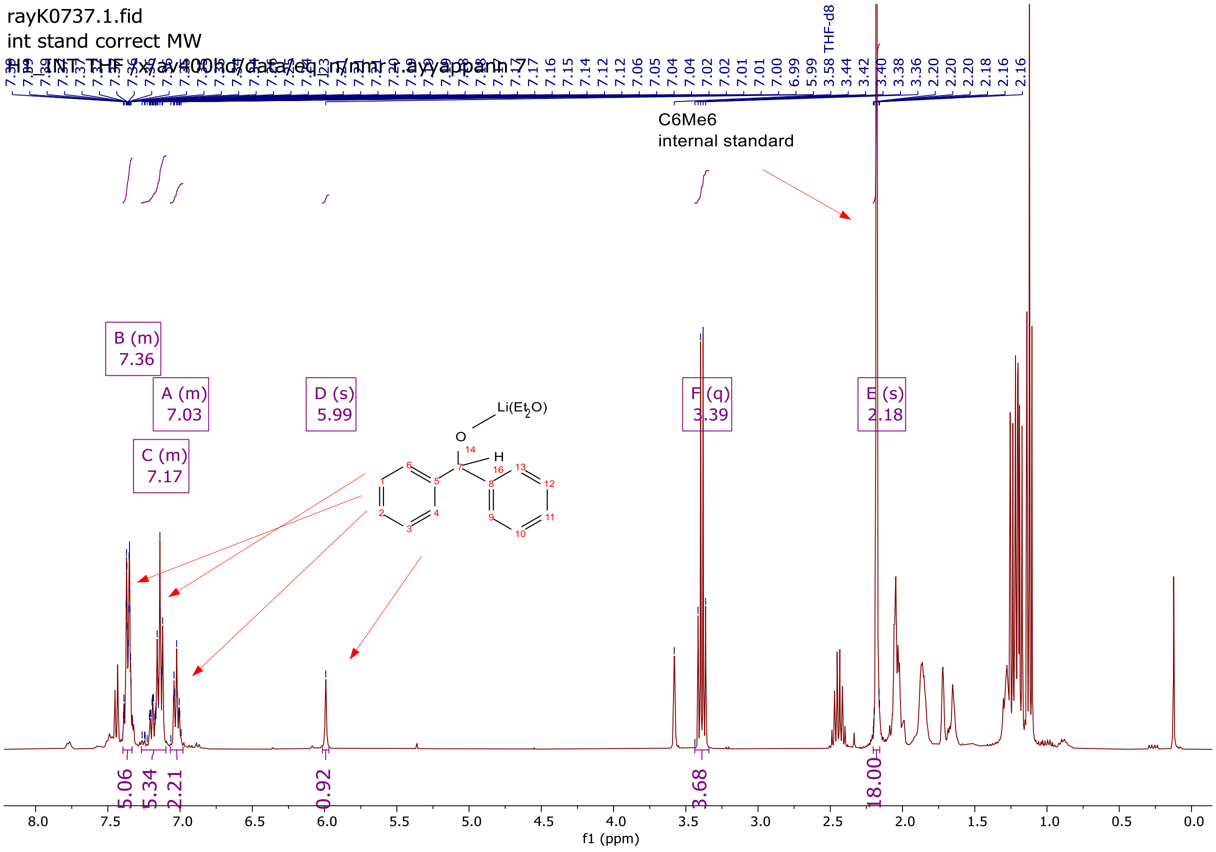

Fig S80. ^{1}H NMR spectrum of the reaction mixture of the hydrolithiation of benzophenone using stoichiometric amount of **1a**. Yield was calculated based on the internal standard C$_6$Me$_6$.

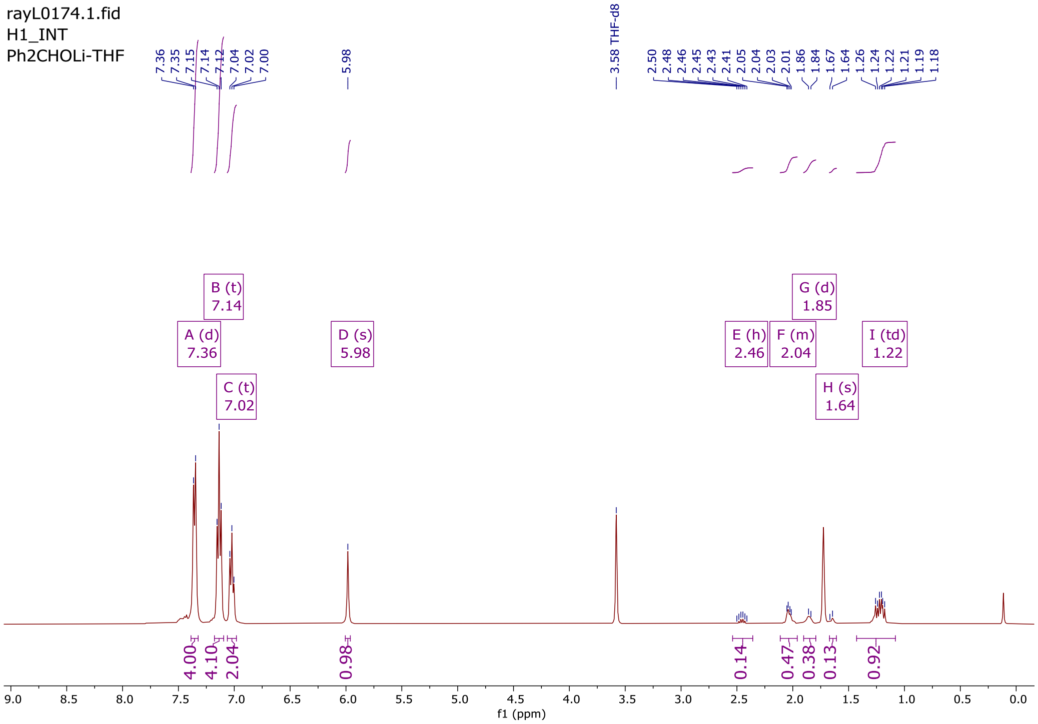

Fig S81. ^{1}H NMR spectrum of the isolated product Ph_2CHOLi in THF-d_8. The peaks in the range 2.5 – 1.25 ppm corresponds to **5a**.

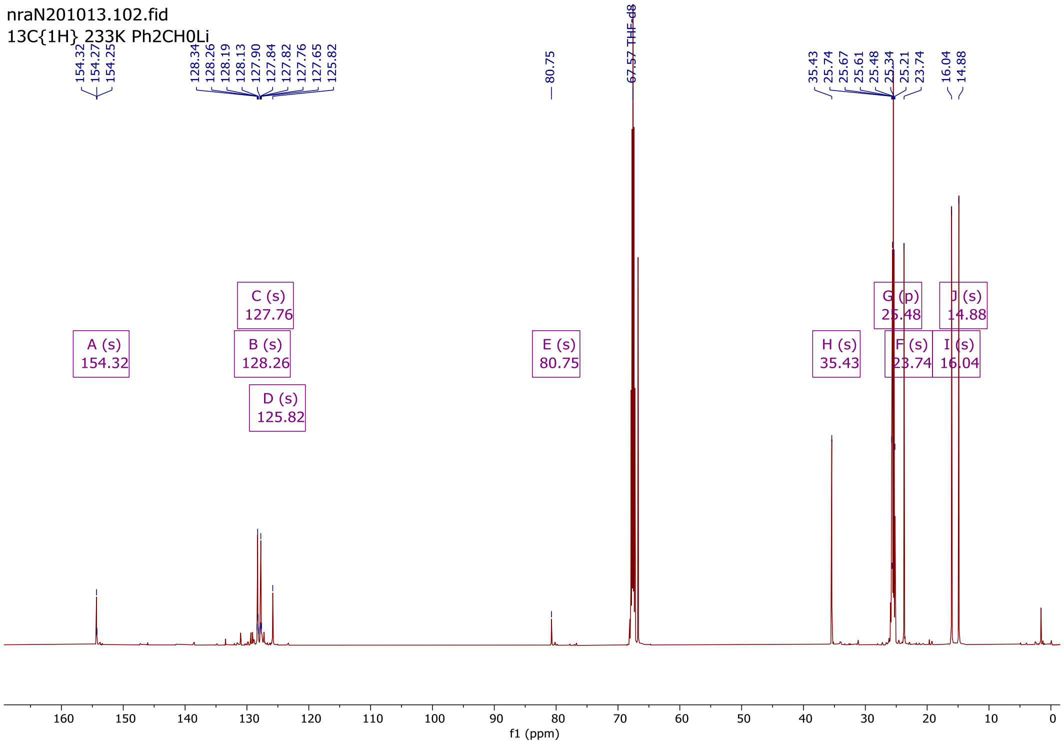

Fig S82. $^{13}C\{^1H\}$ NMR spectrum of Ph_2CHOLi in THF-d_8 at 233 K.

12. Reaction of 2 or 4 with $^{13}CO_2$ (1 bar)

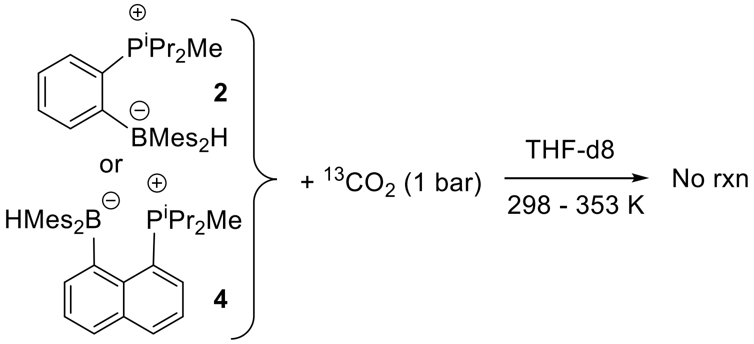

Compound **2** (13.5 mg, 0.030 mmol) or 4 (6.7 mg, 0.013 mmol) was dissolved in THF-d_8 (0.5 mL) in a high-pressure NMR tube at 298 K. Then, $^{13}CO_2$ (1 bar) was introduced into the NMR tube. Monitoring the reaction from 298-353 K by NMR spectroscopy indicated no reaction of **2** with $^{13}CO_2$.

13. Hydrogenation of CO_2 in the presence Li_2CO_3 catalyzed by 5a or 5b

$$\mathrm{H_2\ (1\ bar) + {}^{13}CO_2\ (1\ bar) + Li_2CO_3} \xrightarrow[\text{298 - 353 K} \atop \text{THF-}d_8]{\text{10 mol \% } \mathbf{5a} \text{ or } \mathbf{5b}} \text{No reaction observed}$$

In a high-pressure NMR tube, **5a** or **5b** (5 mg, 0.016 mmol) and lithium carbonate (11.8 mg, 0.160 mmol) were dissolved in THF-d_8 (0.5 mL). After degassing, $^{13}CO_2$ (1 bar) and H_2 (1 bar) were introduced consecutively into the NMR tube. The reaction progress was monitored by NMR spectroscopy using hexamethylbenzene as an internal standard. No reaction was observed and in particular no signal at 9.2 ppm indicative of LiOCHO is observed after 14h at rt nor after 3h at 50°C

14 X-ray crystal diffraction

The crystals were kept in their mother liquor until they were dipped in perfluoropolyether oil and their structure determined. The chosen crystals were mounted on a Mitegen micromount and quickly cooled down to either 100 K or 115 K. The selected crystals were mounted on a Bruker Kappa APEX II using a micro-focus molybdenum Kα radiation (λ = 0.71073 Å) equipped with graphite monochromator which attached with an Oxford Cryosystems Cooler Device. The unit cell determination and data integration were carried out using APEX II.[vi] The structures have been solved by Direct Methods using SHELXS[2], and refined either by least-squares procedures with SHELXL-2016[vii] included in the software packages WinGX version 1.63.[viii] or refined by means of least-squares procedures on a F with the aid of the program CRYSTALS[ix]. Atomic Scattering Factors were taken from the International tables for X-Ray Crystallography[x]. Absorption correction was done using multi-scan DENZO/SCALEPACK (Otwinowski & Minor, 1997) method [xi]. All hydrogen atoms were geometrically placed and refined using a riding model, with the exception of the BH hydrogens, in the structures **1a**, **1b**, **1c** and **3** which were located in the difference Fourier map.

All non-hydrogen atoms were anisotropically refined. Drawings of molecules have been performed with the program Ortep-3[xii] for Windows. Details of the structure solution and refinements are given in the Supporting Information (CIF file), together with a full listing of atomic coordinates, bond lengths and angles, and displacement parameters for all structures. These data have also been deposited at the Cambridge Crystallographic Data Centre. **CCDC numbers 2039383-2039387** contains the supplementary crystallographic data for this paper. These data can be obtained free of charge from The Cambridge Crystallographic Data Centre via www.ccdc.cam.ac.uk/data_request/cif.

Table S2. Crystal data collection and refinement parameters for **1a-c**.

Crystal parameters	**1a**	**1b**	**1c**
Molecular formula	$C_{24}H_{43}BLiOP$	$C_{34}H_{49}BLiOP$	$C_{80}H_{138}B_2Li_2O_4P_2$
Formula weight	396.33	522.49	1261.42
Crystal system	Monoclinic	Triclinic	Orthorhombic
Space group	$P2_1/n$	P-1	$P2_12_12_1$
a (Å)	16.00090(4)	10.21740(2)	11.092900(14)
b (Å)	9.96900(4)	10.90640(3)	19.47580(2)
c (Å)	16.21840(4)	15.03640(3)	35.92390(3)
α (°)	90	77.670(3)	90
β (°)	108.181(4)	74.617(3)	90
γ (°)	90	87.944(3)	90
V ($Å^3$)	2457.89(6)	1577.90(3)	7761.11(2)
Z	4	2	4
F(000)	872	568	2784
Crystal description	Block, colourless	Platelet, colourless	Plate, colourless
Crystal size (mm)	0.25 x 0.12 x 0.05	0.15 x 0.10 x 0.02	0.15 x 0.10 x 0.02
θ (°)	2-28	3-31	3-23
M (mm^{-1})	0.12	0.11	0.10
Independent reflections	7636	10018	17924
R_{int}	0.088	0.047	0.079
θ_{min} - θ_{max} (°)	2.2 – 30.8	1.4 – 31.4	3 – 23

h	-22 to 22	-14 to 14	-14 to 14
k	-14 to 14	-15 to 15	-25 to 22
l	-22 to 23	-19 to 21	-46 to 46
$R[F^2>2\sigma(F^2)]$	0.051	0.053	0.048
$WR(F^2)$	0.048	0.073	0.043
S	1.11	1.07	0.83
(Δ/σ)max	0.001	0.001	0.001
$\Delta\rho_{max}$ (e Å^3)	0.33	0.40	0.38
$\Delta\rho_{min}$ (e Å^3)	–0.25	–0.39	–0.40

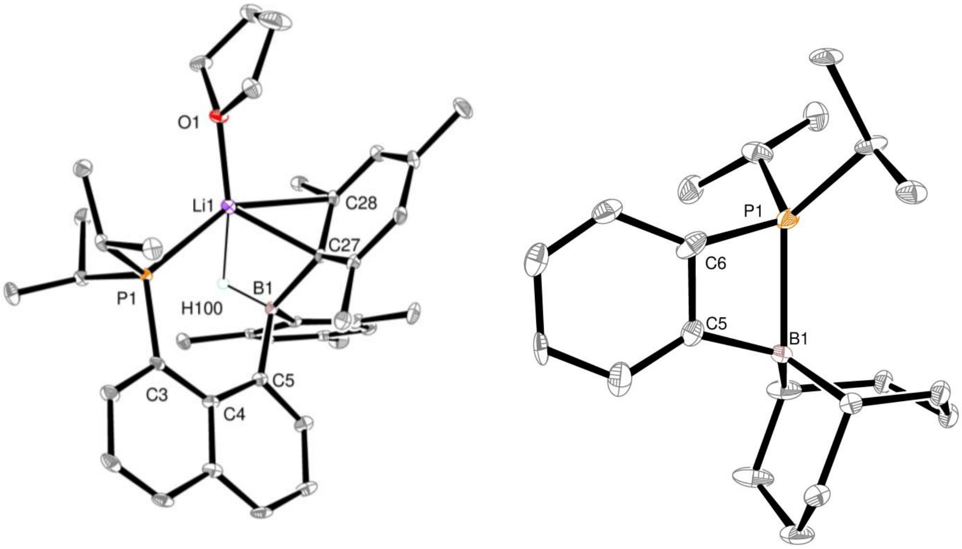

(**3**) (**5a**)

Fig S83. ORTEP views of X-ray structures of **3** and **5a** at 50% thermal ellipsoid probability level. All the hydrogen atoms except B-H were omitted for clarity.

Table S3. Crystal data collection and refinement parameters for **3** and **5a**.

Crystal parameters	**3**	**5a**
Molecular formula	$C_{38}H_{51}B_{Li}OP$	$C_{20}H_{31}BP$
Formula weight	572.5	313.23
Crystal system	Monoclinic	Monoclinic
Space group	$P2_1/c$	$P2_1/c$
a (Å)	17.3854(1)	7.7245(2)
b (Å)	9.637 (0)	11.1972(4)
c (Å)	21.4581 (1)	21.3905(1)
α (°)	90	90
β (°)	109.675 (4)	97.583 (4)
γ (°)	90	90
V (Å^3)	3385.26 (9)	1833.94 (8)
Z	4	4
F(000)	1210	684

Crystal description	Parallelepiped, colourless	Parallelpiped, colourless
Crystal size (mm)	0.15 x 0.06 x 0.02	0.16 x 0.12 x 0.03
θ (°)	2.6 – 28.9	2.7 – 25.3
M (mm^{-1})	0.11	0.14
Independent reflections	5735	684
R_{int}	0.082	0.084
θ_{min} - θ_{max}	2.0-24.7°	2.1-24.7°
h	-20 to 20	-9 to 9
k	-11 to 11	-13 to 13
l	-25 to 25	-25 to 25
$R[F^2>2\sigma(F^2)]$	0.072	0.058
$WR(F^2)$	0.224	0.179
S	1.26	1.12
(Δ/σ)max	0.003	0.004
Δρmax	0.65 e Å3	0.55 e Å3
Δρmin	-0.40 e Å3	-0.61 e Å3

Table S4. Important bond length (Å) and bond *angles (°)*.

Bond length (Å) /*Bond angle (°)*	**1a**	**1b**	**1c** **(molecule 2)**	**3**
P–Li	2.487(3)	2.506(3)	2.535(3)	2.459(7)
B–H	1.18(2)	1.179(18)	1.002	1.17(3)
Li–H	1.78(2)	1.96(2)	2.036	1.92(5)
Li–B	2.373(3)	2.509(3)	3.016(4)	2.485(7)
B–P	3.285(2)	3.283(2)	3.438(2)	3.341(3)
C(R2 on B)–Li	2.323(3)	C6-Li1 2.443(3) C5-Li1 2.214(3)	-	C28-Li1 2.361(7) C27-Li1 2.168(6)
P–Li–H	*94.1(7)*	*79.0(5)*	*78.4*	*74.0(1)*
Li–P–C	*101.87(8)*	*104.19(8)*	*110.98(9)*	*122.8(2)*
Li–H–B	*105.0(1)*	*104.0(1)*	*165.4*	*105.0(2)*
H–B–C	*108.0(1)*	*105.5(9)*	*106.7*	*109.2*

15. References

---

i. Shriver, D. F.; Drezdon, M. A. The Manipulation of Air Sensitive Compounds, 2nd ed.; Wiley: New York, **1986**.

[ii] Andrew Pelter,: Saraswathi Singaram,: Herbert Brown. *Tetrahedron Lett*, **1983**, *24*, 1433-1436.

[iii] Herbert C Brown, Bakthan Singaram, *J. Org. Chem*. **1984**, *49*, 945-947.

[iv] M. Tamm, B. Dreβel, K. Baum, T. Lugger, T. Pape, *J. Organomet. Chem.* **2003**, *677*, 1-9.

[v] Sébastien Bontemps, Marc Devillard, Sonia Mallet-Ladeira, Ghenwa Bouhadir, Karinne Miqueu, Didier Bourissou, *Inorg. Chem*. **2013**, *52*, 4714−4720.

[vi] SAINT Bruker (2007). Bruker AXS Inc., Madison, Wisconsin, USA.

[vii] A short history of SHELX, G. M. Sheldrick, Acta Crystallogr., Sect. A: Found. Crystallogr., **2008**, *64*, 112-122.

[viii] WinGX suite for small-molecule single-crystal crystallography, Farrugia, L. J. J. Appl. Cryst. **1999**, *32*, 837-838.

[ix] CRYSTALS version 12: software for guided crystal structure analysis - PW Betteridge, JR Carruthers, K Prout, DJ Watkin, J. Appl. Cryst. **2003**. *36*, 1487.

[x] INTERNATIONAL tables for X-Ray crystallography, **1974**, Vol IV, Kynoch press, Birmingham, England.

[xi] R. H. Blessing, acta cryst. **1995**, a51, 33-38.

[xii] ORTEP-3 for Windows - a version of ORTEP-III with a Graphical User Interface (GUI)- L. J. Farrugia, J. Appl. Crystallogr. **1997**, *30*, 565.